

UNIVERSITÉ DU QUÉBEC À MONTRÉAL

**THÈSE PRÉSENTÉE À
L'UNIVERSITÉ DU QUÉBEC À CHICOUTIMI
COMME EXIGENCE PARTIELLE
DU DOCTORAT EN RESSOURCES MINÉRALES
OFFERT À
L'UNIVERSITÉ DU QUÉBEC À MONTRÉAL
EN VERTU D'UN PROTOCOLE D'ENTENTE
AVEC L'UNIVERSITÉ DU QUÉBEC À CHICOUTIMI**

PAR

JOSEPH STEPHEN STONER

**MAGNETIC PROPERTIES AND PALEOINTENSITY RECORDS FROM
LATE QUATERNARY LABRADOR SEA SEDIMENTS**

**(PROPRIÉTÉS MAGNÉTIQUES ET ENREGISTREMENTS DE
PALÉOINTENSITÉ DES SÉDIMENTS DU QUATÉNAIRE RÉCENT DE
LA MER DU LABRADOR)**

FÉVRIER 1995



Mise en garde/Advice

Afin de rendre accessible au plus grand nombre le résultat des travaux de recherche menés par ses étudiants gradués et dans l'esprit des règles qui régissent le dépôt et la diffusion des mémoires et thèses produits dans cette Institution, **l'Université du Québec à Chicoutimi (UQAC)** est fière de rendre accessible une version complète et gratuite de cette œuvre.

Motivated by a desire to make the results of its graduate students' research accessible to all, and in accordance with the rules governing the acceptance and diffusion of dissertations and theses in this Institution, the **Université du Québec à Chicoutimi (UQAC)** is proud to make a complete version of this work available at no cost to the reader.

L'auteur conserve néanmoins la propriété du droit d'auteur qui protège ce mémoire ou cette thèse. Ni le mémoire ou la thèse ni des extraits substantiels de ceux-ci ne peuvent être imprimés ou autrement reproduits sans son autorisation.

The author retains ownership of the copyright of this dissertation or thesis. Neither the dissertation or thesis, nor substantial extracts from it, may be printed or otherwise reproduced without the author's permission.

ABSTRACT

This thesis combines results from a high resolution rock magnetic study of three Late Quaternary piston cores from three different oceanographic provinces within the deep Labrador Sea. Paleomagnetic measurements, rock magnetic parameters, hysteresis ratios and low temperature remanence measurements were used in combination with AMS ^{14}C dates, oxygen isotopic ratios, grain-size analyses, carbonate content determinations and detailed core descriptions to delineate the environmental and paleomagnetic record from the deep Labrador Sea.

Core HU90-013-013P (P-013) (lat. $58^{\circ}12.59\text{N}$, long. $48^{\circ}22.40\text{W}$, water depth 3380m) from the Greenland Rise reveals three main features in the downcore variation of the rock magnetic parameters. Two are at the glacial-interglacial transitions (i.e. isotope stage 6/5e and 2/1) showing magnetic grain-size coarsening, increased magnetic concentration and accumulation. Previous studies in this region connected the coarsening of magnetic grain-size during transitions to current winnowing of the finer fraction during interglacial conditions. The interpretation of the present study is that the coarsening is primarily due to increased detrital deposition related to ice retreat and the associated meltwater flux from southern Greenland. The third magnetic feature corresponds to the initial part of stage 2 where there is a distinct interval of higher coercivity. This high coercivity interval has no obvious correlation to climate change, but appears to be related to the increased preservation of ultra fine single domain magnetite due to a lack of reduction diagenesis within the interval.

High-resolution rock magnetic data, AMS ^{14}C dates, $\delta^{18}\text{O}$, and grain-size analyses from P-013 provide a record of the last two deglaciations. During Termination I, a well-defined interval of high volumetric magnetic susceptibility (k) and low anhysteretic susceptibility to volumetric magnetic susceptibility (k_{ARM}/k) postdates the Younger Dryas and the $\delta^{18}\text{O}$ change marking the stage 2/1 boundary and correlates with sedimentological and geomorphological evidence for Greenland ice-sheet retreat from the coastline to the continental interior. During Termination II, a very similar magnetic signal coincides with the $\delta^{18}\text{O}$ shift marking the stage 6/5 glacial-interglacial transition and continues throughout substage 5e. We suggest that this magnetic signal, during both Termination I and Termination II, marks continental meltwater detritus from Greenland. If so, the synchronous changes in magnetic and oxygen isotopic records at Termination II indicate very early and rapid deglaciation of Greenland, in contrast to the relatively late deglaciation observed for Termination I. A distinct fluctuation in k and k_{ARM}/k occurs prior to the onset of the $\delta^{18}\text{O}$ change at Termination I (where it occurs at $\sim 16,900$ yr B.P.) and at Termination II. These are interpreted as due to sudden influx of detritus into the basin caused by unpinning of ice from the continental shelf at the inception of deglaciation.

HU91-045-094P (P-094) (lat. $50^{\circ}12.26\text{N}$, long. $45^{\circ}41.14\text{W}$, water depth 3448 m) was collected from a small deep channel SE of Orphan's Knoll on the Labrador rise. Sedimentation in P-094 contains many distinct intervals of detrital deposition. Variations in magnetic properties and lithology indicate two classes of depositional events during the last glacial cycle. (1) Seven detrital carbonate (DC) layers are recognized by high carbonate content and by magnetite grain-size sensitive parameters (such as k_{ARM}/k and $H_{\text{Cr}}/H_{\text{C}}$) which indicate mean magnetite grain diameters about four times greater than those of the background sediments. (2) Six low detrital carbonate (LDC) layers are recognized by very similar magnetic properties to DC layers but with low carbonate concentrations (similar to the

background sediment). Ice rafted detritus (IRD), recognized by increased percentage of the >125 micron grain-size fraction and by high magnetic susceptibility, is associated with most DC and LDC layers. The large grained magnetite associated with DC and LDC layers is well sorted and relatively constant within and between layers. The correspondence of increased grain-size of well sorted magnetite with the increase in fine grained detrital carbonate content (DC layers) and with the visual record of sediment change (DC and LDC layers), but not with coarse fraction content precludes ice rafting as the primary depositional mechanism. Therefore, DC and LDC events may have been deposited from suspended sediment derived from turbidite activity in the nearby Northwest Atlantic Mid-Ocean Channel. The association of DC layers with IRD and the apparent age correlation of DC layers to North Atlantic Heinrich layers indicate that the ice sheet instability which produced the DC layers is coeval with that which produced many of the Heinrich layers. Several DC and LDC layers, however, do not correlate with recognized Heinrich layers, suggesting even greater instability of the Laurentide ice sheet during the last glacial cycle.

All three deep Labrador Sea piston cores, P-013, P-094 and HU90-013-012 (P-012) (lat. 58°55.35N, long. 47°07.01W, water depth 2830 m) from the Greenland Slope, record Late Quaternary relative paleointensity of the geomagnetic field. Hysteresis ratios, rock magnetic parameters and low temperature remanence measurements indicate that pseudo-single domain magnetite is the dominant magnetic mineral in all three cores. Besides AMS ^{14}C , $\delta^{18}\text{O}$ and $\delta^{13}\text{C}$ stratigraphy, correlation between cores is enhanced by the presence of DC and LDC layers. Apart from deglacial intervals and DC and LDC layers, normalized remanence records show strong correlation for a range of normalizers (k , k_{ARM} and SIRM) and no correlation with bulk magnetic parameters, implying that these cores yield useful relative paleointensity records. Good correlation is observed between cores using only DC and LDC layers as tie points, suggesting that relative paleointensity can be used as a regional correlation tool. Paleointensity records from the Labrador Sea contain many features similar to those observed in the Mediterranean, Indian and Pacific Ocean. A composite record from P-013 and P-012 is matched to a composite of the Mediterranean/Indian Ocean records with high correlation coefficients, however, the chronologies of the two records are inconsistent. The strong correlation of paleointensity features from the Labrador Sea, Indian Ocean and Mediterranean suggests that these sediments are recording synchronous dipole field variations, however, the chronological discrepancy must be rectified before paleointensity can be used with complete confidence as a global correlation tool.

RÉSUMÉ

Ce mémoire présente des études magnétiques à haute résolution sur des sédiments d'âge Quaternaire Supérieur provenant de trois carottes du bassin de la mer du Labrador. Les mesures paléomagnétiques, les paramètres magnétiques, les rapports d'hystérésis et les mesures de rémanence à basse température ont été combinés à d'autres données: datations ^{14}C AMS, rapports isotopiques de l'oxygène, analyses granulométriques, teneurs en carbonate et descriptions détaillées des carottes. Ces données permettent de décrire les enregistrements paléomagnétiques et environnementaux du bassin.

La partie inférieure de la carotte HU90-013-013P (P-013) (lat. $58^{\circ}12.59\text{N}$, long. $48^{\circ}22.40\text{W}$, profondeur 3380m) provenant du talus groenlandais révèle trois événements majeurs concernant les paramètres magnétiques. Deux d'entre eux, qui correspondent à des transitions glaciaire-interglaciaires (stades isotopiques 6/5e et 2/1), montrent une augmentation granulométrique des grains magnétiques, de la concentration magnétique et de l'accumulation. Des études antérieures ont permis d'associer l'augmentation granulométrique des grains magnétiques à un vannage des fractions les plus fines par les courants pendant les intervalles interglaciaires. La présente étude explique cette augmentation granulométrique par un apport détritique accru dû au retrait des glaces au sud du Groenland et à l'eau de fonte qui y est associée. Le troisième événement magnétique, qui correspond au début du stade isotopique 2, est caractérisé par un intervalle à plus grande coercivité. Cet intervalle à forte coercivité semble être relié à une plus grande préservation des magnétites ultrafines à domaine unique, qui serait due à une absence de réduction diagénétique, et non pas à un changement climatique.

Les données magnétiques à haute résolution, les datations ^{14}C AMS, le $\delta^{18}\text{O}$ et la granulométrie de la carotte P-013 offrent un enregistrement des deux dernières déglaciations. Pendant la Terminaison I, un intervalle reconnaissable succède au Dryas Récent et la variation de $\delta^{18}\text{O}$ marquant la limite entre les stades isotopiques 2 et 1. Cet intervalle est défini par une forte susceptibilité magnétique volumétrique (k) et un faible rapport de la susceptibilité "anhystérique" sur la susceptibilité magnétique volumétrique (k_{ARM}/k). Il est corrélé avec des observations sédimentologiques et géomorphologiques correspondant au retrait de la calotte glaciaire groenlandaise vers l'intérieur du continent. Pendant la Terminaison II, un signal magnétique similaire coïncide avec la variation du $\delta^{18}\text{O}$ qui marque la transition glaciaire-interglaciaire des stades 6 à 5; il se prolonge dans le sous-stade isotopique 5e. Ceci suggère que ce signal magnétique est dû à un apport détritique continental par l'eau de fonte provenant du Groenland, pendant les terminaisons I et II. Ainsi, le synchronisme des variations magnétiques et isotopiques indiquerait, pour la Terminaison II, une déglaciation précoce et très rapide du Groenland par comparaison avec une déglaciation relativement lente pour la Terminaison I. Des changements de k et de k_{ARM}/k sont observés avant le début de la variation de $\delta^{18}\text{O}$ aussi bien pour la Terminaison I (i.e. vers 16.900 ans BP) que pour la Terminaison II. Ceci est interprété comme étant dû à un soudain apport détritique dans le bassin causé par le décrochage de la glace du plateau continental au début de la déglaciation.

La carotte HU91-045-094P (P-094) (lat. $50^{\circ}12.26\text{N}$, long. $45^{\circ}41.14\text{W}$, profondeur 3448m) a été échantillonnée dans un chenal sous-marin profond au sud-est de *Orphan's Knoll* sur le talus labradorien. La sédimentologie de la carotte P-094 montre plusieurs horizons détritiques. Les variations des propriétés magnétiques et de la lithologie indiquent deux types

de dépôt pendant le dernier cycle glaciaire.

(1) Sept niveaux de carbonate détritique (DC) sont reconnaissables par leur forte teneur en carbonate et par des paramètres qui sont sensibles à la taille des grains de magnétite (comme k_{ARM}/k et H_{Cr}/H_C). Ces paramètres indiquent un diamètre moyen des grains de magnétite à peu près quatre fois plus grand que les autres grains du sédiment. (2) Six niveaux à faible teneur en carbonate (LDC) sont identifiés, par leurs propriétés magnétiques similaires à celles des niveaux DC et une concentration en carbonate plus faible (équivalente à celle du reste du sédiment). Le sédiment détritique charrié par la glace (IRD), caractérisé par un pourcentage accru de la fraction >125 microns et par une susceptibilité magnétique élevée, est associé à la plupart des couches DC et LDC. Les gros grains de magnétite associés aux niveaux DC et LDC sont bien triés et relativement constant à l'intérieur des niveaux ainsi que d'un niveau à l'autre. L'association de l'augmentation de la taille des grains de magnétite et de la teneur en carbonate détritique fin (couches DC) avec un changement notable de l'enregistrement sédimentaire (couches DC et LDC) exclut l'hypothèse que le charriage par la glace soit le mécanisme de dépôt principal. Par conséquent, les événements DC et LDC ont du être déposés à partir de particules en suspension liées aux activités turbiditiques du chenal mid-océanique du nord-ouest de l'océan Atlantique, le NAMOC. L'association des couches DC et IRD et l'apparente corrélation entre l'âge des couches DC et les niveaux Heinrich de l'Atlantique Nord indiquent que l'instabilité de la calotte glaciaire créant les niveaux DC est contemporaine de celle qui produit les nombreux niveaux d'Heinrich. Toutefois, plusieurs couches DC et LDC ne sont pas corrélables à des niveaux d'Heinrich. Ces données montrent donc une plus grande instabilité de la calotte glaciaire labradorienne pendant le dernier cycle glaciaire que les niveaux d'Heinrich ne le suggère.

Les trois carottes du bassin de la mer du Labrador, P-013, P-094 et HU90-013-012P (P-012) (lat. 58°55.35N, long. 47°07.01W, profondeur 2830m) provenant du talus groenlandais, enregistrent la paléointensité relative du champ magnétique terrestre durant le Quaternaire Supérieur. Les rapports d'hystérésis, les paramètres magnétiques et les mesures de rémanence à basse température indiquent que la magnétite à domaine pseudo-unique est le principal minéral magnétique dans les trois carottes. La corrélation entre les carottes est établie grâce aux données ^{14}C AMS, $\delta^{18}O$ et ^{13}C mais aussi par la présence des niveaux DC et LDC. À l'extérieur des intervalles correspondant à une période de déglaciation et des niveaux DC et LDC, les données de rémanence normalisée montre une forte corrélation pour plusieurs normalisations (k , k_{ARM} et SIRM) apportant ainsi des enregistrements de paléointensité très utiles. Une bonne corrélation est obtenue entre les carottes si l'on utilise uniquement les couches DC et LDC comme des points clés. Ceci suggère que la paléointensité relative peut être utilisée comme outil pour des corrélations régionales. Les enregistrements de paléointensité de la mer du Labrador contiennent plusieurs caractéristiques communes avec ceux de la Méditerranée et des océans Indien et Pacifique. Un enregistrement composé à partir des carottes P-013 et P-012 a un fort coefficient de corrélation avec un enregistrement composite de l'océan Indien et de la Méditerranée bien que la chronologie soit incompatible. La forte corrélation des paléointensités des mers Méditerranée et du Labrador et de l'océan Indien suggère que ces sédiments enregistrent des variations synchrones du champ dipolaire. Toutefois, le problème de la chronologie doit être résolu avant que la paléointensité puisse être utilisée comme outil de corrélation globale.

ACKNOWLEDGMENTS

I am very grateful for the scholarship support I received from the Chaire de recherche en Environnement. I would like to thank my supervisors; Jean-Claude Mareschal for his patience and support; Claude Hillaire-Marcel for his insight, understanding and advice; and Jim Channell for his help, encouragement and friendship. I would also like to thank Anne de Vernal and Dennis Kent for their input and ideas, while taking their time to be on my committee.

I am indebted to Atiur Rahman, Marit-Solveig Seidenkrantz and Guoping Wu for many discussions which greatly helped my understanding of Late Quaternary paleoceanography. To Sylvain Vallières and Isabelle Jacob for their friendship and help whenever or for whatever I asked. To Guy Bilodeau for always answering my sediment requests. To Christine Veiga-Pires for writing a better résumé than my original abstract. To Alice Chassagne for her always kind word and cheerful demeanor. To Céline Hallé-Polèse for being my mother away from home. And to the rest of the Gang du GEOTOP for the friendship and understanding especially toward my lack of French, I may never learn the language but have grown to love the culture.

Last but especially not least, I would like to thank my family. To my parents, Sally and Richard Stoner, for always being there whenever I needed them and never asking anything in return. To my brother Greg Stoner, for his support and friendship. To my Grandmother, "Grandma New York" Mae Leventhal, for her love and encouragement. And finally to Grandpa Eli, Elias Leventhal, unfortunately he is not here to see this day, but because of his love, kindness and encouragement it has finally arrived. I would like to thank all these people for without their help I would have never made it this far.

TABLE OF CONTENTS

ABSTRACT	ii
RÉSUMÉ	iv
ACKNOWLEDGMENTS	vi
TABLE OF CONTENTS	vii
LIST OF FIGURES	x
LIST OF TABLES	xviii
INTRODUCTION	1
REFERENCES	9
CHAPTER I	
HIGH RESOLUTION ROCK MAGNETIC STUDY OF A LATE PLEISTOCENE CORE FROM THE LABRADOR SEA	15
1.1 INTRODUCTION	16
1.2 LOCATION, LITHOLOGY AND CHRONOLOGY	17
1.2.1 Location and Sedimentary Environment	18
1.2.2 Lithology of Core HU90-013-013.....	19
1.2.3 Stratigraphy of Core HU90-013-013.....	21
1.3 METHODS.....	22
1.3.1 Sampling	22
1.3.2 Magnetic Measurements.....	24
1.4 RESULTS.....	25
1.4.1 Down-core Variation of Concentration Dependent Parameters	25
1.4.2 Concentration-Independent rock magnetic Parameters	28
1.5 DISCUSSION.....	32

1.5.1 Intervals of Increased Magnetic Concentration and Grain-size	32
1.5.2 High-coercivity Interval	35
1.6 CONCLUSIONS.....	37
REFERENCES.....	39

CHAPTER II

MAGNETIC PROPERTIES OF DEEP-SEA SEDIMENTS OFF SOUTHWEST GREENLAND: EVIDENCE FOR MAJOR DIFFERENCES BETWEEN THE LAST TWO DEGLACIATIONS	44
2.1 INTRODUCTION	45
2.2 TERMINATION I.....	47
2.3 TERMINATION II.....	51
2.4 DISCUSSION	53
REFERENCES.....	56

CHAPTER III

THE MAGNETIC SIGNATURE OF RAPIDLY DEPOSITED DETRITAL LAYERS FROM THE DEEP LABRADOR SEA: RELATIONSHIP TO NORTH ATLANTIC HEINRICH LAYERS.....	58
3.1 INTRODUCTION	59
3.2 MAGNETIC METHODS	63
3.2.1 Bulk Magnetic Parameters	63
3.2.2 Hysteresis Parameters	65
3.2.3 Low Temperature Remanence	65
3.3 CORE CHARACTERISTICS	66
3.4 MAGNETIC CHARACTERISTICS OF DC AND LDC LAYERS.....	67
3.4.2 Bulk Magnetic Parameters	67
3.4.3 Hysteresis Parameters	74
3.4.4 Low Temperature Remanence	77

3.5 DEPOSITIONAL MECHANISM OF DC AND LDC LAYERS	80
3.4 CHRONOLOGY AND CORRELATION.....	87
3.7 CONCLUSIONS.....	92
REFERENCES.....	94
 CHAPTER IV	
 LATE PLEISTOCENE RELATIVE GEOMAGNETIC FIELD PALEOINTENSITY FROM DEEP LABRADOR SEA SEDIMENTS: REGIONAL AND GLOBAL CORRELATION.....	
4.1 INTRODUCTION	99
4.2 CORE DESCRIPTIONS	100
4.3 ROCK MAGNETIC PROPERTIES	103
4.3.1 Mineralogy	103
4.3.2 Concentration	107
4.3.3 Grain-size	107
4.4 NATURAL REMANENT MAGNETIZATION.....	114
4.5 NORMALIZED REMANENCE.....	114
4.6 RELATIVE PALEOINTENSITY RECORD.....	118
4.7 CHRONOLOGY	123
4.7.1 Chronology of the Labrador Sea Paleointensity Records.....	123
4.8 GLOBAL CORRELATION.....	127
4.8 CONCLUSIONS.....	130
REFERENCES.....	132
 GENERAL CONCLUSIONS.....	 136
REFERENCES.....	139
 APPENDICES	 140

LIST OF FIGURES

CHAPTER I

- Figure 1.1. Site location map. HU90-013-013 is the piston core studied..... 18
- Figure 1.2.. Generalized lithologic section indicating sediment color, lithology, structural features (P. Ferland, personal communication, 1990) and tephra layers (H. Hafliðason, personal communication, 1992), with plots of percent CaCO_3 , mean grain-size $< 160 \mu\text{m}$, the weight percent of the carbonate-free sediment fraction $> 125 \mu\text{m}$, and $\delta^{18}\text{O}$ (‰) vs. depth (cm bs) (Hillaire-Marcel et al., 1994a). Colors are given according to the Munsell soil color charts. bs, below sediment surface. 20
- Figure 1.3. Concentration-dependent rock magnetic parameters k , SIRM, k_{ARM} , HIRM_{0.1} and HIRM_{0.3} versus depth (cm bs), compared with percent CaCO_3 and $\delta^{18}\text{O}$ (‰) vs. depth (cm bs) (Hillaire-Marcel et al., 1994a). Each point represents an average value for approximately 2.5 cm of core. Curve fit is achieved by using the locally weighted least squares method with a 2% weighting function. bs, below sediment surface..... 26
- Figure 1.4. Accumulation rate curve for k vs. depth (cm bs) compared with CaCO_3 , and $\delta^{18}\text{O}$ (‰) versus depth. For the magnetic parameters each point represents an average value for approximately 2.5 cm of core. bs, below sediment surface. 27
- Figure 1.5. Concentration-independent rock magnetic parameters $S_{-0.1}$, $S_{-0.3}$, k_{ARM}/k , $\text{SIRM}/k_{\text{ARM}}$, SIRM/K , and K_f vs. depth (cm bs), compared with percent CaCO_3 and $\delta^{18}\text{O}$ (‰) versus depth (cm bs). Each point represents an average value for approximately 2.5 cm of core. Curve fit is achieved by using the locally weighted least squares method with a 2% weighting function. bs, below sediment surface. 30

CHAPTER II

Figure 2.1. Location map, showing site of piston core HU90-013-013 (P-013).....46

Figure 2.2. Hysteresis ratios of 187 samples from upper 500 cm and from 1200 to 1600 cm open circles from background sediment (outside shaded intervals in Fig. 2.3 and Fig. 2.4). M_r saturation remanence; M_s saturation magnetization; H_{cr} remanent coercivity; H_c coercive force. Single-domain (SD), pseudo-single-domain (PSD), and multidomain (MD) fields after Day et al. (1977).48

Figure 2.3. A: Magnetic grain-size dependent parameter k_{ARM}/k (solid circles) (increased magnetic grain size indicated by smaller values) compared with planktonic $\delta^{18}O$ record from *N. pachyderma* (left coiled) (open circles) for upper 500 cm of P-013. shaded area delineates interval of increased magnetite concentration and grain size interpreted as continental-meltwater-derived detrital flux from southern Greenland; vertical line at 440 cm marks isotopic stage 2/1 boundary. YD = Younger Dryas, H₁ = Heinrich event 1, ME₁ = magnetic event attributed to the beginning of deglaciation prior to Termination I. B: Diagram of k_{ARM}/k (solid circles) compared with corrected (-400 yr for reservoir effect) atomic mass spectroscopy ^{14}C date. C. Diagrams of k_{ARM}/k (solid circles) compared with the magnetic concentration dependent parameter k (open circles). D: k_{ARM}/k (solid circles) compared with percent carbonate (CO_3) (X's), mean grain size (G.S.; in μm) for the < 160 μm fraction (open circles), and percent coarse fraction >125 μm (solid triangles).....50

Figure 2.4. A: Magnetic grain-size dependent parameter k_{ARM}/k (solid circles) (increased magnetic grain-size indicated by smaller values) compared with planktonic $\delta^{18}O$ record from *N. pachyderma* (left coiled) (open circles) for interval from 1200 to 1600 cm of P-013. Shaded area delineates interval of increased magnetite concentration and grain size interpreted as continental-meltwater derived detrital flux from southern Greenland, vertical lines at 1250 and 1440 cm mark isotopic substage 5e/d and stage 6/5 boundaries, respectively. ME₂ = magnetic event attributed to the beginning of deglaciation prior to Termination II. B: Diagram

of k_{ARM}/k (solid circles) compared with magnetic concentration dependent parameter k (open circles). C: Diagram of k_{ARM}/k (solid circles) compared with percent carbonate (X's), mean grain size (G.S.) for the $<160 \mu\text{m}$ grain-size fraction (open circles), and the percent coarse fraction $>125 \mu\text{m}$ (solid triangles). Note: large carbonate spike at 1390 cm is of detrital origin.....52

CHAPTER III

- Figure 3.1. Map of the North Atlantic showing the core locations. References: P-094 and P-013, this study; NOAMP cores, Heinrich, 1988; DSDP site 609, (Broecker et al. 1991; Bond et al. 1992a,b; 1993), SU-9008 (Grousset et al. 1993); 75-55 and 87-009, (Andrews and Tedesco, 1992; Andrews et al. 1993;1994a,b); CHN82-20, (Keigwin and Lehman, 1994). Bathymetric chart of the Labrador Sea modified after Chough et al. (1987). NAMOC: Northwest Atlantic Mid-Ocean Channel; IMOC: Imarssuak Mid-Ocean Channel; Contours in meters.....61
- Figure 3.2. From piston core P-094 generalized lithologic column from onboard core description (A. de Vernal, per comm. 1992), compared with weight percent of carbonate and coarse fraction greater than $125 \mu\text{m}$, the planktonic $\delta^{18}\text{O}$ (‰) and AMS ^{14}C stratigraphy derived from *Neogloboquadrina pachyderma* (L) versus depth (cm) (Hillaire-Marcel et al., 1994a). Shaded areas indicate intervals of visually identified lithologic change.62
- Figure 3.3. Down core profile (P-094) of concentration dependent rock magnetic parameters k , k_{ARM} and SIRM. Shaded areas indicate intervals of visually identified lithologic change.68
- Figure 3.4. Down core profile (P-094) of coercivity dependent rock magnetic ratios $S_{-0.1}$, $S_{-0.3}$, and concentration high coercivity component parameters HIRM $_{-0.1}$ and HIRM $_{-0.3}$. Shaded areas indicate intervals of visually identified lithologic change.....69

- Figure 3.5. Down core profile (P-094) of magnetic grain-size sensitive ratios k_{ARM}/k , $SIRM/k$ and $SIRM/k_{ARM}$. Shaded areas indicate intervals of visually identified lithologic change.....70
- Figure 3.6. Down core profile (P-094) of carbonate (%) data (Hillaire-Marcel et al. 1994a,b) compared with linear interpolation used to calculate carbonate(%) data at the same resolution as the magnetic data.....72
- Figure 3.7. Down core profile (P-094) of concentration dependent rock magnetic parameters k , k_{ARM} and SIRM plotted on a carbonate free basis. Shaded areas indicate intervals of visually identified lithologic change.73
- Figure 3.8. Hysteresis loops of selected samples from P-094.75
- Figure 3.9. Top: Hysteresis parameters for all (316) samples from piston core P-094. M_{rs} , saturation remanence; M_s , saturation magnetization; H_{cr} , remanent coercivity; H_c , coercive force. a. Single domain (SD), pseudo-single domain (PSD), and multidomain (MD) fields after Day et al.(1977). Base: Logarithmic plot of hysteresis parameters with best fitting line plotted as solid line. The results of Parry (1980, 1982) for synthetic samples are shown for reference: broken line a, SD + MD mixtures; broken line b, PSD +MD mixtures; and broken line c, single size magnetite.....76
- Figure 3.10. Down core profile (P-094) of hysteresis parameters M_{rs}/M_s , H_{cr}/H_c , H_{cr} and H_c . Shaded areas indicate intervals of visually identified lithologic change.....78
- Figure 3.11. Normalized isothermal remanence curves of selected samples during warming from 10 K to 160 K. Isothermal remanence acquired in 500 mT field at 10 K.....79
- Figure 3.12. Bivalent plots of mean values of hysteresis parameters M_{rs}/M_s , H_c , and H_{cr}/H_c plotted against mean values of rock magnetic parameter k_{ARM}/k , for individual layers within P-094. Standard error of the mean for each layer shown

on left, labels shown on right.	81
Figure 3.13. Hysteresis parameters of mean values from individual layers within P-094. Psuedo-single domain (PSD), and multidomain (MD) fields after Day et al. (1977). Top: Labels shown. Base: Standard error of the mean for each layer	82
Figure 3.14. High resolution lithologic parameters coarse fraction (>125 μm) and Carbonate (%) compared with magnetic parameters k_{ARM}/k , $H_{\text{cr}}/H_{\text{c}}$, K , $K\text{-CO}_3$, SIRM and $S_{0.3}$ for the interval from 150-350 cm from piston core P-094. Shaded areas indicate intervals of visually identified lithologic change; solid horizontal line indicates sharp sedimentary contact; black bars indicate AMS ^{14}C dated intervals, with dates to the right (Hillaire-Marcel et al., 1994a,b)	83
Figure 3.15. Down core plot from Greenland rise piston core P-013 of lithologic parameters coarse fraction >125 μm and CO_3 (%) compared with hysteresis ratio $H_{\text{cr}}/H_{\text{c}}$. DC = detrital carbonate layers. LDC = possible low detrital carbonate layer.	86
CHAPTER 4	
Figure 4.1. Map of the Labrador Sea showing the location of core sites used in this study. P-012 = piston core HU90-013-012; P-013 = HU90-013-013; P-094 = piston core Hu91-045-094.....	101
Figure 4.2. The S-0.3 ratio versus depth for Labrador Sea piston cores . a.) P-013. b.) P-012. c.) P-094.	104
Figure 4.3. IRM aquisition curves of selected samples for Labrador Sea piston cores. a.) P-013. b.) P-012. c.) P-094.....	105
Figure 4.4. Normalized isothermal remanence curves for selected samples during warming from 10 K to 160 K. IRM acquired in 500 mT field at 10 K. a.) P-013. b.) P-094.	106

- Figure 4.5. Down core profiles of concentration dependent rock magnetic parameters NRM_{20mT}, k , k_{ARM} and SIRM. a.) P-013. b.) P-012. c.) P-094..... 108
- Figure 4.6. Bivariant plot of k_{ARM} versus k (King et al., 1992), both before (left) and after (right) removal of intervals associated with rapid deposition. a.) P-013. b.) P-012. c.) P-094..... 112
- Figure 4.7. Hysteresis parameters both before (left) and after (right) removal of intervals associated with rapid deposition. a.) P-013. b.) P-094. M_{rs} , saturation remanence; M_{s} , saturation magnetization; H_{cr} , remanent coercivity; H_{c} , coercive force. Single domain (SD), psuedo-single domain (PSD), and multidomain (MD) fields after Day et al.(1977). 113
- Figure 4.8. Orthogonal vector projections of alternating field demagnetization for samples from piston cores P-012. The declinations have not been corrected for core orientation. The solid (open) symbols represent the projection of the magnetic vector onto the horizontal (vertical) plane..... 115
- Figure 4.9. Comparisons of normalized remanence, using different normalizing parameters (k , SIRM, k_{ARM}) after removal of intervals associated with rapid deposition. a.) P-013. b.) P-012. c.) P-094 116
- Figure 4.10. Normalized remanence versus the normalizing parameter (k , SIRM, k_{ARM}) after removal of intervals associated with rapid deposition. a.) P-013. b.) P-012. c.) P-094 117
- Figure 4.11. From the 400 to 1800 cm interval of P-013, the normalized remanence (NRM_{20mT}/(SIRM, k_{ARM} , and k)) compared with the planktonic $\delta^{18}\text{O}$ (‰) and AMS ^{14}C stratigraphy derived from *Neogloboquadrina pachyderma* (L) versus depth (cm) (Hillaire-Marcel et al., 1994). Shaded areas indicate intervals of rapid sedimentation and lithologic events. DC= detrital carbonate event and LDC =low detrital carbonate event as defined by Stoner et al. (in press) 119

- Figure 4.12. From piston core P-012, the normalized remanence (NRM_{20mT}/(SIRM, k_{ARM} , and k)) compared with the planktonic $\delta^{18}O$ (‰) stratigraphy derived from *Neogloboquadrina pachyderma* (L) versus depth (cm) (Hillaire-Marcel et al., 1994). Shaded areas indicate intervals associated with lithologic events. DC= detrital carbonate event and LDC =low detrital carbonate event as defined by Stoner et al., (in press)..... 120
- Figure 4.13. From the 500 to 1100 cm interval of piston core P-094, the normalized remanence (NRM_{20mT}/(SIRM, k_{ARM} , and k)) compared with the planktonic $\delta^{18}O$ (‰) and AMS ^{14}C stratigraphy derived from *Neogloboquadrina pachyderma* (L) versus depth (cm) (Hillaire-Marcel et al., 1994). Shaded areas indicate intervals associated with lithologic events. DC= detrital carbonate event and LDC =low detrital carbonate event as defined by Stoner et al., (in press) 121
- Figure 4.14. Normalized remanence plotted versus common arbitrary depth scale. Correlation of records using only tie points from detrital layers (DC1,2, 4,5,6,7 and LDC 5/6) as defined by Hillaire-Marcel et al. (1994) and Stoner et al.(in press). a.) NRM_{20mT}/ k_{ARM} versus arbitrary depth for P-013, P-012, and P-094. b.) NRM_{20mT}/SIRM versus arbitrary depth for P-013, P-012, and P-094..... 122
- Figure 4.15. Normalized remanence plotted versus common arbitrary depth scale. Correlation of records based on tie points from detrital layers (DC1,2, 4,5,6,7 and LDC 5/6) as defined by Hillaire-Marcel et al. (1994) and Stoner et al. (in press) and visual peak matching. a.) NRM_{20mT}/ k_{ARM} versus arbitrary depth for P-013, P-012, and P-094. b.) NRM_{20mT}/SIRM versus arbitrary depth for P-013, P-012, and P-094 124
- Figure 4.16. Age depth profile for P-013, P-012 and P-094..... 125
- Figure 4.17. a.) The Labrador Sea relative paleointensity stack from P-013 and P-012 (dashed line) versus Labrador Sea age model derived from AMS ^{14}C dates, and isotopic stage determinations. Also plotted on the same scale, the Mediterranean,

Indian Ocean paleointensity stack (solid line) (Meynadier et al., 1992; Tric et al., 1992) versus the bulk sediment $\delta^{18}\text{O}$ derived age model of Shackelton et al., (1993) (Indian Ocean) and $\delta^{18}\text{O}$, tephrochronology derived age model of Paterne et al., (1986) (Mediterranean). No correction was made for the difference between ^{14}C and calendar years. b.) Tuned record showing strong correlation when placed on common Mediterranean, Indian Ocean time scale.. c.) Tuned record showing strong correlation when placed on common Labrador Sea time scale. 128

APPENDICES

Figure A.1. Paleomagnetic remanence data after 20 mT AF demagnetization for core HU90-013-013 (P-013). a.) Magnetic intensity shown with isotopic stage determinations (Hillaire-Marcel et al., 1994). b.) Magnetic inclination with solid horizontal line indicating expected geocentric axial dipole inclination for this site. c.) Magnetic declination. Dashed vertical lines indicate piston core section breaks 144

Figure A.2. Paleomagnetic remanence data after 20 mT AF demagnetization for core HU90-013-012 (P-012). a.) Magnetic intensity shown with isotopic stage determinations (Hillaire-Marcel et al., 1994). b.) Magnetic inclination with the solid horizontal line indicating expected geocentric axial dipole inclination for this site. c.) Magnetic declination. Dashed vertical lines indicate piston core section breaks. 145

Figure A.3. Paleomagnetic remanence data after 20 mT AF demagnetization for core HU91-045-094 (P-094). a.) Magnetic intensity shown with isotopic stage determinations (Hillaire-Marcel et al., 1994). b.) Magnetic inclination with solid horizontal line indicating expected geocentric axial dipole inclination for this site. c.) Magnetic declination. Dashed vertical lines indicate piston core section breaks. 146

LIST OF TABLES**CHAPTER I**

Table 1.1. Depth to age profile with intervening sedimentation rates.....	23
---	----

CHAPTER III

Table 3.1. Correlation of Labrador Sea detrital layers with North Atlantic Heinrich layers	88
---	----

APPENDICES

Table A.1. Generalized table of downcore magnetic parameters and their interpretations.....	141
--	-----

GENERAL INTRODUCTION

During the last few years, the record of climate change during the Late Quaternary has improved dramatically, pointing to a significantly more dynamic climate system than previously thought. Ice core evidence indicates that temperature and dustiness of the air over the Greenland ice cap underwent large and rapid changes on short time scales. The Younger Dryas (YD) is the best studied example of abrupt climate change (Broecker and Denton 1989; Broecker, et al., 1990; Lehman and Keigwin 1992; Alley et al., 1993). The short duration (~1,000 years) of the YD with abrupt cooling and reintroduction of glacial conditions in the midst of deglaciation cannot be tied to orbital cycles that have a period 20,000 years or more. The prevailing theory links the YD to oceanic thermohaline circulation and major changes in North Atlantic Deep Water (NADW) formation (Broecker, et al., 1990; Lehman and Keigwin 1992). Recent Greenland ice core data have yielded new constraints on the YD (Alley et al., 1993) suggesting that the transition from YD to the Preboreal deglacial period took place in less than 10 years. A similar change is also noted for the transition from the Oldest Dryas to Bolling/Allerod warm period.

Abrupt transitions between cold and warm epochs also appear to be a common feature of the last glacial cycle. The Dansgaard-Oeschger interstadial events, recently identified in

the Greenland Summit ice core (Johnsen et al., 1992), lasted between 500 and 2,000 years and appear to be characterized by rapid oscillations in atmospheric circulation (Taylor et al. 1993a). These changes have also been attributed to a turning on and off of heat released to the atmosphere over the northern Atlantic by thermohaline circulation (Broecker et al., 1990, Bond et al., 1993a). Broecker et al. (1990) proposed that changes in North Atlantic water's salinity due to growth and decay of the ice sheets switched on and off the thermohaline circulation, although variations in the hydrologic cycle may also play a role (Duplessy et. al., 1992). For the last interglacial (isotope sub-stage 5e), even larger instabilities in the climate system have been interpreted from the Summit ice core (Dansgaard et al., 1993, GRIP, 1993). However, the validity of this interpretation of the ice core record is still being debated (Grootes et al., 1993; Taylor et al., 1993b, Charles et al., 1994). Such instabilities during a period with less continental ice than the present would support the hydrologic cycle hypothesis (Duplessy et. al., 1992; Weaver and Hughes 1994). If large shifts in climate occurred during the last interglacial they should be observed in other climate indicators. European lake (Thouveny et al., 1994; Field et al., 1994) and shallow marine (M-S. Seidenkrantz per. comm.) records suggest that these climatic changes did occur, but have presently not been corroborated by deep sea records (Keigwin et al., 1994; McManus et al., 1994).

Recent evidence has also complicated the understanding of how climate is controlled by Milankovitch cycles. The increased quality of terrestrial and marine records has cast doubt about the timing of the 6/5 glacial-interglacial transition and the response of climate to orbital forcing. The coral record indicates that sea level was as high as present about 132,000 yr BP (Stein et al., 1993; Gallup, et al., 1994). This is significantly earlier than the 125,000 yr BP indicated by the SPECMAP time-scale (Martinson et al, 1987). Yet, as new evidence suggests that the SPECMAP time-scale will have to be adjusted (Winowgrad et al.,

1992, Dansgaard et al., 1993; Jouzel et al., 1993, Stein et al., 1993; Gallup, et al., 1994; Lambeck and Nakada, 1992), little is known about the timing of events associated with the 6/5 transition. The lack of absolute age control and environmentally independent stratigraphic methods in deep sea records has precluded high resolution correlations so important for spatial and temporal reconstructions. Therefore, Termination II, generally characterized in the marine record by a fairly sudden and simple $\delta^{18}\text{O}$ decrease (e.g., Broecker and van Donk, 1970; Martinson et al., 1987), has not been adequately studied.

Only the most recent climatic oscillation of millennial duration (Allerod-Younger Dryas) has been fully documented outside Greenland. During the last glacial period, the Dansgaard-Oeschger warming events recognized in the Greenland ice core record as lasting longer than 2,000 years, have been correlated to warming events in the Antarctic (Vostok) ice core (Bender et al., 1994). Evidence for millennial scale climatic events has been found in the oceanic sedimentary record as brief but massive discharge of icebergs into the North Atlantic (Heinrich, 1988). Initial correlation of the Greenland ice core record with the marine sediment record suggests that following each of the iceberg discharge events, sea and air temperatures both rose sharply, marking the start of another cycle (Bond et al., 1993a). The YD may be related to one of these events (Bond et al., 1993b; Hillaire-Marcel et al., 1994). During the last glacial, at least six distinct layers of increased lithic to planktic concentration known as Heinrich events, appear to occur synchronously across the North Atlantic from the Labrador Sea to Portugal (Andrews and Tedesco, 1992; Bond et al., 1992; Broecker et al., 1992; Hillaire-Marcel et al., 1994). Heinrich events, are thought to be a result of quasi-periodic ice rafted deposition (IRD) due to massive discharge of icebergs from the Laurentide ice sheet (Heinrich 1988; Bond et al., 1992). At present these events are poorly understood with questions surrounding the number of events, depositional mechanisms, source area as well as their cause and climatic significance. A binge-purge model has been proposed to

explain the origin of Heinrich events as Laurentide ice sheet glacial surges (MacAyeal, 1993). There is some evidence that other ice sheets might also be involved (Grousset et al., 1993, Bond et al., 1993b) pointing to a climatic rather than internal ice sheet control. The apparent correlation of Heinrich events to climatic variations observed in a Florida lake (Grimm et al., 1993) suggests that these ice sheet/ocean interactions may have global climatic significance.

The Labrador Sea provides a unique link between ice sheets and open ocean, being the subarctic basin that was most directly influenced by continental ice sheets. Their control on sedimentation is shown by the accumulation of up to 500 m of Pleistocene clastic sediments in the central Labrador Basin (Hesse et al., 1987). This transitional basin also received large amounts of meltwater directly (de Vernal and Hillaire-Marcel 1987; Hillaire-Marcel and de Vernal 1989), or from ice surges such as the Heinrich events (Andrews and Tedesco, 1992; Bond et al., 1992; Broecker et al., 1992; Hillaire-Marcel et al., 1994), or from calving due to destabilization of the ice margins (Ruddiman and McIntyre, 1981). These meltwater fluctuations strongly affected sedimentation (Fillon et al., 1981; Fillon, 1985; Piper et al., 1990; Hillaire-Marcel et al., 1994). Sedimentation in this basin was also affected by ice advances triggering turbidite flow down the Northwest Atlantic Mid-Ocean Channel (NAMOC) (Chough et al., 1987; Hesse et al., 1987). The NAMOC, the main "basin-draining" channel of the Labrador Sea, is over 3800 km long and 100 to 200 m deep. It is one of the largest deep sea channels known (Hesse, 1989). The control of ice sheets on NAMOC activity is shown by the cessation of turbidite flow down this conduit at ca. 7.1 ka (Hesse et al., 1987).

The Laurentide ice sheet was by far the dominant source of terrigenous material to the Labrador Sea. The asymmetry of the Labrador Basin fill, with an over supplied Labrador margin and a starved Greenland margin, suggests that the Greenland ice sheet was more stable than the Laurentide ice sheet (Hesse et al., 1990) It is likely that sedimentation

observed from deep Labrador Sea cores provide a record of the past variations of these ice sheets. Changes in the sedimentation pattern during the last climatic cycle are expected to contain high frequency variations related to the influence of the Laurentide ice sheet, and longer period variations from the Greenland ice sheet. If Heinrich events in the North Atlantic are associated with Laurentide ice sheet instability, a detailed record should be preserved in Labrador Sea sediments. Therefore, the sedimentation in the Labrador Sea might not only provide a record of the response of the ice sheets to orbital forcing, but also of millennial scale events whose importance for the climate system begins to be recognized.

Rock magnetic measurements provide a high speed, high resolution, highly sensitive, non-destructive, quantitative record of lithologic variations. Previous magnetic studies from Late Pleistocene cores have been correlated to paleoclimatic and paleoceanographic conditions (Kent, 1982; Robinson 1986, 1990; Bloemendal 1983; Bloemendal et al., 1988, 1992, 1993; Doh et al., 1988; Bloemendal and de Menocal 1989; Hall et al., 1989a, b). Composition, concentration and grain-size of the magnetic material have been shown to vary from glacial to interglacial times. These variations are explained by changes in the mechanism of transport of detrital magnetic material to the ocean basin (e.g., bottom currents, fluvial, eolian activity, and ice rafting) and dilution by biogenic material (e.g. carbonate, silica). Therefore, magnetic parameters can be used to assess paleoenvironmental change (see Table A.1). Magnetic methods have also been used for rapid characterization of diagenetic variations associated with reducing conditions (Karlin and Levi, 1983, 1985, Bloemendal et al., 1989; Channell and Hawthorne, 1990; Leslie et al., 1990 a, b; Karlin, 1990 a, b; Robinson, 1990; Bloemendal et al., 1993) They are also effective in identifying relict oxic zones in non steady-state diagenetic environments (Karlin, 1990b). Because of the large number and confusing nature of magnetic parameters, a table is included in the Appendix (Table A.1).

Paleomagnetic measurements provide one of the only direct records of past geophysical conditions. Fluctuations of the Earth's magnetic field have been widely used for correlation. Magnetostratigraphy has been used to develop a time scale for the last 200 m.y. relying primarily on the sequence of magnetic polarity reversals in marine and terrestrial records. For much shorter time intervals (< 100 kyr), variations in secular variation records have been used for correlation with good success in lake sediments, however the records from marine sediments are not as convincing. Secular variations generally do not exceed a few tens of degrees, therefore sampling and measurement techniques as well as sedimentary disturbances are particularly critical. Because the dynamic sedimentary environment of the Labrador Sea could perturb the directional data and the lack of high quality records to which this data could be compared, it was decided that this area of research would be given low priority (the directional data is included in the Appendix as Figures A.1, A.2, and A.3). However, several recent studies have suggested that marine sediments may preserve a record of geomagnetic field intensity (i.e. dipole field paleointensity) (Kent and Opdyke, 1977; Tauxe and Wu, 1990; Meynadier et al., 1992; Tric et al., 1992; Valet and Meynadier, 1993; Schneider, 1994; Tauxe and Shackleton, 1994; Yamazaki and Ioka, 1994). Therefore, it was decided to focus on the intensity component of the magnetic vector in hope that a record could be extracted from high sedimentation rate Labrador Sea cores.

The detailed magnetic study of sediments from the deep Labrador Sea was part of a larger study including isotopic, geochemical, lithologic and paleontological analyses, in order to characterize the climatic and environmental changes within the Labrador Sea during the last climate cycle. The objective of the magnetic study was: (1) to characterize the sediment by magnetic properties; (2) to interpret this record in terms of ice sheet activity and (3) determine if sediment from this basin reliably recorded intensity variations of the geomagnetic field.

This thesis is a compilation of four articles: two published and two in press. The articles concern high resolution magnetic studies of three Late Quaternary piston cores from the Labrador Sea. The first article, "High-resolution rock magnetic study of a Late Pleistocene core from the Labrador Sea" published in *Canadian Journal of Earth Sciences*, deals with the high resolution rock magnetic study of piston core HU90-013-013 (P-013) (Stoner et al., 1994). This work defines the magnetic mineralogy of this core and presents a model explaining several features of the rock magnetic parameters. The second article, "Magnetic properties of deep-sea sediments off southwest Greenland: Evidence for major differences between the last two deglaciations" published in *Geology*, is a detailed study of the changes in magnetic properties at Termination I and Termination II (Stoner et al., 1995). The magnetic data are combined with oxygen isotope, AMS ^{14}C and lithologic data. The marine record can be correlated to the stages of glacial retreat recognized for the Greenland ice sheet. Although the records for the two terminations have similarities, the timing of glacial retreat appears to have been very different for the two terminations. The third article, "The magnetic signature of rapidly deposited detrital layers from the deep Labrador Sea: Relationship to North Atlantic Heinrich layers" to be published in *Paleoceanography* concerns the magnetic properties of piston core HU91-045-094 (P-094) from the Labrador Rise (Stoner et al., in press a). This paper uses high resolution bulk magnetic, hysteresis and low temperature remanence measurements to examine the sedimentary environment and depositional mechanism associated with distinct rapidly deposited detrital layers. These layers are extremely well defined by the magnetic parameters. This record is correlated with the Heinrich layer stratigraphy from the northern Labrador Sea and the North Atlantic. The magnetic record from P-094 is compared with the magnetic record from P-013 to look at the basinal variation associated with these layers.

The fourth and final article, "Late Pleistocene relative geomagnetic field paleointensity from deep Labrador Sea sediments: Regional and global correlation" to be published in *Earth and Planetary Science Letters*, shows that although sedimentation within the Labrador Sea was very dynamic, the sediments yield reproducible relative paleointensity records (Stoner et al., in press b). Rapidly deposited detrital layers, recognized by their lithologic, geochemical and magnetic characteristics, can be removed from the record for the purposes of constructing relative paleointensities. These detrital layers, although not used in the paleointensity records, provide a means of correlation among the three cores. The chronology of the record from the Labrador Sea appears inconsistent with that of records from the Mediterranean and Indian Ocean. However, after adjustment of the chronology the records are strongly correlated. The high degree of reproducibility in the Labrador Sea paleointensity records, and the correlation of the Labrador Sea records with those from the Indian Ocean and Mediterranean Sea, lead us to conclude that the paleointensity records from the Labrador Sea are indicative of dipole geomagnetic relative paleointensity and therefore useful for high resolution global correlation. Although the paleointensity variations from the Labrador Sea are consistent with those from outside the region, the chronology of the records are inconsistent. The chronologic discrepancy within these records may indicate fundamental problems with correlation of AMS ^{14}C ages (used in the Labrador Sea) to the oxygen isotope (SPECMAP) time-scale used elsewhere.

REFERENCES

- Alley, R. B., Meese, D. A., Shuman, C. A., Gow, A. J., Taylor, K. C., Grootes, P. M., et al. 1993. Abrupt increase in Greenland snow accumulation at the end of the Younger Dryas event. *Nature*, **362**: 527-529.
- Andrews, J. T. and Tedesco, K. 1992. Detrital carbonate-rich sediments, northwest Labrador Sea: implications for ice-sheet dynamics and iceberg rafting Heinrich events in the North Atlantic. *Geology*, **20**: 1087-1090.
- Bender, M., Sowers, T., Dickson, M-L., Orchard, J., Grootes, P., Meyewski, P. A., and Meese, D. A., 1994. Climate correlations between Greenland and Antarctica during the past 100,000 years. *Nature*, **372**: 663-666.
- Bloemendal, J. 1983. Paleoenvironmental implications of the magnetic characteristics of sediments from DSDP Site 514, Southeast Argentine Basin, Initial Reports of the Deep Sea Drilling Project, **71**: 1097-1108.
- Bloemendal, J., Lamb, B., and King, J. W. 1988. Paleoenvironmental implications of rock-magnetic properties of Late Quaternary sediment cores from the eastern equatorial Atlantic. *Paleoceanography*, **3**: 61-87.
- Bloemendal J., King, J. W., Hall, F. R., and Doh, S.J. 1992. Rock magnetism of Late Neogene and Pleistocene deep-sea sediments: relationship to sediment source, diagenetic processes, and sediment lithology. *Journal of Geophysical Research*, **97**: 4361-4375.
- Bloemendal, J., King, J. W., Hunt, A. deMenocal, P. B., and Hayahida, A. Origin of the sedimentary magnetic record at ocean drilling program sites on the Owen Ridge, Western Arabian Sea. *Journal of Geophysical Research*, **98**: 4199-4219 (1993)
- Bloemendal J., and deMenocal, P. B. 1989. Evidence for a change in the periodicity of tropical climate cycles at 2.4 Myr from whole-core magnetic susceptibility measurements. *Nature*, **342**: 897-900.
- Bond, G., Heinrich, H., Broecker, W., Labeyrie, L., McManus, J., Andrews, J., Huon, s., Jantsschik, R., Clasen, S., Simet, C., Tedesco, K., Kias, M., Bonani, G., and Ivy, S. 1992. Evidence for massive discharges of icebergs into the North Atlantic ocean during the last glacial period. *Nature*, **360**: 245-249
- Bond, G., Broecker, W., Johnsen, S., McManus, J., Laberyie, L., Jouzel, J., and Bonani, G. 1993a. Correlations between climate records from North Atlantic sediments and Greenland ice. *Nature*, **365**: 143-147.
- Bond, G., Broecker, W., McManus, J. and Higgins, S., 1993b. The Younger Dryas: one more Heinrich event in the North Atlantic? *Transactions, American Geophysical Union*, **74**(43): 357

- Broecker, W. S., Bond, G., Klas, M., Bonani, B., and Wolfli, W. 1990. A Salt oscillator in the Glacial Atlantic? 1. the concept. *Paleoceanography* **5**: 469-477.
- Broecker, W.S., Bond, G., McManus, J., Klas, M., and Clarke, E. 1992. Origin of the Northern Atlantic's Heinrich events. *Climate Dynamics*, **6**: 265-273.
- Broecker, W., and Van Donk, J., 1970, Insolation changes, ice volumes, and ^{18}O record in deep sea cores: *Reviews of Geophysics*, **8**: 169-198.
- Broecker, W. S., and Denton, G. H. 1989. The role of ocean-atmosphere reorganizations in glacial cycles. *Geochimica et Cosmochimica Acta*, **53**: 2465-2501.
- Channell, J. E. T. and Hawthorne, T. 1990. Progressive dissolution of titanomagnetites at ODP Site 653 (Tyrrhenian Sea). *Earth and Planetary Science Letters*, **96**, 469-480.
- Charles, C. D., Rind, D., Jouzel, J., Koster, R. D., and Fairbank, R. G. 1994. Glacial-interglacial changes in moisture sources for Greenland: Influences on the ice core record of climate. *Science*, **263**: 508-511.
- Chough, S. K., Hesse, R., and Müller, J. 1987. The Northwest Atlantic Mid-Ocean Channel of the Labrador Sea. IV. Petrography and provenance of the sediments. *Canadian Journal of Earth Sciences*, **24**: 731-740.
- Dansgaard, W., Johnsen, S.J., Clausen, H.B., Dahl-Jensen, D. Gundestrup, N. S., Hammer, C.U., Hvidberg, C. S., Steffensen, J. P., Sveinbjornsdottir, A. E., Jouzel, J., and Bond, G. 1993. Evidence for general instability of past climate from a 250-kyr ice-core record. *Nature*, **364**. 218-220.
- de Vernal, A. and Hillaire-Marcel, C. 1987. Paleoenvironments along the eastern Laurentide Ice Sheet margin and timing of the last ice maximum and retreat. *Géographie physique et Quaternaire*, **41**: 265-277.
- Doh, S. J., King, J. W., and Leinen, M. 1988. A rock-magnetic study of Giant Piston Core LL44-GPC from the Central North Pacific and its paleoceanographic significance. *Paleoceanography*, **3**: 89-111.
- Duplessy, J-C, Labeyrie, L., Arnold, M., Paterne, M., Duprat, J. and van Weering, T. C. E., 1982. Changes in surface salinity of the North Atlantic Ocean during the last deglaciation. *Nature*, **358**: 485-488.
- Field, M. H., Huntley, B., and Müller, H. 1994. Eemian climate fluctuations observed in a European pollen record. *Nature*, **371**: 779-783.
- Fillon, R. H., Miller, G. H., and Andrews, J. T., 1981. Terrigenous sand in Labrador Sea hemipelagic sediments and paleoglacial events on Baffin Island over the last 100,000 years. *Boreas*, **10**: 107-124.
- Fillon, R. H., 1985, Northwest Labrador Sea stratigraphy, sand input and Paleoceanography during the last 160,000 years, *in* Andrews, J. T., ed.,

- Quaternary environments, eastern Canadian Arctic, Baffin Bay and western Greenland: Boston, Allen & Unwin, p. 211-247.
- Gallup, C. D., Edwards, R. L., and Johnson, R. G., 1994. The timing of high sea levels over the past 200,000 years: *Science*, **263**: 796-800.
- Grimm, E. C., Jacobson, G. L., Watts, W. A., Hansen, B. and Maasch, K. A. 1993. A 50,000-year record of climate oscillations from Florida and its temporal correlation with the Heinrich Events. *Science*, **261**: 198-200.
- GRIP members, 1993. Climate instability during the last interglacial period recorded in the GRIP ice core. *Nature*, **364**: 203-207
- Grootes, P. M., Stulver, M., White, J. W. C., Johnsen, S., and Jouzel, J. 1993. Comparison of oxygen isotope records from the GISP2 and GRIP Greenland ice cores. *Nature*, **366**: 552-554.
- Grousset, F., Labeyrie, L., Sinko, A., Cremer, M. Bond, G., Duprat, J. Cortijo, E. and Huon, S. 1993. Patterns of ice-rafted detritus in the glacial North Atlantic (40-65°N). *Paleoceanography*, **8**: 175-192
- Hall, F. R., Bloemendal, J., King, J. W. Arthur, M. A., and Aksu, A. E. 1989a. Middle to Late Quaternary sediment fluxes in the Labrador Sea, ODP Leg 105, Site 646: A synthesis of rock-magnetic, Oxygen isotopic, carbonate, and planktonic foraminiferal data B. et al, *Proceedings of the Ocean Drilling Program, Scientific Results*, **105**: 653-665.
- Hall, F. R., Busch, W. H., and King, J. W. 1989b. The relationship between variations in rock-magnetic properties and grain size of sediments from ODP hole 645C, *In* Srivastava, S. P., Arthur, M. and Clement, B. et al, *Proceedings of the Ocean Drilling Program, Scientific Results*, **105**: 837- 841.
- Heinrich, H. 1988. Origin and consequences of cyclic ice rafting in the northeast Atlantic Ocean during the past 130 000 years. *Quaternary Research*, **29**: 143-152
- Hesse, R. 1989. "Drainage systems" associated with mid-ocean channels and submarine yazoos: Alternative to submarine fan depositional systems. *Geology*, **17**: 1148-1151.
- Hesse, R., Chough, S. K., and Rakofsky, A. 1987. The Northwest Atlantic Mid-Ocean Channel of the Labrador Sea. V. Sedimentology of a giant deep-sea channel. *Canadian Journal of Earth Sciences*, **24**: 1595-1624
- Hesse, R., Rakofsky, A., and Chough, S. K., 1990. The central Labrador Sea: facies and dispersal patterns of clastic sediments in a small ocean basin. *Marine and Petroleum Geology*, **7**: 13-28.
- Hillaire-Marcel, C., and de Vernal, A. 1989. Isotopic and palynological records of the Late Pleistocene in Eastern Canada and adjacent ocean basins. *Géographie Physique et Quaternaire*, **43**: 263-290.

- Hillaire-Marcel, C., de Vernal, A., Bilodeau, G. and Wu, G. 1993a. Isotope stratigraphy, sedimentation rates, deep circulation and carbonate events in the Labrador Sea during the last ~ 200 ka. *Canadian Journal of Earth Sciences*, **31**: 63-89.
- Johnsen, S. K., Clausen, H. B., Dansgaard, W., Fuhrer, K., Gundestrup, N., Hammer, C. U., Iverson, P., Jouzel, J., Stauffer, B. and Steffensen, J. P. 1992. Irregular glacial interstadials recorded in a new Greenland ice core. *Nature*, **359**: 311-313.
- Jouzel, J., Barkov, N. I., Barnola, J. M., Bender, M., Chappellaz, J., Genthon, C., Kotlyakov, V. M., Lipenkov, V., Lorius, C., Petit, J. R., Raynaud, D., Raisbeck, G., Ritz, C., Sowers, T., Stievenard, M., Yiou, F., and Yiou, P., 1993. Extending the Vostok ice core record of paleoclimate to the penultimate glacial period. *Nature* **364**: 407-412.
- Karlin, R. and Levi, S. 1983. Diagenesis of magnetic minerals in recent hemipelagic sediments. *Nature* **303**: 327-330.
- Karlin, R. and Levi, S. 1985. Geochemical and sedimentological control on the magnetic properties of hemipelagic sediments. *Journal of Geophysical Research*, **90**: 10,373-10,392.
- Karlin, R. 1990a. Magnetic diagenesis in marine sediments from the Oregon continental margin. *Journal of Geophysical Research*, **95**: 4405-4419.
- Karlin, R. 1990b. Magnetic mineral diagenesis in suboxic sediments at Bettis site W-N, NE Pacific Ocean. *Journal of Geophysical Research*, **95**: 4421-4436.
- Keigwin, L. D., Curry, W. B., Lehman, S. J., and Johnsen, S., 1994. The role of the deep ocean in North Atlantic climate change between 70 and 130 kyr ago. *Nature*, **371**: 323-326.
- Kent, D. V. 1982. Apparent correlation of paleomagnetic intensity and climatic records in deep-sea sediments. *Nature*, **299**: 538-539
- Kent, D. V., and Opdyke, N. 1977. Paleomagnetic field intensity and climatic records in deep-sea sediment core. *Nature*, **266**: 156-159.
- Lambeck, K., and Nakada, M., 1992. Constraints on the age and duration of the last interglacial period and on sea-level variations. *Nature* **357**: 125-128.
- Lehman, S. J., and Keigwin, L. D. 1992. Sudden changes in North Atlantic circulation during the last deglaciation. *Nature*, **356**: 757-762.
- Leslie, B. W., Hammond, D. E., Berelson, W. M and Lund, S. P. 1990a. Diagenesis in anoxic sediments from the California continental Borderland and its influence on iron, sulfur, and magnetite behavior. *Journal of Geophysical Research*, **95**: 4453-4470.
- Leslie, B. W., Lund, S. P and Hammond, D. E. 1990b Rock magnetic evidence for the dissolution and authigenic growth of magnetic minerals within anoxic marine

- sediments of the California continental borderland. *Journal of Geophysical Research*, **95**: 4437-4452.
- MacAyeal, D. R., 1993. Binge/purge oscillations of the Laurentide ice sheet as a cause of the North Atlantic's Heinrich events. *Paleoceanography*, **8**: 775-784.
- Martinson, D. G., Pisias, N. G., Hays, J. D., Imbrie, J., Moore, T. C. Jr. and Shackleton, N. J. 1987. Age dating and the orbital theory of the Ice Ages: development of a high-resolution 0 to 300,000-year chronostratigraphy. *Quaternary Research*, **27**: 1-29.
- McManus, J.F., Bond, G.C., Broecker, W.S., Johnsen, S., Labeyrie, L., and Higgins, S., 1994. High-resolution climate records from the North Atlantic during the last interglacial. *Nature*, **371**: 326-329.
- Meynadier, L., Valet, J.P., Weeks, R., Shackleton, N.J., and Hagee, V.L. 1992. Relative geomagnetic intensity of the field during the last 140 ka. *Earth and Planetary Science Letters*, **114**: 39-57.
- Piper, D. J. W., Mudie, P. J., Fader, G. B., Josenhans, H. W., MacLean, B., and Vilks, G., 1991. Quaternary geology. *In* *Geology of the continental margin of eastern Canada*. Edited by M. J. Keen, and G. L. Williams. Geological Survey of Canada, *Geology of Canada*, No 2, pp 475-607.
- Robinson, S. G. 1986. The Late Pleistocene paleoclimatic record of North Atlantic deep-sea sediments revealed by mineral-magnetic measurements. *Physics of the Earth Planetary Interiors*, **42**: 22-46.
- Robinson, S. G. 1990. Applications of whole-core magnetic susceptibility measurements of deep-sea sediments, *In* Duncan, R. A., Backman, J., Peterson, L. C. et al., *Proceedings of the Ocean Drilling Program, Scientific Results*, **115**: 737-771.
- Ruddiman W. F. and McIntyre A., 1981. The North Atlantic Ocean during the last deglaciation. *Palaeogeography, Palaeoclimatology, Palaeoecology*, **35**: 145-214.
- Schneider, D.A., 1994. An estimate of late Pleistocene geomagnetic intensity variation from Sulu Sea sediments. *Earth and Planetary Science Letters*, **120**:301-310.
- Seidenkrantz, M.-S., 1993. Benthic foraminiferal and stable isotope evidence for a "Younger Dryas-style" cold spell at the Saalian-Eemian transition, Denmark, *Palaeogeography, Palaeoclimatology, Palaeoecology*, **102**: 103-120.
- Stein, M., Wasserburg, G. J., Aharon, P., Chen, J. H., Zhu, Z. R. Bloom, A., and Chappell, J., 1993. TIMS U-series dating and stable isotopes of the last interglacial event in Papua New Guinea. *Geochimica et Cosmochimica Acta*. **57**: 2541-2554.
- Stoner, J. S., Channell, J. E. T., Hillaire-Marcel C. and Mareschal J.-C., 1994. High resolution rock magnetic study of a Late Pleistocene core from the Labrador Sea. *Canadian Journal of Earth Sciences*, **31**: 104-114.

- Stoner, J. S., Channell, J. E. T., and Hillaire-Marcel C., 1995. Magnetic properties of deep sea sediment off SW Greenland: Major differences between the last two deglaciations. *Geology*, **23**: 241-244.
- Stoner, J. S., Channell, J. E. T. and Hillaire-Marcel, C., (in press a). The magnetic signature of rapidly deposited detrital layers from the deep Labrador Sea: relationship to North Atlantic Heinrich layers. *Paleoceanography*.
- Stoner, J. S., Channell, J. E. T. and Hillaire-Marcel, C., (in press b). Late Pleistocene relative geomagnetic field paleointensity from deep Labrador Sea sediments: Regional and global correlation. *Earth and Planetary Science Letters*.
- Tauxe, L., and Wu, G. (1990). Normalized remanence in sediments from western equatorial Pacific: relative paleointensity of the geomagnetic field. *Journal of Geophysical Research*, **95**: 12337-12350.
- Tauxe, L., and Shackleton, N.J. (1994). Relative paleointensity records from the Ontong-Java plateau. *Geophysical Journal International* **117**: 769-782.
- Taylor, K. C., Lamorey, G. W., Doyle, G. A., Alley, R. B., Grootes, P. M., Mayewski, P. A., White, J. W. C., and Barlow, L. K. 1993. The 'flickering switch' of Late Pleistocene climate change. *Nature* **361**: 432-436.
- Taylor, K. C., Hammer, C. U., Alley, R. B., Clausen, H. B., Dahl-Jensen, D., Gow, A. J., Gundestrup, N. S., Kipfstuhl, J., Moore, J. C., and Waddington, E. D.. 1993. Electrical conductivity measurements from the GISP2 and GRIP Greenland ice cores. *Nature* **366**: 549-552.
- Thouveny, N., de Beaulieu, J.-L., Bonifay, E., Creer, K., Guiot, J., Icole, M. Johnsen, S., Jouzel, J., Reille, M., Williams, T., Williamson, D. 1994. Climate variations in Europe over the past 140 kyr deduced from rock magnetism. *Nature*, **371**: 503-506.
- Tric, E., Valet, J.P., Tucholka, P., Paterne, M., Labeyrie, L., Guichard, F., Tauxe, L., and Fontugne, M. (1992). Paleointensity of the geomagnetic field for the last 80,000 years. *Journal of Geophysical Research*, **97**: 9337-9351.
- Valet, J.-P., and Meynadier, L., 1993. Geomagnetic field intensity and reversals during the last four million years. *Nature*, **366**: 234-238.
- Weaver, A.J., and Huges, T. M. C., 1994. Rapid interglacial climate fluctuations driven by North Atlantic ocean circulation. *Nature*, **367**: 447-450.
- Winograd, I. J., Coplen, T. B., Landwehr, J. M., Riggs, A. C., Ludwig, K. R., Szabo, B. J., Kolesar, P. T., and Revesz, K. M., 1992. Continuous 500,000-year climate record from vein calcite in Devils Hole, Nevada. *Science*, **258**: 255-260.
- Yamazaki, T., and Ioka, N., 1994. Long-term secular variation of the geomagnetic field during the last 200 kyr recorded in sediment cores from the western equatorial Pacific. *Earth and Planetary Science Letters*, **128**: 527-544.

CHAPTER I

HIGH RESOLUTION ROCK MAGNETIC STUDY OF A LATE PLEISTOCENE CORE FROM THE LABRADOR SEA.

1.1 INTRODUCTION

Pleistocene climatic fluctuations that are characterized by ice sheet growth and decay are related to reorganization of the oceanic and atmospheric paleocirculation patterns (Broecker and Denton 1989, 1990; Hillaire-Marcel and de Vernal 1989). The basins off eastern Canada were the primary transitional basins between ice sheets and open oceans and received large amounts of melt water (de Vernal and Hillaire-Marcel 1987a-b; Hillaire-Marcel and de Vernal 1989). Sedimentation in these basins is sensitive to climatic fluctuations which should affect the rock magnetic character of the sediments.

High resolution rock magnetic studies from Late Pleistocene cores have correlated rock magnetic variations to paleoclimatic and paleoceanographic conditions (Robinson 1986; and Bloemendal et al. 1988, 1992). In older sequences, rock magnetic studies have detected changes in terrigenous source regions (Bloemendal 1983; Robinson 1986, 1990; Doh et al. 1988; DeMenocal et al. 1988; Bloemendal et al. 1988; Mead et al. 1986; Bloemendal and DeMenocal 1989; Mienert and Bloemendal 1989). Open ocean sites have generally indicated that relatively high magnetic concentrations occur during glacial periods while low magnetic concentrations occur during interglacials, primarily due to dilution of the magnetic fraction by increased biogenic sedimentation (e.g. calcium carbonate, silica). Composition and grain-size were also shown to vary from glacial to interglacial times. In contrast to the open ocean studies of Robinson (1986) and Bloemendal et al. (1988), a study of ODP-Site 646 (Leg

105) in the Labrador Sea concluded that the finer grained magnetic material deposited during glacial periods shows no significant correlation between magnetic concentration and percentage CaCO_3 (Hall et al. 1989a). Changes in the intensity of bottom current activity, which are related to the climatic conditions (e.g. glacial/interglacial) (Duplessy et al. 1988, Broecker 1990, Broecker et al. 1990, Labeyrie et al. 1992), were considered to be responsible for glacial-interglacial variations in grain-size of the magnetic material (Hall et al. 1989a).

The Late Pleistocene piston core HU 90-013-013 (PC-013) was taken at approximately the same location as ODP-Site 646 (Leg 105) (Fig. 1.1). Although PC-013 represents a much shorter interval of time than the ODP core (isotopic stages 1 through at least 5e compared to stages 1-21) back-to-back sampling, with each sample representing approximately 2.5 cm of core, allows definition of magnetic features not available from ODP cores due to sampling restrictions.

1.2 LOCATION, LITHOLOGY AND CHRONOLOGY

1.2.1 Location and Sedimentary Environment

PC-013 was collected from the Greenland Rise, north of the of the Eirik Ridge on the northern flank of a subsidiary ridge ($58^{\circ}13'N$, $48^{\circ}22'W$), at a water depth of 3380 m (Fig. 1.1). The Eirik Ridge, a sediment drift, results from a combination of sediment erosion, redeposition, and smoothing of the seafloor by strong contour currents (Srivastava, Arthur et al. 1987). The Eirik Ridge is a depositional feature associated with the circulation of the Western Boundary Under Current (WBUC) around the southern tip of Greenland before it turns northwest into the main part of the Labrador Sea. Though the Eirik Ridge appears to be primarily a relict feature (Hiscott et al. 1989), moderate bottom currents are still active in the Labrador Sea, with maximum velocities of 20 cm/s near the southern tip of Greenland

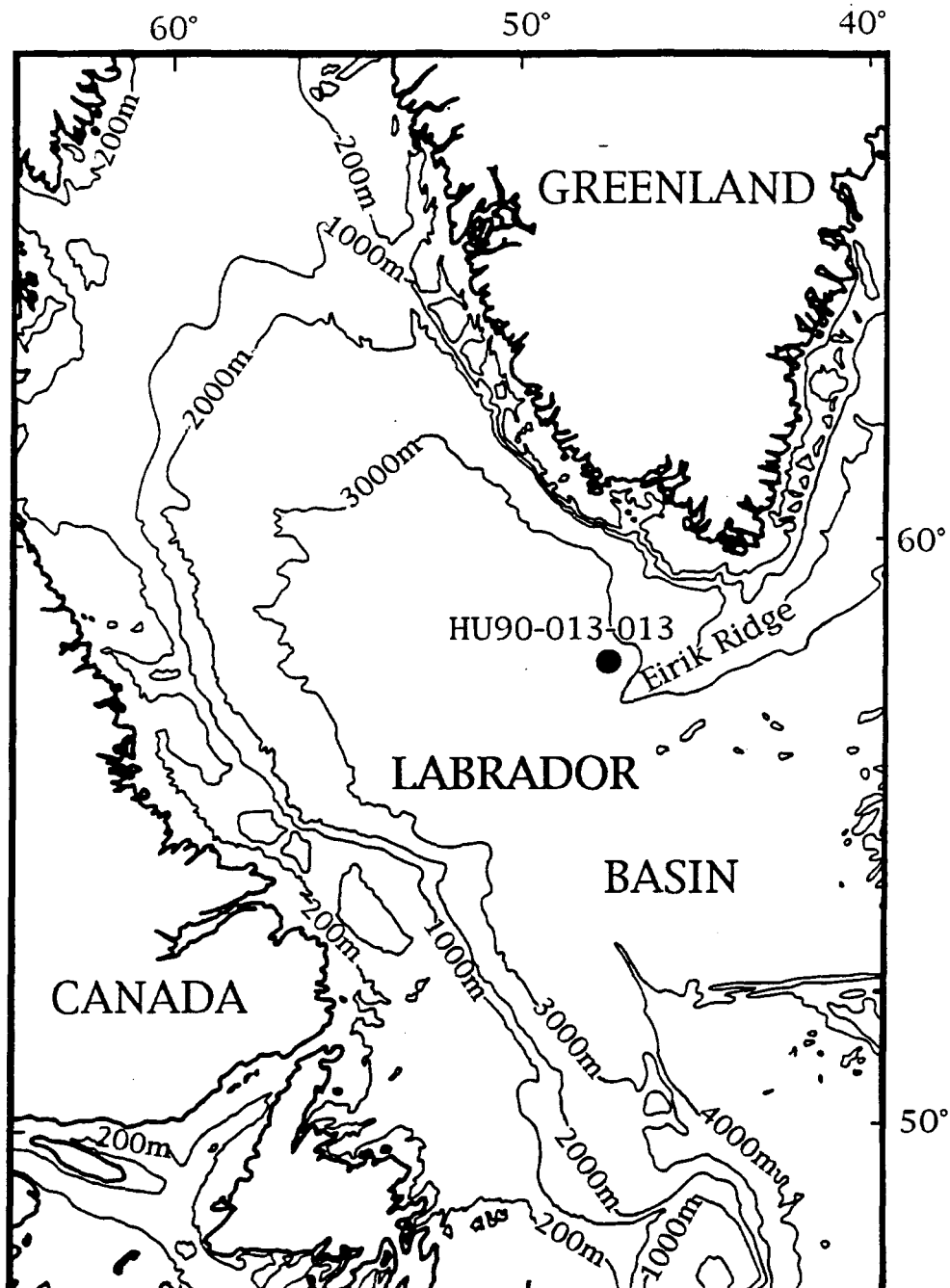


Figure 1.1. Site location map. HU90-013-013 is the piston core studied.

(Rabinowitz and Eitrem 1974). Currently the WBUC corresponds to the maximum velocity core of North West Atlantic Bottom Water (NWABW), which is found between 2500-3000 m in depth, at the edge of the Eirik Ridge (Clarke 1984; McCartney 1992). While this circulation existed during most of the Holocene, the WBUC is generally considered to have been inactive during the last glacial maximum (Duplessy et al. 1988, Broecker 1990, Broecker et al. 1990, Labeyrie et al. 1992, Lehman and Keigwin 1992).

Chough and Hesse (1985) from piston cores on the southern flank of the Eirik Ridge, found the drift sediments to be dominantly clayey silts and silty clays which could be characterized as “reworked” hemipelagic and pelagic sediments, while Hiscott et al (1989) from Site 646 found 95% of the Late Pliocene and younger age sediment to be structureless or bioturbated. Sedimentation processes observed at Site 646 are by three dominant agents; ice rafting, turbidity currents, and contour currents (Chough and Hesse 1985; Cremer 1989; Hiscott et al 1989). Through the Late Pleistocene a pronounced weakening of bottom current intensity is observed (Cremer 1989; Cremer et al 1989), with decantation of hemipelagic suspension and sporadic ice-rafted detritus (IRD) as the dominant settling processes during this interval (Cremer 1989; Cremer et al 1989). Turbidite sequences are generally composed of detrital carbonate (Cremer 1989; Hiscott et al 1989) and are considered to be similar to those described on the levees of the Northwest Atlantic Mid-Ocean Channel (NAMOC) (Hesse and Chough, 1980). These turbiditic layers are often observed in the same intervals as ice rafted detritus (Cremer 1989).

1.2.2 Lithology of Core HU90-013-013

The 1744 cm long core PC-013, consists of alternating sections of clayey silts, silty clays, and clays (Hillaire-Marcel and Rochon et al. 1990) (Fig. 1.2). The top twenty centimeters consist of an oxidized horizon of brown, carbonate-rich clayey silts. This

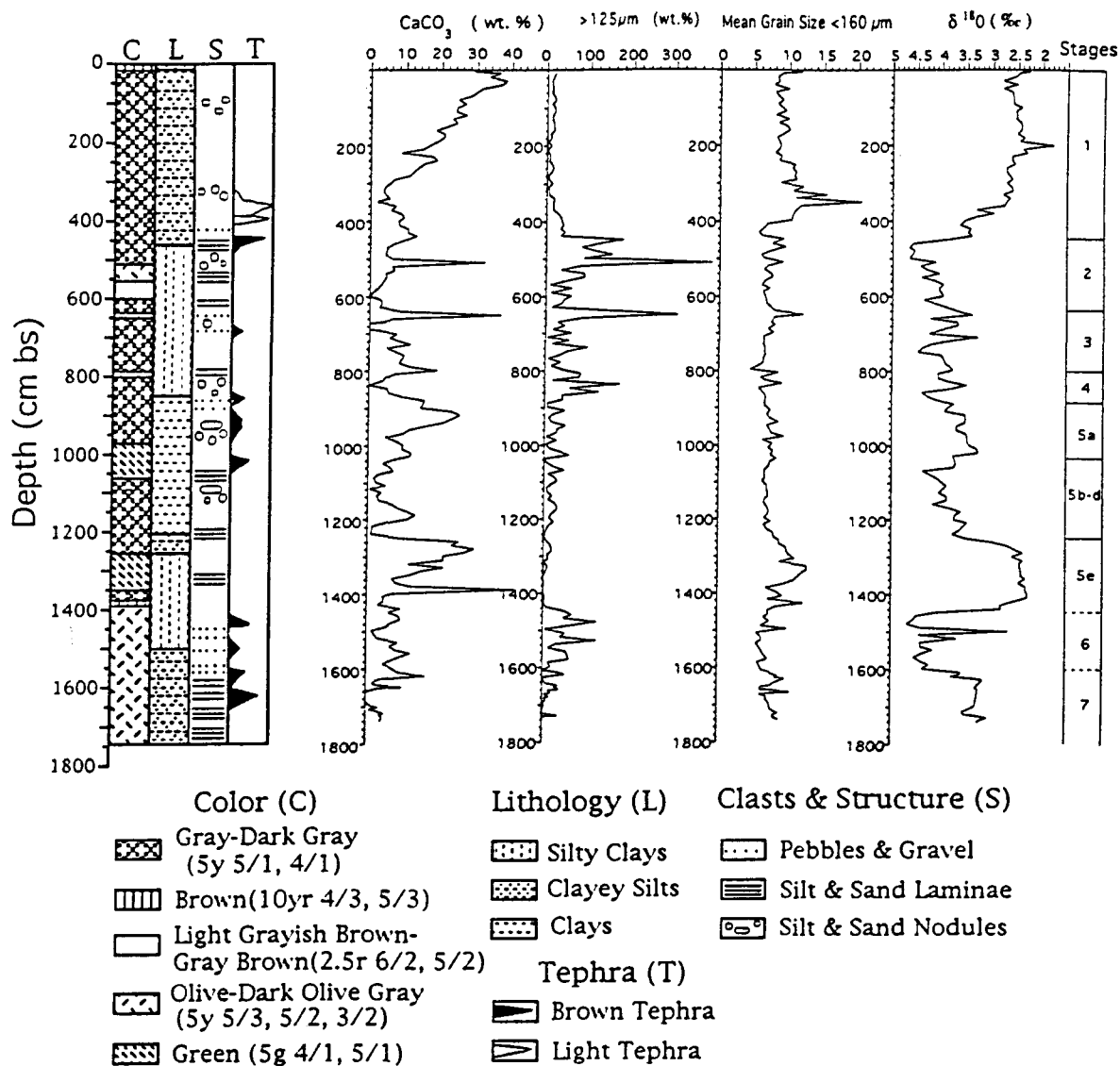


Figure 1.2. Generalized lithologic section indicating sediment color, lithology, structural features (P. Ferland, personal communication, 1990) and tephra layers (H. Haflidason, personal communication, 1992), with plots of percent CaCO_3 , mean grain-size $<160\mu\text{m}$, the weight percent of the carbonate-free sediment fraction $>125\mu\text{m}$, and $\delta^{18}\text{O}$ (‰) vs. depth (cm bs) (Hillaire-Marcel et al., 1994a). Colors are given according to the Munsell soil color charts. bs, below sediment surface.

AMS ^{14}C ages (Table 1). The stage 2/3 transition, indistinct in the oxygen isotope record, has been identified at approximately 620 cmbs based on ^{14}C ages and the occurrence of Heinrich event 3 at 640 cmbs with an approximate age of 28 kyr (Bond et al. 1992) or 30 kyr (Andrews et al. 1994, Hillaire-Marcel et al. 1994 a). Stage 4 is considered to occur in the \approx 800 to 880 cmbs interval based on micropaleontological data (see de Vernal et al. 1994) and the presence of a light $\delta^{13}\text{C}$ event. The short length of stage 4 is believed to be a general feature of the Labrador Sea (Hillaire-Marcel and de Vernal 1989). Isotopic substage 5a is distinct in the record (Fig. 1.2) while the interval from substage 5b-5d exhibits heavier than expected $\delta^{18}\text{O}$ values. These higher values may be related to rapid ice growth over Greenland and Arctic Canada during this interval as postulated by Miller and de Vernal (1992). The transitions from stage 5d to 5e and 5e to what is generally accepted as stage 6 are marked by abrupt changes in the $\delta^{18}\text{O}$ due to full interglacial conditions of substage 5e. The light $\delta^{18}\text{O}$ peak in stage 6 may indicate that the interval above, interpreted as stage 6 (Fig. 1.2), may represent a "Younger Dryas Type" event of substage 5e (see Hillaire-Marcel et al. 1994 a). The transition from stage 6 to stage 7 has been placed at 1600 cmbs, based on the oxygen isotope record and micropaleontological data (Hillaire-Marcel et al. 1994 a,b).

1.3 METHODS

1.3.1 Sampling

PC-013's core sections were cut with a rotary saw and the sediment split with an electric knife. The split core sections were sampled on board for magnetic measurement by continuous subsampling with 7 cc plastic cubes back-to-back, along the central axis, down the entire length of the core (708 total samples). Duplicate samples were taken approximately every 10 cm (173 total samples). All magnetic measurements were made in the magnetically-shielded laboratory at the University of Florida.

Table 1. Depth to age profile with intervening sedimentation rates.

Depth (cm bs) ^a	¹⁴ C Age (years BP)	$\delta^{18}\text{O}$ Chronostratigraphy (years)	Sedimentation rate (cm/ka)
			28
98-100	3,980 \pm 70		28
188-190	6,810 \pm 100		28
208-210	7,580 \pm 70		90
238-240	7,790 \pm 80		90
338-340	8,830 \pm 90		90
358-360	9,230 \pm 360		30
368-370	10,040 \pm 120		30
388-390	10,430 \pm 80		30
398-400	10,720 \pm 90		15
418-420	11990 \pm 90		15
430		12,500	25
428-430	12,450 \pm 120		25
438-440	12,560 \pm 90		9
448-450	14,150 \pm 110		9
478-480	16,990 \pm 110		8
508-510	20,950 \pm 150		16
528-530	22,190 \pm 200		16
698-700	33,000 \pm 340		9
756-758	41,380 \pm 590		5
860		64,000	7
1236		122,000	21
1406		130,000	4
1630		190,000	

Note: Reservoir-corrected AMS ¹⁴C ages are from Wu and Hillaire-Marcel (1994), sedimentation rates are from Hillaire-Marcel et al. (1994). The $\delta^{18}\text{O}$ record allowed identification of 5 events which were correlated with the orbitally based chronostratigraphy of Martinson et al. (1987) and assigned ages.

^aGiven as centimeters below the sediment surface (bs)

1.3.2 Magnetic Measurements

All samples were measured for: low (k at 0.47 kHz) and high-frequency (k_{hf} at 4.7 kHz) volumetric magnetic susceptibility, the ratio of k to k_{hf} gives the frequency dependent magnetic susceptibility (k_{f}); natural remanent magnetization (NRM) and the NRM after 20 mT alternating field (AF) demagnetization; anhysteretic remanent magnetization (ARM) using a 99 mT peak AF and a 0.04 mT direct current (DC) biasing field (this is expressed as an anhysteretic susceptibility (k_{ARM}) by dividing by the strength of the biasing field); saturation isothermal remanent magnetization (SIRM) produced in a DC field of 1 T (the authors realize that antiferromagnetic grains may not be completely saturated at a field of this intensity); back field isothermal remanent magnetization (BIRM) using DC fields of -0.1 T (BIRM_{-0.1}) and -0.3 T (BIRM_{-0.3}).

The BIRMs and SIRM were used to obtain the S-ratios (BIRM_{-0.1}/SIRM = $S_{-0.1}$) and (BIRM_{-0.3}/SIRM = $S_{-0.3}$) and hard isothermal remanent magnetization (HIRM). HIRM_{-0.1} is defined as (SIRM + BIRM_{-0.1}) / 2, while HIRM_{-0.3} is defined as (SIRM + BIRM_{-0.3}) / 2.

Stepwise AF demagnetization in peak fields up to 99 mT as well as progressive IRM acquisitions were measured on selected samples. These parameters are fully defined by Collinson (1983), O'Reilly (1984), and Thompson and Oldfield (1986).

Magnetic accumulation rates were calculated by multiplying the magnetic concentration dependent parameter k by the sedimentation rates (Table 1) and the bulk density (Hillaire-Marcel et al. 1994 a). Only sedimentation rates based on ¹⁴C dates were used, due to uncertainties in relating the isotopic stratigraphy of the lower section of PC-013 with ages derived from the chronostratigraphy of Martinson et al. (1987) (for discussion, see above and Hillaire-Marcel et al. 1994 a).

1.4 RESULTS

1.4.1 Downcore Variation of Concentration Dependent Parameters

Figure 1.3 shows k and the intensities of SIRM, K_{arm} , HIRM_{0.1} and HIRM_{0.3} plotted versus depth. In general, increasing magnetic mineral content, indicated by peaks in the k and SIRM curves occur during glacial to interglacial transitions (i.e. isotope stage 6/5e and 2/1). Magnetically, tephra-rich intervals (Fig. 1.2) are not always distinguishable from IRD (fraction > 125 μm) (Fig. 1.2). Both are characterized by high k , however, there is a tendency for SIRM to be lower for IRD. Although k_{ARM} displays the same general response to intervals of high magnetic concentration identified by k and SIRM, it also displays a much greater downcore variability due to its greater sensitivity to ferrimagnetic grain-size.

Downcore variation in the concentration of higher coercivity components, indicated by HIRM_{0.1}, does not consistently follow the transitions from glacial to interglacial periods. Generally the highest HIRM_{0.1} values are associated with intermediate $\delta^{18}\text{O}$ values, during the stage 2/1 transition, the initial part of stage 2, substages 5a-d and stage 7. The lowest HIRM_{0.1} values are associated with heavy $\delta^{18}\text{O}$ values of stage 2 and stage 6 and intermediate HIRM_{0.1} values are associated with the light $\delta^{18}\text{O}$ values of stage 1 and substage 5e. The association of high HIRM_{0.1} with intermediate $\delta^{18}\text{O}$ indicates that the concentration of higher coercivity magnetic materials (e.g.. single domain magnetite and/or antiferromagnetic material) is controlled by a different set of factors than magnetic concentration in general. The HIRM_{0.3} curve shows a similar trend to that of the HIRM_{0.1} curve, but with much less variation and much greater scatter due to the dominance of ferrimagnetic minerals on the magnetic properties of this core.

In agreement with the results of Hall et al. (1989a), the concentration dependent parameters k , SIRM, HIRM_{0.1} and HIRM_{0.3} show no clear correlation with percent CaCO_3 (Fig. 1.3 & 1.4), with correlation coefficients of $r = -0.26, -0.43, -0.42$ and -0.27

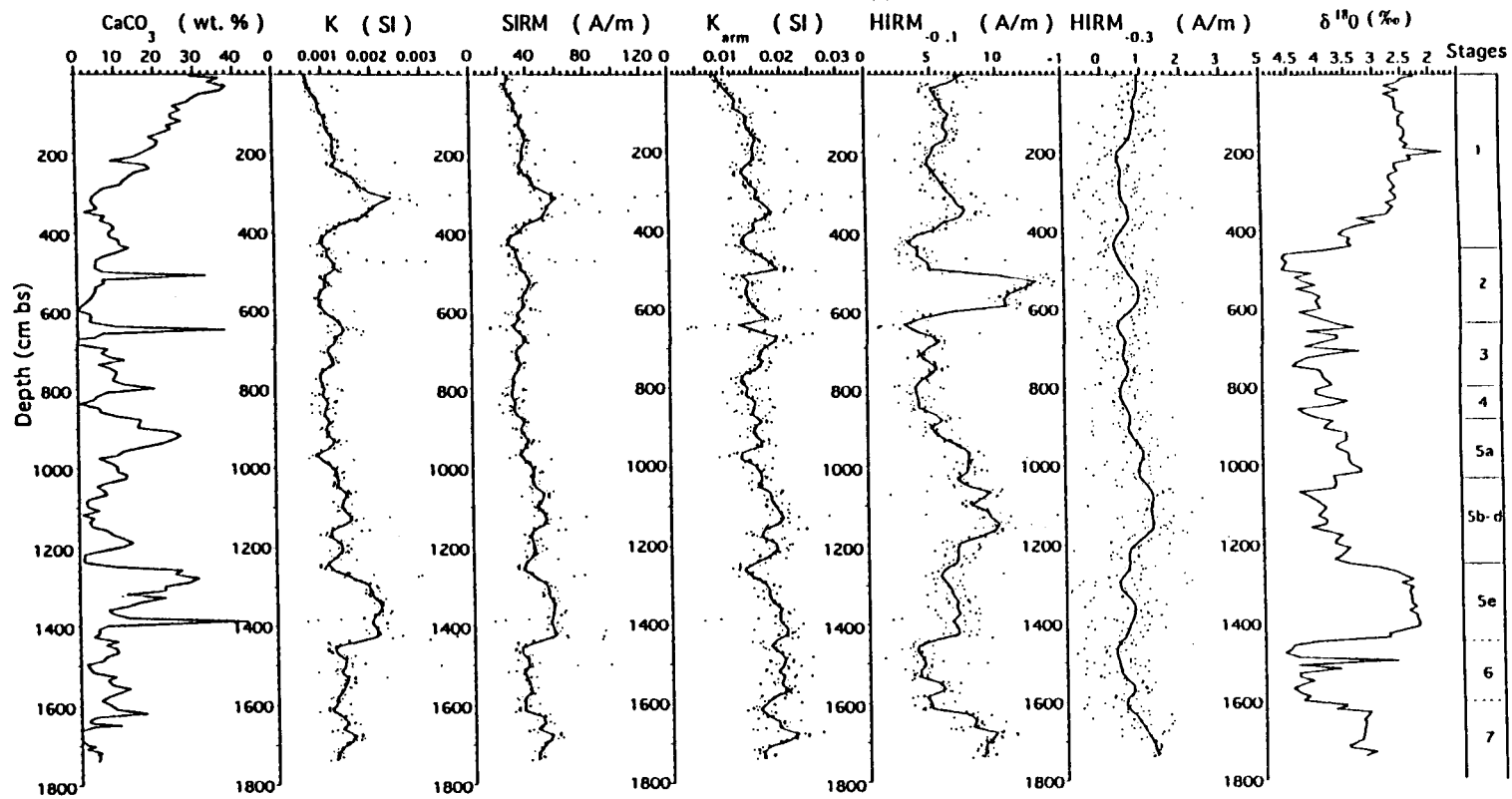


Figure 1.3. Concentration-dependent rock magnetic parameters K , SIRM, K_{ARM} , HIRM_{0.1} and HIRM_{0.3} versus depth (cm bs), compared with percent CaCO_3 and $\delta^{18}\text{O}$ (‰) vs. depth (cm bs) (Hillaire-Marcel et al., 1994a). Each point represents an average value for approximately 2.5 cm of core. Curve fit is achieved by using the locally weighted least squares method with a 2% weighting function. bs, below sediment surface.

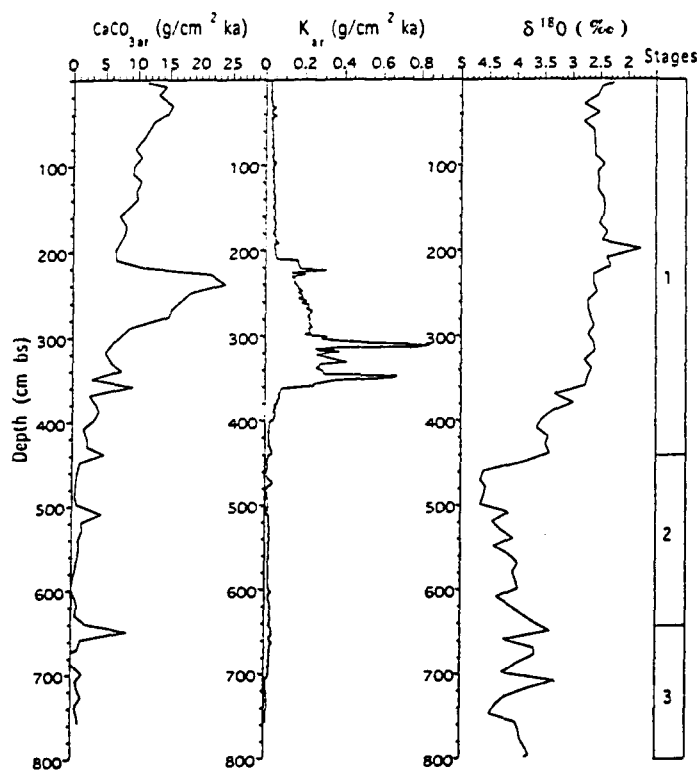


Figure 1.4. Accumulation rate curve for K vs. depth (cm bs) compared with CaCO_3 , and $\delta^{18}\text{O}$ (‰) versus depth. For the magnetic parameters each point represents an average value for approximately 2.5 cm of core. bs, below sediment surface.

respectively. On the other hand, k_{ARM} has a more negative correlation with percent $CaCO_3$, with $r = -0.63$, possibly due to lower concentrations of magnetic material and relatively larger magnetic grain-sizes during periods of increased $CaCO_3$ content.

Magnetic concentration may be influenced by dilution from other components (e.g. $CaCO_3$ and/or silica) which may obscure changes in the magnetic input. One way to eliminate this problem is to recalculate the magnetic parameters as if they were accumulation rates or fluxes (Bloemendal 1983; Bloemendal et al. 1988; Doh et al. 1988; and Hall et al. 1989a). Figure 1.4 shows $CaCO_3$ and k plotted as accumulation rates ($CaCO_{3ar}$ and k_{ar} respectively) versus depth (cmbs). As is to be expected, very high accumulation rates are found when the maximum sedimentation rates (Table 1) and highest values for the parameters (Fig. 1.3) coincide. The interval of maximum magnetic accumulation corresponds to the glacial to interglacial transition 2/1. Even though the magnetic accumulation was not calculated for the bottom half of the core, high accumulation rates would also be expected for substage 5e due to its higher sedimentation rates (Table 1) and higher values of magnetic concentration (Fig. 1.3) relative to the surrounding intervals.

1.4.2 Concentration Independent Rock Magnetic Parameters

To eliminate the dependence on magnetic concentration, ratios between individual magnetic parameters can be calculated which are essentially concentration independent. Six interparametric ratios were used in this study: the 2 S-ratios and k_f (defined above), $SIRM/K$; $SIRM/k_{ARM}$, and k_{ARM}/k . The S-ratios are primarily indicative of changes in the coercivity of the sediment's magnetic assemblage. The $S_{-0.3}$ is used as an indicator of the proportion of high coercivity particularly antiferromagnetic (hematite and goethite) to the lower coercivity ferrimagnetic (magnetite and maghemite), but is only discriminatory ($S_{-0.3} > -0.9$) when the proportion of antiferromagnetic material is greater than 80% of the magnetic

assemblage (Bloemendal et al. 1992). While, $S_{-0.1}$ is also sensitive to the proportion of antiferromagnetic to ferrimagnetic minerals in the assemblage, but it also exhibits a strong secondary response to ferrimagnetic grain-size (Robinson 1986). The k_{ARM} ratios, k_{ARM}/k and $SIRM/k_{ARM}$ are primarily responsive to the dominant ferrimagnetic grain-size of the magnetic minerals in the assemblage. k_{ARM}/k decreases with increasing grain-size (King et al. 1982), while $SIRM/k_{ARM}$ increases with increasing grain-size. $SIRM/k$ also decreases with increasing grain-size, but it also responds to the magnetic mineralogy (Thompson 1986). $SIRM/k_{ARM}$ is less responsive and k_{ARM}/k is the least responsive to magnetic mineralogy. While k_f is used to indicate the presence of superparamagnetic material (Thompson and Oldfield 1986; Maher 1988). For further explanation on the empirical and theoretical basis of these ratios see Dunlop (1981); King et al. (1982); O'Reilly (1984); Thompson and Oldfield (1986); Thompson (1986); Hall and King (1989); Yu and Oldfield (1989); King and Channell (1991) and Bloemendal et al. (1992).

The largest feature associated with all the rock magnetic parameters is the high coercivity interval indicated by low negative $S_{-0.1}$ ratio and high $HIRM_{0.1}$ values observed from approximately 500-600 cmbs (Fig. 1.5). The transition to the low negative $S_{-0.1}$ ratio is rather abrupt, occurring over 2 or 3 samples (approximately 5 cm) both above and below the interval. The low negative $S_{-0.1}$ ratio tends to indicate a magnetic assemblage dominated by ferrimagnetic grains of finer SD grain-size or an assemblage with a small antiferromagnetic component, or both (Robinson 1986). $SIRM/k$ shows a similar peak at this interval indicating a similar magnetic assemblage. In contradiction, however, $SIRM/k_{ARM}$ also shows a peak in this interval which is indicative of a coarser grained magnetic assemblage, while k_{ARM}/k shows a mixed signal in this interval, indicative of a slight fining from top to bottom. The apparent contradiction between these magnetic ratios can be explained by either small proportion of the magnetic mineral assemblage containing a

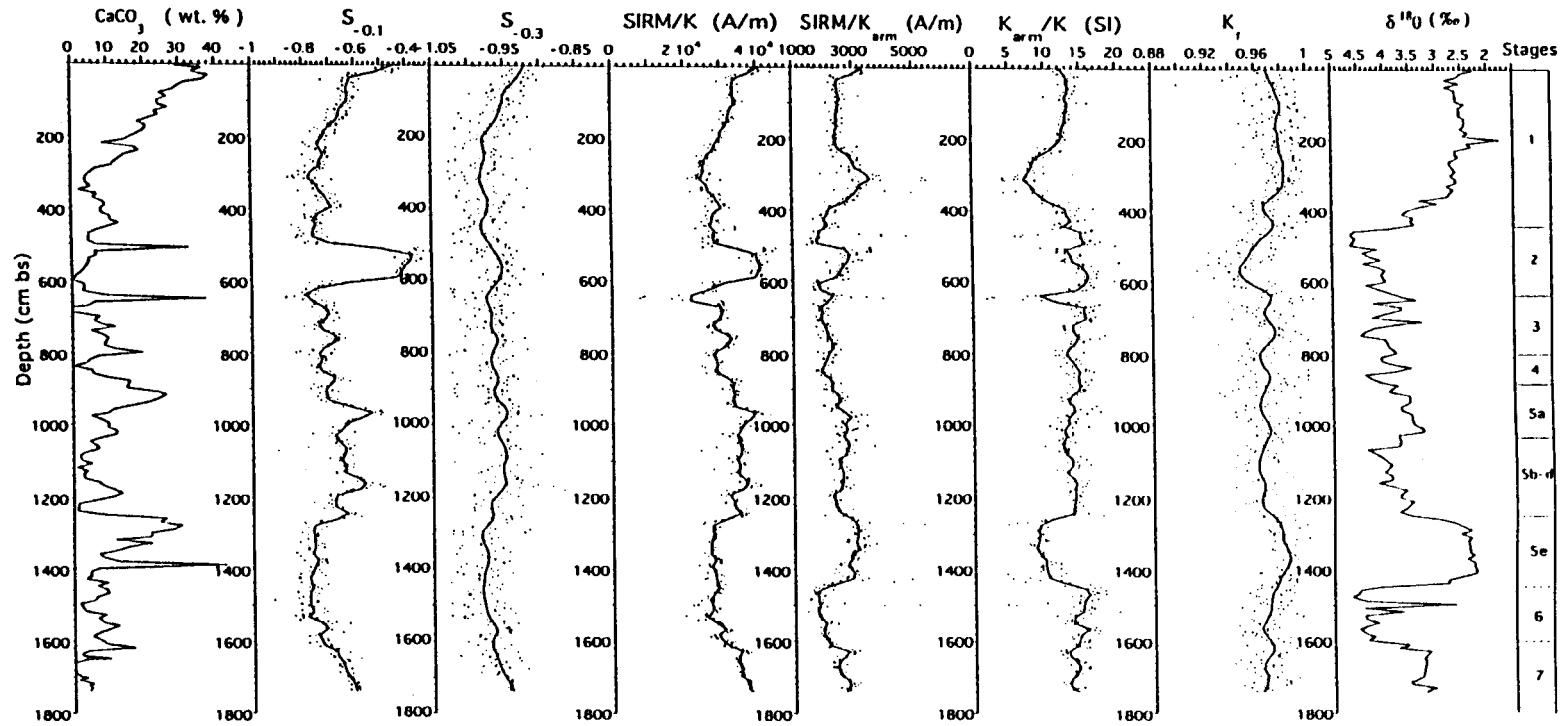


Figure 1.5. Concentration-independent rock magnetic parameters $S_{-0.1}$, $S_{-0.3}$, K_{ARM}/K , $\text{SIRM}K_{\text{ARM}}$, SIRM/K , and K_f vs. depth (cm bs), compared with percent CaCO_3 and $\delta^{18}\text{O}$ (‰) versus depth (cm bs). Each point represents an average value for approximately 2.5 cm of core. Curve fit is achieved by using the locally weighted least squares method with a 2% weighting function. bs, below sediment surface.

higher coercivity antiferromagnetic mineral (hematite or goethite) or a magnetic assemblage that has a significant proportion of ultrafine SD magnetite. Karlin (1990) indicated that k_{ARM} might not activate the smallest fraction whose coercivities are greater than the peak applied AF field of 100 mT. This interval also exhibits greater frequency dependence of susceptibility (k_f) (Fig. 1.5) indicating a greater proportion of grains close to the superparamagnetic-SD grain-size threshold and possibly indicative of a finer overall magnetic assemblage. Although, the decrease in k_f is only on the order of 6%.

The top twenty centimeters are also characterized by a low negative $S_{-0.1}$ values (Fig 5). This corresponds to the well oxidized, bioturbated, surficial layer above the level of iron reduction (Lucotte et al. 1994). The magnetic parameters of the top 20 cm are similar in all respects to those from the 500-600 cmbs interval which may indicate similarities between the depositional or post-depositional nature of these sediments, though the paleoenvironments were very different during these times. Two other middle to low negative $S_{-0.1}$ peaks are observed at 950-990 cmbs and 1140-1180 cmbs, and are contained within a broad zone of $S_{-0.1}$ values greater than -0.7 from 950 to 1240 cmbs (substages 5a-d). This high coercivity interval is also displayed by $HIRM_{-0.1}$ (Fig. 1.3) and SIRM/K curves. Little variation is observed from the k_{ARM} ratios during this interval (Fig 5). Below this interval is a zone of low negative $S_{-0.1}$ values, indicating an interval of lower coercivity from 1250 to 1550 cmbs. Low values for SIRM/K are also observed during this interval. From 1600 cmbs to the base of the core increasing $S_{-0.1}$ values are observed. This higher coercivity interval correlates with a decrease in $\delta^{18}O$ and is also observed as an increase in SIRM/ k values.

The k_{arm} ratios especially k_{ARM}/k show three distinct intervals indicative of a coarser grained magnetic assemblage (Fig 5). The three intervals occur at: 220-380 cmbs, 640-650 cmbs and 1240-1420 cmbs. These intervals correspond to high negative values of $S_{-0.1}$ and lows on the SIRM/ k curve, probably indicative of coarse grained ferrimagnetic, MD

magnetite dominated, magnetic assemblage. Though, for both the $S_{0.1}$ and the $SIRM/k$ curves, the transition to a finer grain-sized magnetic assemblage at 1440 cmbs as indicated by the k_{ARM} ratios is not observed, probably due to the increase in IRD (Fig. 1.2) during this interval.

The intervals of coarser magnetic grain-size (220-380 cmbs and 1240-1420 cmbs) correspond to the glacial to interglacial transition 2/1 and the last interglacial 5e. The other interval (640-650 cmbs), correlates with a short carbonate peak, and is identified as Heinrich event 3 (Hillaire-Marcel et al. 1994 a) as indicated by the poorly sorted sand and gravel, the large increase in the fraction greater than $125 \mu\text{m}$ (Fig. 1.2), as well as the change in color from gray to brown. Very low $SIRM/k$ values are observed during this interval, probably indicating the affect of coarse MD magnetite on the magnetic properties in this layer. Other Heinrich events (notably 1, 2, & 6) have been identified within PC-013 (Hillaire-Marcel et al. 1994 a) but do not produce major features in the magnetic record.

1.5 DISCUSSION

1.5.1 Intervals of Increased Magnetic Concentration and Grain-size

The two prominent intervals of increased magnetic grain-size and concentration are associated with glacial to interglacial transition 2/1 and interglacial 5e. The increase in magnetic grain-size is inferred from a decrease in k_{ARM}/k and an increase in $SIRM/k_{ARM}$ values. This is further corroborated by an observed increase in the grain-size of the whole sediment for the fraction less than $160 \mu\text{m}$ during the same intervals (Fig. 1.2) (Hillaire-Marcel et al. 1994 a). The strong negative correlation between k_{ARM}/k and the grain-size analysis of the mean grain-size (in μm) for the less than $160 \mu\text{m}$ fraction of $r = -0.74$, is consistent with findings of Hall et al. (1989b) in Baffin Bay, and indicates that k_{ARM}/k is a

useful proxy for grain-size changes within the smaller grain-size fraction of the sediment as a whole.

The increase in magnetic concentration associated with substage 5e is assumed to be related to the change in climatic conditions. The change in magnetic concentration associated with the 2/1 transition cannot unequivocally be associated with the climate change in view of the large volcanic input in this interval. But, the range of high tephra count in the core is primarily between 350-400 cmbs and the high magnetic concentration and increased grain-size occurs from 220 to 380 cmbs. Therefore, we consider that the volcanogenic detritus contributes to the increased magnetic concentration in the lower part of the interval, but is not the only source of increased magnetic concentration during this interval.

From site 646, Hall et al. (1989a) concluded that the changes in k_{ARM}/v reflect changes in bottom current activity and that the low values of k_{ARM}/k , indicative of larger magnetic grain-sizes, reflect increased bottom current activity and winnowing of the finer fractions. They also concluded that the bottom current activity, as determined from k_{ARM}/k , and the terrigenous flux indicated by magnetic accumulation rates lag the SPECMAP oxygen-isotope curve by 14 and 18 kyr respectively from stage 11 to 1. For PC-013, the increase in magnetic grain-size and concentration occurs at precisely the same level (Figs 3 and 5). The magnetic accumulation rate for the 2/1 transition (Fig.3) lags the increase in magnetic grain-size by 20 cm or approximately 1000 yrs from the ^{14}C dates of Wu and Hillaire-marcel (1994). However little emphasis can be given to this since the accumulation rates are proportional to sedimentation rates (Table 1) which are not accurately determined (due to the changing rate of sedimentation during this interval), but are simply interpolated between ^{14}C dates. The low carbonate percentages in this interval (Figs. 1.2,1.3 and 1.5) appear to be related to low productivity rather than significant dissolution (de Vernal et al. 1994). Therefore it appears that the increase in concentration reflects magnetic accumulation and, at

least for the last and the present interglacials, increases in grain-size and concentration occur during the same intervals and are therefore probably due to the same cause.

Current winnowing of the finer fraction has been suggested to be the primary mechanism for the larger magnetic grain-size. This hypothesis does not appear to be supported in this core for several reasons. First, the location of this site at a depth of 3380 m is beneath the main axis of WBUC activity (Clarke 1984; McCartney 1992; McCave and Tucholke 1986; Hillaire-Marcel et al. 1994 a , Lucotte and Hillaire-Marcel 1994), which may explain the lack of sedimentary structures related to current processes at this site (Cremer 1989). The site position below the WBUC is further established by comparing sedimentation rates from PC-013 with piston core HU90-13-012 (PC-012) which is approximately 100 km away and 600 m higher up the Greenland slope. In PC-012 the Holocene section is represented by 30 cm of core due to its location in the main axis of the WBUC (Lucotte and Hillaire-Marcel, Hillaire-Marcel et al. 1994 a) and stage 2 extends over an interval of 2 m, during a period with little or no bottom current activity. On the other hand, PC-013 contains an extended Holocene section of approximately 4 m and a relatively condensed stage 2 of approximately 2 m, due to the activity and inactivity of the WBUC during these times respectively. The effect of WBUC on the sedimentation rate of PC-013 can be further illustrated by the decrease in sedimentation rates during the Younger Dryas, when deep water flow was turned off (Broecker et al. 1990; Lehman and Keigwin 1992, Veum et al 1992, Charles and Fairbanks 1992, Alley et al. 1993). The sedimentation rate during this time was reduced by a factor of 2 relative to the intervals both before and after, when the WBUC was active (Hillaire-Marcel et al 1994). Therefore, PC-013 is located at a site characterized by high sediment accumulation (rather than by erosion) during WBUC activity.

The fact that the increases in mean grain-size, magnetic grain-size and accumulation are observed during periods of significant decrease in $\delta^{18}\text{O}$ values indicates that significant

ice retreat was occurring during these times. Therefore we consider that these increases are a reflection of increased detrital component due to a strong melt water flux from southern Greenland. This interpretation is supported by an increase in detrital silicate flux during the interval from 220 to 380 cmbs. This flux was 4 times the amount of the preceding glacial period and twice as much as the rest of the Holocene (Hillaire-Marcel et al 1994). The increase in magnetic grain-size associated with the glacial to interglacial transitions and the increase in the mean grain-size (in μm) of the whole sediment ($< 160 \mu\text{m}$) (Fig 2) should not be confused with an increased input of IRD, which is indicated by increases in the percent of the sediment greater than $120 \mu\text{m}$ (Fig. 1.2). This IRD indicator is highest during glacials and at a maximum during Heinrich events (Hillaire-Marcel et al. 1994 a), but is significantly reduced during interglacials (Fig. 1.2).

1.5.2 High Coercivity Interval

The variations in the $S_{0.1}$ ratio and $\text{HIRM}_{0.1}$ (Figs 3 and 5) show an interval (between 500 and 600 cmbs) with much higher coercivity than the intervals above or below. The magnetic assemblage in this interval is probably dominated by SD magnetite, with possibly a small proportion of antiferromagnetic material (hematite or goethite). The interpretation that SD ferrimagnetic material is the dominant magnetic mineralogy in this interval is supported by the greater frequency dependence of susceptibility indicating an increased ultrafine fraction. Because the transition from lower to higher coercivity is so abrupt (about 5 cm) a dramatic change in sediment source at both the initiation and termination of this interval would be needed. There is no evidence indicating that an increase in a detrital source could account for the large and rapid change in coercivity during the interval.

The similarity of magnetic behavior between the high coercivity interval and the oxidized surficial layer above the zone of iron reduction may indicate that the high coercivity corresponds to a relict oxidized zone. The presence of oxidizing conditions in this interval is indicated by a marked color change (on board core description), large manganese peak at 580 cmbs (Lucotte et al. 1994) and an uranium low with a sharp increase in the interval just below (Vallières, S. pers. comm., 1992). The color change from dark gray above this interval, to an olive to olive gray at the top of the interval, changes to a light brownish gray in the lower part of the interval, followed by a sharp transition to gray immediately below the interval. A more oxic sedimentary environment is assumed during stage 2 due to lower sedimentation rates and reduced organic carbon burial (Lucotte et al, 1994). Therefore it seems probable that a diagenetic mechanism similar to that postulated by Karlin (1990) for Pacific sediments might be involved. This mechanism involves the preferential dissolution of SD ferrimagnetic component just below the zone of iron reduction in all but relict oxidized zones within the core. These conditions lead to a magnetic assemblage dominated by a coarser grained ferrimagnetic mineralogy with an overall lower coercivity in all but the surficial and relict oxidized zones. The mechanism for this paleoxidization zone is still unclear, but it may be related to a mechanism proposed by Finney et al. (1988), where the oxidized zone is buried by an upward shift in the redox boundary due to an increased sedimentation rate. For PC-013, this could be related to the increase in sedimentation observed during stage 1.

An alternative mechanism involves a progressive oxidation front, usually associated with turbidite emplacement (Colley et al. 1984; Wilson et al. 1985), but which may be initiated by any relatively sudden change in sedimentary conditions. Such change causes the actual thickness of the oxidized sediment surface layer to become less than the equilibrium steady-state layer thickness (e.g. turbidite, decrease in organic sedimentation, increase in

oxygen) (Wilson et al. 1986, Dean et al. 1989, Pruyssers et al. 1993). The top of this interval coincides with Heinrich event 2 which is rich in detrital carbonate (Fig 2 and 5) and whose origin may be related to overflow turbidites from the NAMOC (Cremer 1989; Hillaire-Marcel et al. 1994 a).

1.6 CONCLUSIONS

1. Increasing magnetic grain-size correlates with glacial to interglacial transition 6/5e and 2/1. The coarsening of magnetic grain-size is associated with a large increase in magnetic concentration, and higher sedimentation rates due to reinitiation of the WBUC. These factors also correlate with an increase in the mean grain-size of the whole sediment for the fraction less than 160 μm and an increased silica flux during the 2/1 transition. These changes at the glacial-interglacial transitions (6/5e and 2/1) are considered to be due to an increase in detrital components related to glacial retreat and an associated large melt water flux from southern Greenland.

2. An interval of increased magnetic coercivity recognized by the variations in the $S_{0.1}$ ratio and $\text{HIRM}_{0.1}$ from 500 to 600 cmts, appears to be related to the preservation of SD ferrimagnetic component due to a lack of reduction diagenesis during this interval. The mechanism for preservation of this relict oxic zone is presently undetermined. Other intervals of higher coercivity within this core might be related to similar oxidation events that have been only tentatively identified.

3. Most concentration dependent magnetic parameters (k , SIRM, $\text{HIRM}_{0.1}$ and $\text{HIRM}_{0.3}$) show no correlation to percent carbonate in agreement with the study of Hall et al. (1989a). Whereas, k_{ARM} shows a more negative correlation with percent carbonate due to its greater grain-size sensitivity, and the general correlation in this core of higher (lower) percent carbonate with larger (smaller) magnetic grain-size. These results are in contrast to the deep

sea cores studied by Robinson (1986,1990) and Bloemendal et al. (1988) owing to the more complicated sedimentation patterns observed in transitional basins like the Labrador Sea.

4. The strong negative correlation between the magnetic grain-size sensitive parameter k_{ARM}/k and the mean grain-size of the fraction less than 160 μm indicates that k_{ARM}/k can be used as a proxy for grain-size change in the small grain-size fraction of the sediment.

REFERENCES

- Alley, R. B., Meese, D. A., Shuman, C. A., Gow, A. J., Taylor, K. C., Grooter, P. M., White, J. W. C., Ram, M., Waddington, E. D., Mayewski, P. A., and Zielinski, G. A. 1993. Abrupt increase in Greenland snow accumulation at the end of the Younger Dryas event. *Nature (London)*, **362**: 527-529.
- Andrews, J. T., Tedesco, K., Briggs, W. M., and Evans, L. M. 1994. Sediments, sedimentation rates, and environments, SE Baffin Shelf and NW Labrador Sea 8 to 26 Ka. *Canadian Journal of Earth Sciences*, **31**: 90-103
- Bloemendal, J. 1983. Paleoenvironmental implications of the magnetic characteristics of sediments from DSDP Site 514, Southeast Argentine Basin, Initial Reports of the Deep Sea Drilling Project, **71**: 1097-1108.
- Bloemendal J., and deMenocal, P. B. 1989. Evidence for a change in the periodicity of tropical climate cycles at 2.4 Myr from whole-core magnetic susceptibility measurements. *Nature (London)*, **342**: 897-900.
- Bloemendal, J., Lamb, B., and King, J. W. 1988. Paleoenvironmental implications of rock-magnetic properties of Late Quaternary sediment cores from the eastern equatorial Atlantic. *Paleoceanography*, **3**: 61-87.
- Bloemendal J., King, J. W., Hall, F. R., and Doh, S.J. 1992. Rock magnetism of Late Neogene and Pleistocene deep-sea sediments: relationship to sediment source, diagenetic processes, and sediment lithology. *Journal of Geophysical Research*, **97**: 4361-4375.
- Bond, G., Heinrich, H., Broecker, W., Labeyrie, L., McManus, J., Andrews, J., Huon, s., Jantsschik, R., Clasen, S., Simet, C., Tedesco, K., Kias, M., Bonani, G., and Ivy, S. 1992. Evidence for massive discharges of icebergs into the North Atlantic ocean during the last glacial period. *Nature (London)*, **360**: 245-249.
- Broecker, W. S. 1990. Salinity history of the northern Atlantic during the last deglaciation. *Paleoceanography*, **5**: 459-467.
- Broecker, W. S., and Denton, G. H. 1990. The role of ocean-atmosphere reorganizations in glacial cycles. *Quaternary Science Reviews*, **9**: 305-341.
- Broecker, W.S., Bond, G., McManus, J., Klas, M., and Clarke, E. 1992. Origin of the Northern Atlantic's Heinrich events. *Climate Dynamics*, **6**: 265-273.
- Charles, C. D., and Fairbanks, R. G. 1992. Evidence from Southern Ocean sediments for the effect of North Atlantic deep-water flux on climate. *Nature*, **353**: 720-725.
- Chough, S. K., and Hesse, R. 1985. Contourites from Eirik Ridge, south of Greenland. *Sedimentary Geology*, **41**: 185-199.

- Clarke, R. A. 1984. Transport through the Cape Farewell-Flemish Cape section. Rapports et procès verbaux des réunions. Extrait du Journal du conseil international pour l'exploration de la mer, **185**: 120-130.
- Colley, S., Thomson, J., Wilson, T. R. S., and Higgs, N. C. 1984. Post-depositional migration of elements during diagenesis in brown clay and turbidite sequences in the North East Atlantic. *Geochimica et Cosmochimica Acta*, **48**: 1223-1235.
- Collinson, D. W. 1983. *Methods in Rock-Magnetism and Paleomagnetism: Techniques and Instrumentation*. Chapman and Hall, London, 503 p.
- Cremer, M. 1989. Texture and Microstructure of Neogene-Quaternary sediments, ODP Sites 645 and 646, Baffin Bay and Labrador Sea. Proceedings of the Ocean Drilling Program, Scientific Results, **105**: 7-16.
- Cremer, M., Maillet, N., and Latouche, C. 1989. Analysis of sedimentary facies and clay mineralogy of the Neogene-Quaternary sediments in ODP Site 646, Proceedings of the Ocean Drilling Program, Scientific Results, **105**: 71-82.
- Dean, W. E., Gardner, J. V., and Hemphill-Haley, E. 1989. Changes in redox conditions in deep-sea sediments of the subarctic North Pacific Ocean: possible evidence for the presence of North Pacific Deep Water. *Paleoceanography*, **4**: 639-653.
- deMenocal, P. B., Laine, E. P., and Ciesielski, P. F. 1988. A magnetic signature of bottom current erosion. *Physics of the Earth and Planetary Interiors*, **51**: 326-348.
- de Vernal, A., and Hillaire-Marcel, C. 1987a. Climatostatigraphie du Pléistocène supérieur dans les Provinces Atlantique du Canada. *L'Anthropologie*, **91**: 93-107.
- de Vernal, A. and Hillaire-Marcel, C. 1987b. Paleoenvironments along the eastern Laurentide Ice Sheet margin and timing of the last ice maximum and retreat. *Géographie physique et Quaternaire*, **41**: 265-277.
- de Vernal, A., Turon, J-L., and Guiot, J. 1994. Dinoflagellate cyst distribution in high latitude environments and development of transfer function for the reconstruction of sea-surface temperature, salinity and seasonality. *Canadian Journal of Earth Sciences*, **31**: 93-107.
- Doh, S. J., King, J. W., and Leinen, M. 1988. A rock-magnetic study of Giant Piston Core LL44-GPC from the Central North Pacific and its paleoceanographic significance. *Paleoceanography*, **3**: 89-111.
- Dunlop, D. J. 1981. The rock magnetism of fine particles. *Physics of the Earth and Planetary Interiors*, **26**: 1-26.
- Duplessy, J. C., Shackleton, N. J., Fairbanks, R. G., Labeyrie, L., Oppo, D., and Kallel, N. 1988. Deep water source variations during the last climatic cycle and their impact on the global deepwater circulation. *Paleoceanography* **3**: 343-360.

- Finney, B. P. Mitchell, W. L. and Heath, G. R. 1988. Sedimentation at MANOP site H (eastern equatorial Pacific) over the past 400,000 years: climatically induced redox variations and their effects on transition metal cycling. *Paleocenography*, **3**: 169-189.
- Hall, F. R. and King, J. W. 1989. Rock-magnetic stratigraphy of site 645 (Baffin Bay) from ODP leg 105. *Proceedings of the Ocean Drilling Program: Scientific Results*, **105**: 843-849.
- Hall, F. R., Bloemendal, J., King, J. W. Arthur, M. A., and Aksu, A. E. 1989a. Middle to Late Quaternary sediment fluxes in the Labrador Sea, ODP Leg 105, Site 646: A synthesis of rock-magnetic, Oxygen isotopic, carbonate, and planktonic foraminiferal data. *Proceedings of the Ocean Drilling Program: Scientific Results*, **105**: 653-665.
- Hall, F. R., Busch, W. H., and King, J. W. 1989b. The relationship between variations in rock-magnetic properties and grain size of sediments from ODP hole 645C. *Proceedings of the Ocean Drilling Program: Scientific Results*, **105**: 837-841.
- Hesse, R., and Chough, S. K. 1980. The Northwestern Atlantic Mid-Ocean Channel of the Labrador Sea: II, depositional of parallel laminated levee-muds from the viscous sublayer of low density turbidity currents. *Sedimentology*, **27**: 697-711.
- Hillaire-Marcel, C., and de Vernal, A. 1989. Isotopic and palynological records of the Late Pleistocene in Eastern Canada and adjacent ocean basins. *Géographie Physique et Quaternaire*, **43**: 263-290.
- Hillaire-Marcel, C., and Rochon, A. and onboard participants. 1990. Cruise report and onboard studies, CSS *Hudson* 90-013, May 29th-June 22nd 1990, leg 1: the Labrador Sea. Geological Survey of Canada, Open-File 2531.
- Hillaire-Marcel, C., de Vernal, A., Bilodeau, G. and Wu, G. 1993a. Isotope stratigraphy, sedimentation rates, deep circulation and carbonate events in the Labrador Sea during the last ~ 200 ka. *Canadian Journal of Earth Sciences*, **31**: 63-89.
- Hillaire-Marcel, C., de Vernal, A., Lucotte, M., Mucci, A., Bilodeau, G., Rochon, A., Vallières, S., and Wu, G., 1993b. Productivité et flux de carbone dans la mer du Labrador au cours des derniers 40 000 ans. *Canadian Journal of Earth Sciences*, **31**: 139-158.
- Hiscott, R. N., Cremer, M., and Aksu, A. E. 1989. Evidence from sedimentary structures for processes of sediment transport and deposition during Post-Miocene time at Sites 645, 646, and 647, Baffin Bay and the Labrador Sea. *Proceedings of the Ocean Drilling Program: Scientific Results*, **105**: 53-64.
- Karlin, R. 1990. Magnetic mineral diagenesis in suboxic sediments at Bettis site W-N, NE Pacific Ocean. *Journal of Geophysical Research*, **95**: 4421-4436.
- King, J. W., and Channell, J. E. T. 1991. Sedimentary magnetism, environmental magnetism, and magnetostratigraphy. *In* U.S. National Report to International Union of Geodesy and Geophysics, *Reviews of Geophysics, Supplement*, pp. 358-370.

- King, J. W., Banerjee, S. K., Marvin, J., and Ozdemir, O. 1982. A comparison of different magnetic methods for determining the relative grain size of magnetite in natural materials: some results from lake sediments. *Earth and Planetary Science Letters*, **59**: 404-419.
- Labeyrie, L. D., Duplessy, J.-C., Duprat, J., Juillet-Leclerc, A., Moyes, J., Michel, E., Kallel, N., and Shackleton, N.J. 1992. Changes in the vertical structure of the North Atlantic ocean between glacial and modern times. *Quaternary Science Reviews*, **11**: 401-413.
- Lehman, S. J., and Keigwin, L. D. 1992. Sudden changes in North Atlantic circulation during the last deglaciation. *Nature (London)*, **356**: 757-762.
- Lucotte, M., and Hillaire-Marcel, C. 1994. Identification et distribution des grandes masses d'eau dans les mers du Labrador et d'Irminger. *Canadian Journal of Earth Sciences*, **31**: 5-13.
- Lucotte, M., Mucci, A., Hillaire-Marcel, C., and Tran, S. 1994. Early diagenetic processes in deep Labrador Sea sediments: reactive and non reactive iron and phosphorous. *Canadian Journal of Earth Sciences*, **31**: 14-27.
- Maher, B. A. 1988. Magnetic properties of some synthetic sub-micron magnetites. *Geophysical Journal of the Royal Astronomical Society*, **94**: 83-96.
- Mangerud, J., Lie, S. E., Furnes, H., Kristiansen, I. L., and Lømo, L. 1984. A Younger Dryas ash bed in western Norway, and its possible correlations with Tephra in cores from the Norwegian Sea and the North Atlantic. *Quaternary Research*, **21**: 85-104.
- Martinson, D. G., Pisias, N. G., Hays, J. D., Imbrie, J., Moore, T. C. Jr. and Shackleton, N. J. 1987. Age dating and the orbital theory of the Ice Ages: development of a high-resolution 0 to 300,000-year chronostratigraphy. *Quaternary Research*, **27**: 1-29.
- McCartney, M. S. 1992. Recirculating components to the deep boundary current of the North Atlantic. *Progress in Oceanography*, **29**: 283-383.
- McCave, I. N., and Tucholke, B. E. 1986. Deep current-controlled sedimentation in western North Atlantic. *In The Western North Atlantic Region. Edited by P. R. Vogt, and B. E. Tucholke. Geological Society of America, The Geology of North America, Volume M, pp. 451-468.*
- Mead, G. A., Tauxe, L., and LaBrecque, J. L. 1986. Oligocene paleoceanography of the South Atlantic: paleoclimatic implications of sediments accumulation rates and magnetic susceptibility. *Paleoceanography*, **1**: 272-284.
- Mienert, J., and Bloemendal, J. 1989. A comparison of acoustic and rock magnetic properties of equatorial Atlantic deep-sea sediments: paleoclimatic implications. *Earth and Planetary Science Letter*, **94**: 291-300.

- Miller, G. H., and de Vernal, A. 1992. Will greenhouse warming lead to northern hemisphere ice sheet growth? *Nature (London)*, **357**: 244-247
- O'Reilly, W. 1984. *Rock and Mineral Magnetism*. Blackie & Son Ltd., Glasgow and London.
- Pruysers, P., de Lange, G. J., Middelburg, J. J., and Hydes, D. J. 1993. The diagenetic formation of metal-rich layers in sapropel-containing sediments in the eastern Mediterranean. *Geochimica et Cosmochimica Acta*, **57**: 527-536.
- Rabinowitz, P. D., and Eittreim, S. L. 1974. Bottom Current measurements in the Labrador Sea. *Journal of Geophysical Research*, **79**: 4085-4090.
- Robinson, S. G. 1986. The Late Pleistocene palaeoclimatic record of North Atlantic deep-sea sediments revealed by mineral-magnetic measurements. *Physics of the Earth Planetary Interiors*, **42**: 22-46.
- Robinson, S. G. 1990. Applications of whole-core magnetic susceptibility measurements of deep-sea sediments, *In* Duncan, R. A., Backman, J., Peterson, L. C. et al., *Proceedings of the Ocean Drilling Program, Scientific Results*, **115**: 737-771.
- Srivastava, S., Arthur, M. A., and Shipboard Party 1987. Initial Report of the Ocean Drilling Program 105. Part A, U.S. Government Printing Office, Washington D. C.
- Thompson, R. 1986. Modeling magnetization data using SIMPLEX. *Physics of the Earth and Planetary Interiors*, **42**: 113-127.
- Thompson, R., and Oldfield, F. 1986. *Environmental Magnetism*. Allen & Unwin, New York.
- Veum, T., Jansen, E., Arnold, M., Seyer, I., and Duplessy, J.-C. 1992. Water mass exchange between the North Atlantic and the Norwegian Sea during the past 28,000 years. *Nature (London)*, **356**: 783-785.
- Wison, T. R. S., Thomson, J., Colley, S., Hydes, D. J., Higgs, N. C., and Sorensen, J. 1985. Early organic diagenesis: The significance of progressive subsurface oxidation fronts in pelagic sediments. *Geochimica et Cosmochimica Acta*, **49**: 811-822.
- Wison, T. R. S., Thomson, J., Hydes, D. J., Colley, S., Culkin, F., and Sorensen, J. 1986. Oxidation fronts in pelagic sediments: Diagenetic formation of metal-rich layers. *Science (Washington, D.C.)*, **232**: 972-975.
- Wu, G.-P. and Hillaire-Marcel, C. 1993. AMS radiocarbon stratigraphies in deep Labrador Sea Cores: paleoceanographic implications. *Canadian Journal of Earth Science*, **31**: 38-47.
- Yu, L. and Oldfield, F. 1989. A multivariate mixing model for identifying sediment source from magnetic measurements, *Quaternary Research*, **32**: 168-181.

CHAPTER II

MAGNETIC PROPERTIES OF DEEP-SEA SEDIMENTS OFF SOUTHWEST GREENLAND: EVIDENCE FOR MAJOR DIFFERENCES BETWEEN THE LAST TWO DEGLACIATIONS

2.1 INTRODUCTION

Piston core HU90-013-013 (P-013) was taken from the Labrador Sea, on the Greenland rise, northwest of the of the Eirik Ridge (lat 58°13'N, long 48°22'W, present water depth: 3380 m), at approximately the same location as Ocean Drilling Program Site 646 (Leg 105) (Fig. 2.1). The *N. pachyderma* (left-coiled) derived planktonic $\delta^{18}\text{O}$ record for this 17.4 m core indicates that the base was deposited during an interstadial period in isotopic stage 6 or in stage 7 (Hillaire-Marcel et al., 1994). Late Pleistocene sedimentation in the deep Labrador Sea was largely detrital. The coarse sediment fraction ($>125\ \mu\text{m}$) primarily reflects ice-rafted debris (IRD), which was almost exclusively deposited during glacial isotopic stages 6 and 4 to 2 and was at a maximum during Heinrich events. During interglacial periods, deposition was primarily from hemipelagic suspension with much higher sedimentation rates during the Holocene (32-54 cm/ka) than during the preceding glacial interval (10-15 cm/ka) (Hillaire-Marcel et al., 1994).

Magnetic measurements were carried out on 7 cm³ cubic samples collected back-to-back downcore, with each sample representing ~2.0 cm of core length. Although a wide range of magnetic measurements have been carried out on this core (see Stoner et al., 1994), we restrict our discussion to the records at Termination I and Termination II of two parameters: volumetric magnetic susceptibility (k) and

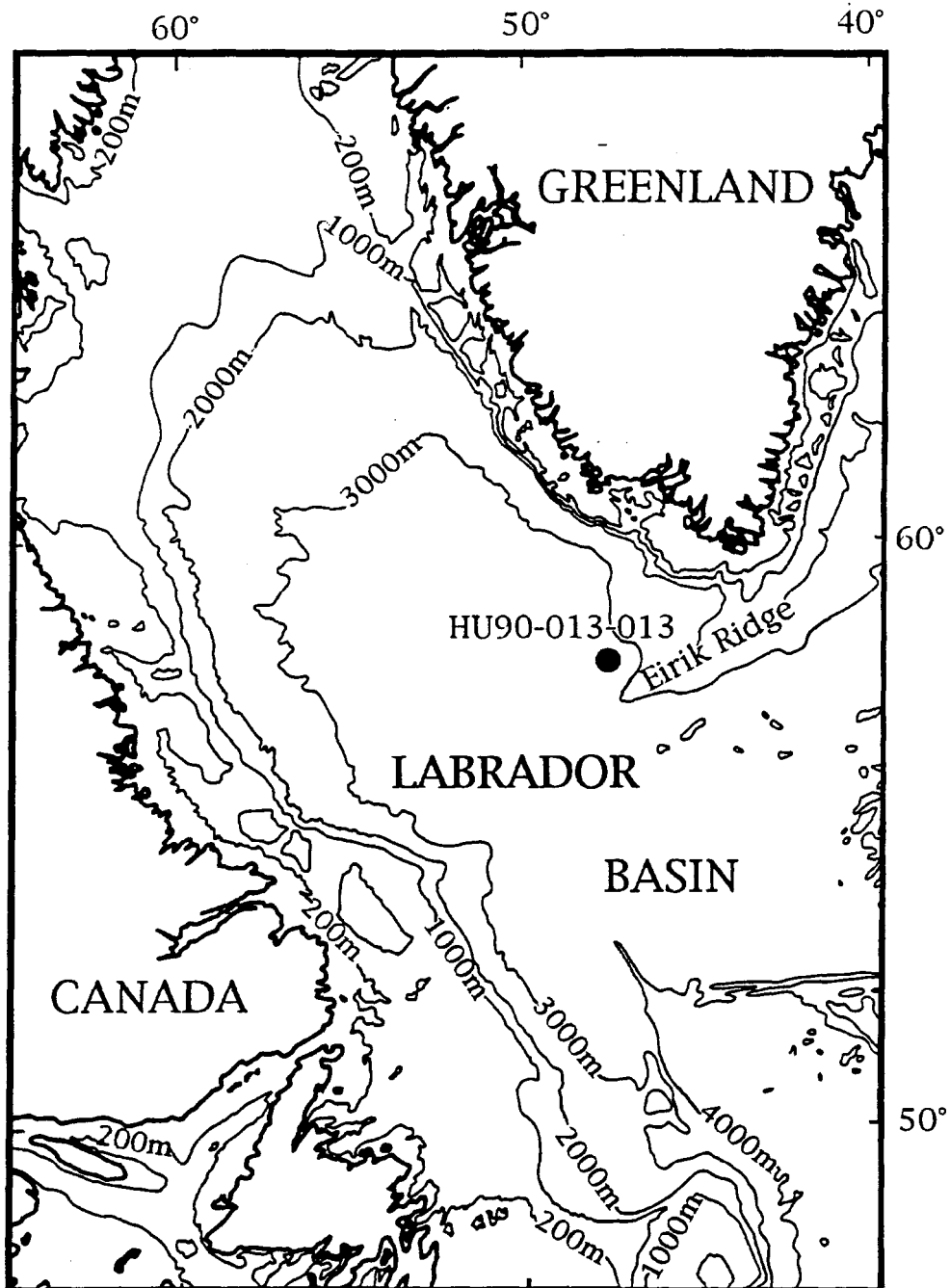


Figure 2.1. Location map, showing site of piston core HU90-013-013 (P-013).

anhysteretic remanent magnetization expressed as anhysteretic susceptibility (k_{ARM}). Numerous magnetic hysteresis loops from these intervals indicate that magnetite is the only magnetic mineral present in detectable quantity. Hysteresis ratios lie in the pseudo-single domain field of the Day et al. (1977) plot and display a grain-size mixing trend (Fig. 2.2). In this core, k is therefore primarily a measure of the concentration of magnetite, and variations in the ratio k_{ARM}/k are inversely related to changes in the fine (~ 0.1 - $20 \mu\text{m}$) magnetite grain-size (see King et al., 1982; Bloemendal et al., 1992, 1993). We document changes in magnetic parameters during Termination I (stage 2/1) and Termination II (stage 6/5) and compare these changes with $\delta^{18}\text{O}$, atomic mass spectroscopy (AMS) ^{14}C dates, percent carbonate, laser microgranulometer-determined mean grain-size (in μm) of the $<160 \mu\text{m}$ fraction, and coarse fraction percent $>125 \mu\text{m}$ (Hillaire-Marcel et al., 1994). The magnetic parameters at this location appear to be particularly sensitive to environmental changes during the last two deglaciations, providing a link between ice-sheet behavior and the marine-sediment record.

2.2 TERMINATION I

The dominant feature of the magnetic record at Termination I is a broad low in k_{ARM}/k (between 235 and 375 cm below the sea floor) coinciding with a high in k (Fig. 2.3). These changes in magnetic parameters, indicating an increase in magnetite (fine-fraction) grain-size and concentration, postdate the $\delta^{18}\text{O}$ change defining the stage 2/1 transition (~ 440 cm). The onset of the change in magnetic properties coincides with (1) the end of a distinct fluctuation in k_{ARM}/k , which is coeval with the Younger Dryas (Fig. 2.3); (2) a marked decrease in IRD indicated by the coarse fraction percent $>125 \mu\text{m}$ (Fig. 2.3D); (3) an increase in the mean grain-size of the $<160 \mu\text{m}$ fraction (Fig. 2.3D); (4) low carbonate percent (Fig. 2.3D); and (5) the highest sedimentation rates in

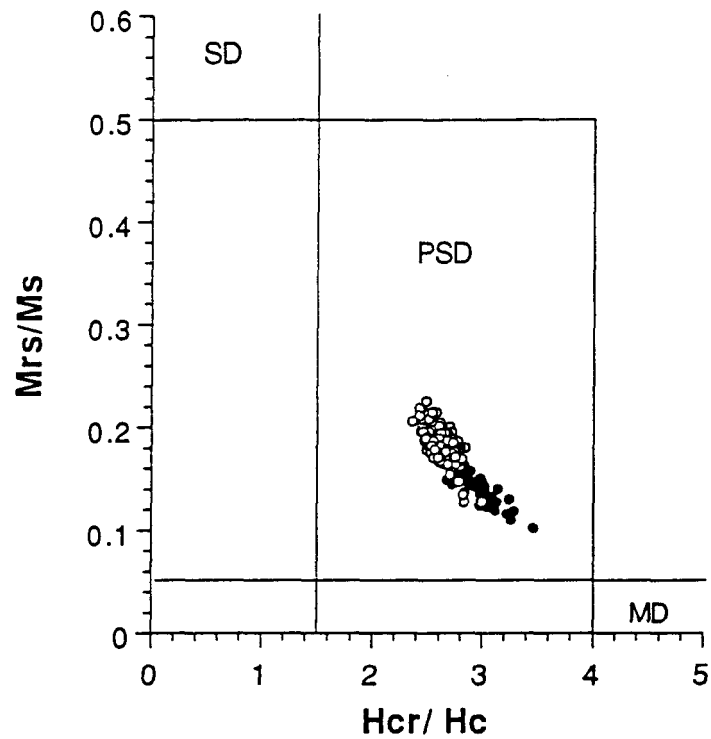


Figure 2.2. Hysteresis ratios of 187 samples from upper 500 cm and from 1200 to 1600 cm of P-013. Solid circles from ME events and shaded core intervals (see Fig. 3 and Fig. 4); open circles from background sediment (outside shaded intervals in Fig. 3 and Fig. 4). M_{rs} saturation remanence; M_s saturation magnetization; H_{cr} remanent coercivity; H_c coercive force. Single-domain (SD), pseudo-single-domain (PSD), and multidomain (MD) fields after Day et al. (1977).

the core (Fig. 2.3B). The AMS ^{14}C dates bracket this broad change in magnetic properties within the 10-7.7 ka interval (Fig. 2.3B).

Three short-lived fluctuations in k_{ARM}/k precede the broad change in magnetic properties mentioned above. (1) Increased k_{ARM}/k (with little change in k) at ~11 to 10.4 ka is correlated to the Younger Dryas as defined by $\delta^{18}\text{O}$, the Vedde ash, and AMS ^{14}C dates (Hillaire-Marcel et al. 1994) (Fig. 2.3, B and C). (2) Decreased k_{ARM}/k at ~14 ka is correlated to Heinrich Event 1 (Fig. 2.3, A and B). This fluctuation occurs just prior to the change in $\delta^{18}\text{O}$ marking the stage 2/1 boundary (Fig. 2.3A) and is associated with an increase in IRD (Fig. 2.3D). (3) A distinct fluctuation in k_{ARM}/k and k (ME_1 in Fig. 2.3) after 16 990 yr B.P. (^{14}C dating), and prior to the $\delta^{18}\text{O}$ shift at the stage 2/1 transition, correlates with a decrease in IRD and carbonate and an increase in the mean grain-size (Fig. 2.3D).

The geologic record of deglaciation in this region indicates two distinct stages, disintegration of marine ice and melting of continental ice (Funder, 1989). The onset of deglaciation is poorly determined; however, radiocarbon dates indicate that the ice margin in all parts of Greenland was located near the present coastline by 10-11 ka (Funder, 1989). The second stage in the retreat of the Greenland ice-sheet involved melting of land-based ice, which retreated to approximately its present position in southwestern Greenland by 8 ka (Kelly, 1985), and continued to retreat to inside its present position until ~7 ka (Funder, 1989).

The magnetic interval of high k and low k_{ARM}/k at 10-7.7 ka (Fig. 2.3) is interpreted to be caused by the transfer of large amounts of glacially eroded detritus to the deep sea by meltwater as the Greenland ice-sheet retreated from the coast into the continental interior. According to this hypothesis, the increased magnetic grain-size and concentration is due to a proximal meltwater source carrying detritus from the crystalline

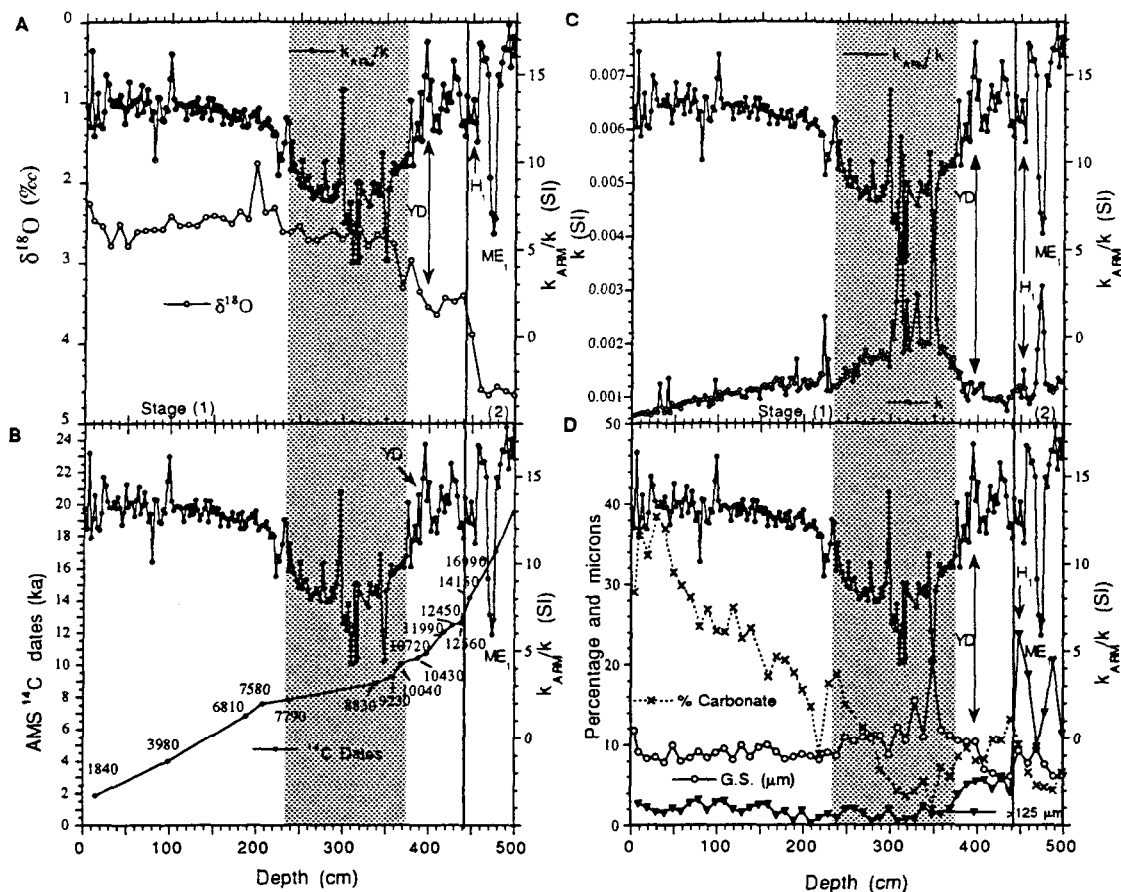


Figure 2.3. A: Magnetic grain-size dependent parameter k_{ARM}/k (solid circles) (increased magnetic grain size indicated by smaller values) compared with planktonic $\delta^{18}\text{O}$ record from *N. pachyderma* (left coiled) (open circles) for upper 500 cm of P-013. Shaded area delineates interval of increased magnetite concentration and grain size interpreted as continental-meltwater-derived detrital flux from southern Greenland; vertical line at 440 cm marks isotopic stage 2/1 boundary. YD = Younger Dryas, H₁ = Heinrich event 1, ME₁ = magnetic event attributed to the beginning of deglaciation prior to Termination I. B: Diagram of k_{ARM}/k (solid circles) compared with corrected (-400 yr for reservoir effect) atomic mass spectroscopy ^{14}C dates. C: Diagrams of k_{ARM}/k (solid circles) compared with the magnetic concentration dependent parameter k (open circles). D: k_{ARM}/k (solid circles) compared with percent carbonate (CO_3) (X's), mean grain size (G.S.; in μm) for the $< 160 \mu\text{m}$ fraction (open circles), and percent coarse fraction $> 125 \mu\text{m}$ (solid triangles).

bedrock of Greenland. Because the interval coincides with the highest sedimentation rates in the core, the record cannot be an artifact of sediment winnowing. The interpretation is supported by high silicate flux during this interval (Hillaire-Marcel et al., 1994) and by a distinct change in the solid phase Fe, Mn, and P which has been attributed to a shift from a distal to a proximal detrital source (Lucotte et al., 1994). The lack of a large magnetic response to the first (marine) stage of deglaciation (characterized by high IRD) indicates that k and k_{ARM}/k (at this location) were relatively insensitive to IRD deposition associated with marine deglaciation, possibly due to different sources for some of this detrital material. The end of the magnetic interval at ~ 7.7 ka occurs at approximately the time of maximum ice retreat on Greenland (Funder, 1989) and a return to relatively stable ice-sheet conditions.

2.3 TERMINATION II

A broad change in k_{ARM}/k and k is associated with the isotopic substage 5e (Fig. 4). As with Termination I, the change in magnetic properties indicates an increase in magnetite grain-size and concentration which coincides with a marked decrease in IRD and carbonate, and an increase in the mean grain-size (in μm) of the $<160 \mu\text{m}$ fraction (Fig. 2.4C). As for Termination I, we interpret this magnetic signal to be due to an influx of continental meltwater detritus. For Termination II, however, the onset of the change in magnetic properties coincides with the $\delta^{18}\text{O}$ shift defining the stage 6/5 glacial-interglacial transition (Fig. 2.4A). The magnetic signal continues throughout substage 5e, implying a source of land-derived detrital input until just prior to the 5e/5d boundary (Fig. 2.4A).

An additional distinct fluctuation in k_{ARM}/k and k (ME₂ in Fig. 2.4) precedes the $\delta^{18}\text{O}$ shift of the stage 6/5 boundary. This fluctuation is similar in all respects to

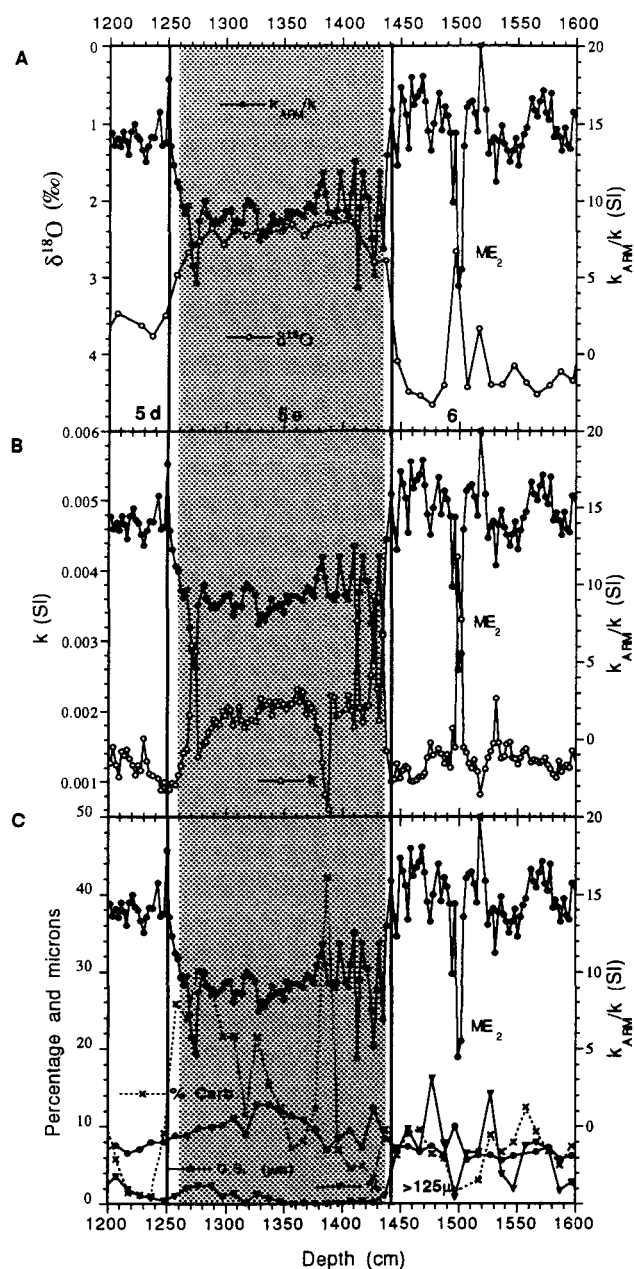


Figure 2.4. A: Magnetic grain-size dependent parameter k_{ARM}/k (solid circles) (increased magnetic grain-size indicated by smaller values) compared with planktonic $\delta^{18}O$ record from *N. pachyderma* (left coiled) (open circles) for interval from 1200 to 1600 cm of P-013. Shaded area delineates interval of increased magnetite concentration and grain size interpreted as continental-meltwater derived detrital flux from southern Greenland, vertical lines at 1250 and 1440 cm mark isotopic substage 5e/d and stage 6/5 boundaries, respectively. ME₂ = magnetic event attributed to the beginning of deglaciation prior to Termination II. B: Diagram of k_{ARM}/k (solid circles) compared with magnetic concentration dependent parameter k (open circles). C: Diagram of k_{ARM}/k (solid circles) compared with percent carbonate (X's), mean grain size (G.S.) for the <160 μ m grain-size fraction (open circles), and the percent coarse fraction >125 μ m (solid triangles). Note: large carbonate spike at 1390 cm is of detrital origin.

ME₁ prior to Termination I (Fig. 2.3). However, at Termination II, the magnetic event coincides with a light peak in the $\delta^{18}\text{O}$ record (Fig. 2.4A).

2.4 DISCUSSION

The coincidence of the onset of the change in k and k_{ARM}/k with an almost complete cessation in IRD deposition and, for Termination I, with the time at which the Greenland ice sheet reached the present coastline is consistent with the interpretation that the onset of the change in magnetic properties marks the disappearance of marine-based ice and the beginning of continental-derived meltwater flux. The change in magnetic parameters is associated with an increased contribution from a proximal highly magnetic detrital source as compared to a more distal and less magnetic source associated with much of the IRD (i.e., Hudson Straits for the Heinrich events). The return to background magnetic properties at ~ 7.7 ka is consistent with the time at which the ice-sheet was stabilized.

The AMS ^{14}C stratigraphy indicates that the temporary increase in magnetite grain-size and concentration at Termination I occurred between 10 and 7.7 ka (Fig. 2.3B). Peak values occurred between 9.2 and 8.5 ka correlating with the later part of the Fairbanks (1989) meltwater pulse Ib, whereas the entire magnetic episode occurs during Termination Ib (Duplessy et al., 1981, 1986). No corresponding magnetic signal is associated with the Fairbanks (1989) meltwater pulse Ia or Termination Ia (Duplessy et al., 1981, 1986).

In contrast to the two-step deglaciation associated with Termination I, Termination II is generally characterized in the marine record by a fairly sudden and simple $\delta^{18}\text{O}$ decrease (e.g., Broecker and van Donk, 1970; Martinson et al., 1987). In our record of Termination II (Fig. 2.4), a $\delta^{18}\text{O}$ shift of 2.4‰ occurs over an interval of 70 cm from glacial maximum values of 4.7‰ at 1477 cm to full interglacial $\delta^{18}\text{O}$ values of 2.3‰ at

1407 cm. The change in $\delta^{18}\text{O}$ from 4.1‰ to 2.8‰ in 10 cm coincides with a factor of two increase in k and a 50% decrease in k_{ARM}/k (Fig. 2.4A). This large and rapid increase in magnetite grain-size and concentration coincides with an almost complete disappearance of IRD, an increase in mean grain size, and low carbonate percentage (Fig. 2.4C). If, as postulated, this magnetic signal is due to land-derived meltwater detritus, then substantial ice retreat must have occurred extremely early in Termination II. As the Greenland ice-sheet is believed to have been more extensive during isotopic stage 6 than during the last glacial maximum (Kelly, 1985; Funder, 1989), an extremely high rate of Greenland margin deglaciation is required to explain the synchronicity of the magnetic and $\delta^{18}\text{O}$ records. Alternatively, significant deglaciation of the marine-based Greenland ice margin prior to the decrease in $\delta^{18}\text{O}$ (see Crowley, 1994) could also explain the synchronicity of the records. The early deglaciation of the Greenland continent, independent of the deglaciation rate, suggests a much greater sensitivity of the Greenland ice-sheet to initial deglacial forcing during Termination II than is observed for Termination I. This implies that initial stages of deglaciation had a different geographical distribution for the two terminations.

Distinct fluctuations in k_{ARM}/k and k prior to Termination I (ME₁; Fig. 2.3) and Termination II (ME₂; Fig. 2.4) are interpreted to be due to a sudden pulse of detritus into the basin. Both events correlate with an increase in mean grain-size and a decrease in IRD and carbonate and are characterized by laminated sediments; ME₂ also correlates with a large decrease in $\delta^{18}\text{O}$ indicative of a meltwater pulse. These events are interpreted to signify the beginning of deglaciation, marking the unpinning of grounded ice from the continental shelf, leading to a short-term depositional event at this site. ME₁ during stage 2 occurs just above an AMS ^{14}C date of 16 990 yr B.P., which places this event at the time of the beginning of eustatic sea-level rise (Fairbanks 1989) and with established melt events in the Davis Strait and the Labrador Sea (Hillaire-Marcel and de Vernal, 1989; Andrews et al.,

1994). During isotopic stage 6, light $\delta^{18}\text{O}$ events have also been observed in the Labrador Sea (Fillon, 1985) and Norwegian Sea (Kellogg et al., 1978). Therefore the ME events may be equivalent to the Imbrie et al. (1993) "Major Nordic" deglaciation events postulated to indicate early response to insolation changes.

REFERENCES

- Andrews, J. T., Erlenkeuser, H., Tedesco, K., Aksu, A. E., and Jull, A. J. T., 1994, Late Quaternary (Stage 2 and 3) meltwater and Heinrich events northwest Labrador Sea: *Quaternary Research*, v. 41, p. 26-34.
- Bloemendal, J., King, J. W., Hall, F. R., and Doh, S. J. 1992, Rock magnetism of Late Neogene and Pleistocene deep-sea sediments: relationship to sediment source, diagenetic processes, and sediment lithology: *Journal of Geophysical Research*, v. 97, p. 4361-4375.
- Bloemendal, J., King, J. W., Hunt, A., DeMenocal, P. B., and Hayahida, A., 1993, Origin of the sedimentary magnetic record at ocean drilling program sites on the Owen Ridge, Western Arabian Sea: *Journal of Geophysical Research*, v. 98, p. 4199-4219.
- Broecker, W., and Van Donk, J., 1970, Insolation changes, ice volumes, and ^{18}O record in deep sea cores: *Reviews of Geophysics*, v. 8, p. 169-198.
- Crowley, T. J., 1994. Potential reconciliation of Devils Hole and deep-sea Pleistocene chronologies: *Paleoceanography*, v. 9, p. 1-5.
- Day, R., Fuller, M., and Schimdt, V. A., 1977, Hysteresis properties of titanomagnetites: Grain size and compositional dependence: *Physics of the Earth and Planetary Interiors*, v. 13, p. 260-267.
- Duplessy, J.-C., Delibrias, G., Turon, J. L., Pujol, C., and Duprat, J., 1981, Deglacial warming of the northeastern Atlantic Ocean: Correlation with the paleoclimatic evolution of the European continent: *Paleogeography, Paleoclimatology, Paleoecology*, v. 35, p. 121-144.
- Duplessy, J.-C., Arnold, M., Maurice, P., Bard, E., Duprat, J., and Moyes, J., 1986, Direct dating of the oxygen-isotope record of the last deglaciation by ^{14}C accelerator mass spectrometry: *Nature*, v. 320, p. 350-352.
- Fairbanks, R. G., 1989, A 17,000-year glacio-eustatic sea level record: Influence of glacial melting rates on the Younger Dryas event and deep-ocean circulation: *Nature*, v. 342, p. 637-642.
- Fillon, R. H., 1985, Northwest Labrador Sea stratigraphy, sand input and Paleooceanography during the last 160,000 years, *in* Andrews, J. T., ed., *Quaternary environments, eastern Canadian Arctic, Baffin Bay and western Greenland*: Boston, Allen & Unwin, p. 211-247.
- Funder, S., 1989, Quaternary geology of the ice-free areas and adjacent shelves of Greenland, *in* Fulton, R.J., ed., *Quaternary geology of Canada and Greenland*: Geological Survey of Canada, *Geology of Canada*, no. 1, p. 743-792.

- Hillaire-Marcel, C., and de Vernal, A., 1989, Isotopic and palynological records of the Late Pleistocene in Eastern Canada and adjacent ocean basins. *Géographie physique et Quaternaire*, v. 43, p. 263-290.
- Hillaire-Marcel, C., de Vernal, A., Bilodeau, G., and Wu, G. 1994, Isotope stratigraphy, sedimentation rates, deep circulation and carbonate events in the Labrador Sea during the last ~ 200 ka: *Canadian Journal of Earth Sciences*, v. 31, p. 63-89.
- Imbrie, J., and 18 others, 1993, On the structure and origin of major glaciation cycles 2. The 100,000-year cycle: *Paleoceanography*, v. 8, p. 699-735.
- Kelly, M., 1985. A review of the Quaternary geology of western Greenland, *in* Andrews, J. T.ed., *Quaternary environments eastern Canadian Arctic, Baffin Bay and Western Greenland*: Allen & Unwin, Boston, p. 461-501.
- Kellogg, T. B., Duplessy, J.-C., and Shackleton, N. J., 1978, Planktonic foraminiferal and oxygen isotopic stratigraphy and paleoclimatology of Norwegian Sea deep-sea cores: *Boreas*, v. 7, p. 61-73.
- King, J. W., Banerjee, S. K., Marvin, J., and Ozdemir, O., 1982, A comparison of different magnetic methods for determining the relative grain size of magnetite in natural materials: some results from lake sediments: *Earth and Planetary Science Letters*, v. 59, p. 404-419.
- Lucotte, M., Mucci, A., Hillaire-Marcel, C., and Tran, S., 1994. Early diagenetic processes in deep Labrador Sea sediments: Reactive and nonreactive iron and phosphorus, *Canadian Journal of Earth Sciences*, v. 31 p. 14-27.
- Martinson, D. G., Pisias, N. G., Hays, J. D., Imbrie, J., Moore, T. C. Jr. and Shackleton, N. J. 1987, Age dating and the orbital theory of the Ice Ages: Development of a high-resolution 0 to 300,000-year chronostratigraphy: *Quaternary Research*, v. 27, p. 1-29.
- Stoner, J. S., Channell, J. E. T., Hillaire-Marcel, C., and Mareschal, J.-C., 1994, High resolution rock magnetic study of a Late Pleistocene core from the Labrador Sea: *Canadian Journal of Earth Sciences*, v. 31, p. 104-114.

CHAPTER III

THE MAGNETIC SIGNATURE OF RAPIDLY DEPOSITED DETRITAL LAYERS FROM THE DEEP LABRADOR SEA: RELATIONSHIP TO NORTH ATLANTIC HEINRICH LAYERS

3.1 INTRODUCTION

From several North Atlantic cores, Heinrich (1988) observed six distinct layers of high lithic content during the last ice age (oxygen isotope stages 2-4). These intervals, which correspond to low planktonic foraminifera abundance dominated by polar species *N. pachyderma* (left coiled) (Broecker et al., 1992), appear to occur synchronously across the North Atlantic from the Labrador Sea to Portugal (Bond et al., 1992a; Broecker et al., 1992; Hillaire-Marcel et al., 1994a). Heinrich layers were assumed to result from catastrophic surging of the Laurentide ice sheet, sending huge streams of icebergs which rapidly deposited carbonate-rich ice rafted debris (IRD) as they melted on their way across the North Atlantic (Bond et al., 1992a). Andrews and Tedesco (1992) used AMS ^{14}C dates and mineralogy to correlate two intervals of high detrital carbonate, labeled DC1 and DC2, from two northern Labrador Sea cores to the North Atlantic Heinrich layers H1 and H2, and proposed that these layers resulted from ice surges down Hudson Strait. Further south in the Labrador Sea, Hillaire-Marcel et al. (1994a) demonstrated that detrital carbonate deposition was decoupled from IRD deposition, suggesting two different depositional mechanisms for these layers within this basin.

Rock magnetic measurements in sediments are useful for detecting subtle lithologic changes. Composition, concentration and grain-size of magnetic minerals have been shown to vary from glacial to interglacial, due to dilution by biogenic material and

changing sources and transport mechanisms of magnetic minerals (e.g., bottom currents, fluvial, eolian activity, meltwater and ice rafting) (Kent, 1982; Robinson 1986, 1990; Bloemendal, 1983; Bloemendal et al., 1988, 1992, 1993; Doh et al., 1988; Bloemendal and de Menocal 1989; Stoner et al., 1994, 1995). The use of magnetic parameters to document sedimentological changes associated with sub-Milankovitch scale environmental variability in the deep North Atlantic has been restricted to susceptibility measurements. Troughs in magnetic susceptibility are associated with detrital carbonate (DC) layers from the northern Labrador Sea (Andrews and Tedesco, 1982; Andrews et al., 1993; 1994a,b) while Grousset et al. (1993) reported distinct peaks in susceptibility from Heinrich layers in the North Atlantic. Although the Heinrich and DC layers are interpreted to be derived from surging of the Laurentide ice sheet (Andrews and Tedesco 1992; Bond et al., 1992a; Hillaire-Marcel et al., 1994a), the contrasting susceptibility records suggest different depositional processes.

We present a high resolution magnetic study of core HU91-045-094 (P-094) raised from a small channel on the Labrador rise, southeast of Orphan's Knoll (50°12.26N, 45°41.14W, 3448 m; Fig. 3.1). This location, sheltered from major deep water current influence, was along the route of icebergs and meltwater from Hudson Strait to the North Atlantic during the last glacial period. This site is also near the Northwest Atlantic Mid-Ocean Channel (NAMOC) and within an area that may have been influenced by spill over turbidites from this conduit (Chough et al., 1987; Hesse et al., 1987) (Fig. 3.1). The 1098 cm piston core extends into oxygen isotope stage 5 clearly preserving a high quality record of Heinrich and detrital carbonate layers deposited during the last glacial interval (Hillaire-Marcel et al., 1994a).(Fig. 3.2). The magnetic and lithologic records from P-094 are compared with the records from piston core HU90-013-013 (P-013) (58°12.59N, 48°22.40W, water depth 3380 m; Fig. 3.1) taken from the Greenland Rise (Hillaire-Marcel

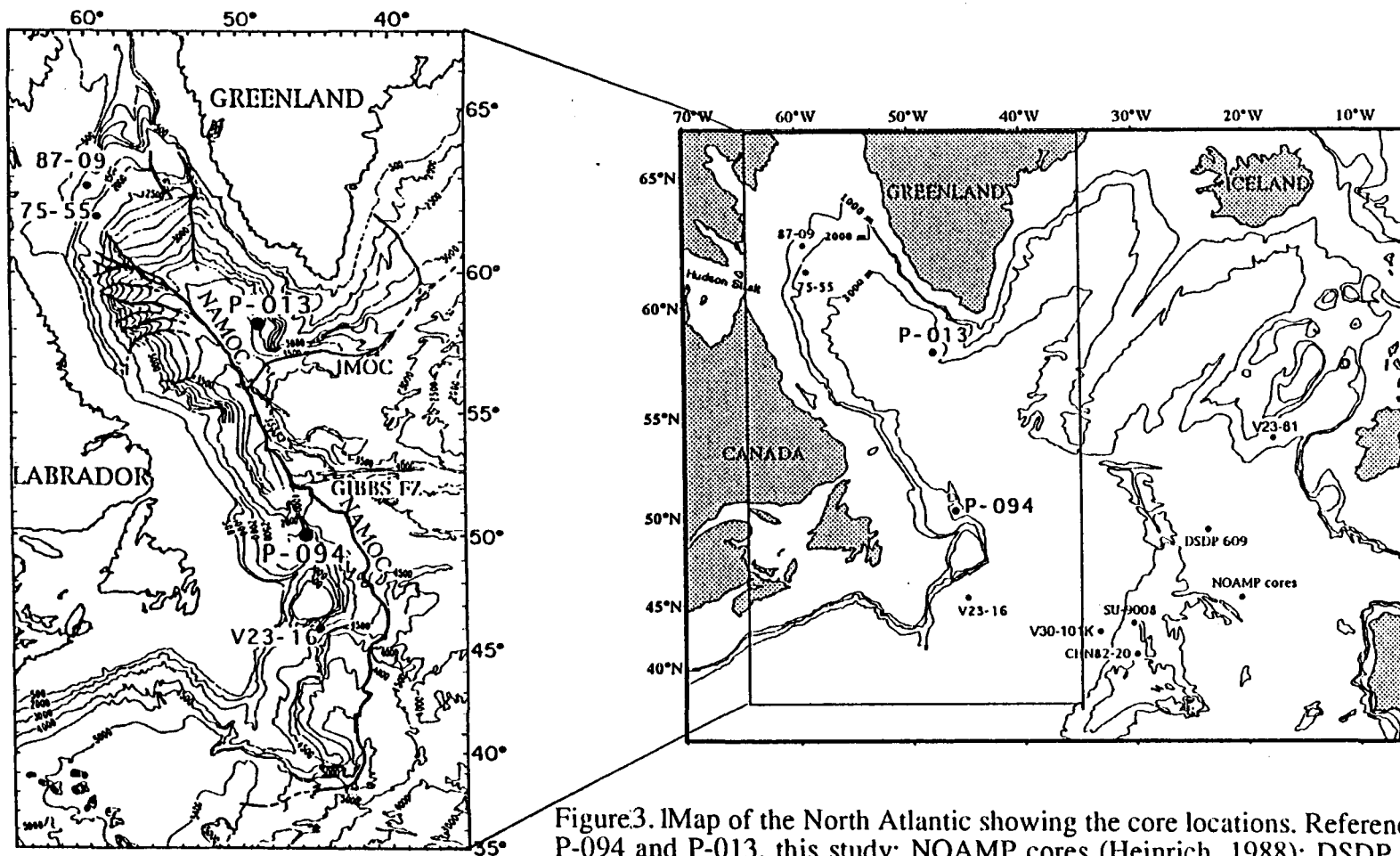


Figure 3. Map of the North Atlantic showing the core locations. References: P-094 and P-013, this study; NOAMP cores (Heinrich, 1988); DSDP site 609, V23-81, V30-101k, V23-16 (Broecker et al. 1991; Bond et al. 1992a,b; 1993), SU-9008 (Grousset et al. 1993); 75-55 and 87-009, (Andrews and Tedesco, 1992; Andrews et al. 1993;1994a,b); CHN82-20, (Keigwin and Lehman, 1994). Bathymetric chart of the Labrador Sea modified after Chough et al. (1987). NAMOC: Northwest Atlantic Mid-Ocean Channel; IMOC: Imarssuak Mid-Ocean Channel; Contours in meters.

et al., 1994a, Stoner et al., 1994; 1995). We intend to use these records to document and assess possible depositional mechanisms of "Heinrich" type layers in the deep Labrador Sea.

3.2 MAGNETIC METHODS

The P-094 core sections were cut with a rotary saw and the sediment split with an electric knife. The split core sections were continuously sampled onboard ship using 7.2 cc plastic cubes back-to-back, along the central axis, down the entire length of the core (473 total samples). The cubic samples were used for bulk rock magnetic measurement and were later subsampled for hysteresis and low temperature remanence experiments. The rock magnetic measurements were made in the magnetically-shielded laboratory at the University of Florida, while the hysteresis and low temperature experiments were made at the Institute for Rock Magnetism at the University of Minnesota.

3.2.1 Bulk Magnetic Parameters

The following magnetic measurements were made on all samples. (1) Low (k at 0.47 kHz) and high-frequency (k_{hf} at 4.7 kHz) volumetric magnetic susceptibility, the ratio of k to k_{hf} gives the frequency dependent magnetic susceptibility (k_f). (2) Natural remanent magnetization (NRM) and the NRM after 20 mT alternating field (AF) demagnetization. (3) Anhysteretic remanent magnetization (ARM) using a 99 mT peak AF and a 0.04 mT direct current biasing field (this is expressed as an anhysteretic susceptibility (k_{ARM}) by dividing by the strength of the biasing field). (4) Saturation isothermal remanent magnetization (SIRM) produced in a DC field of 1 T. (5) Back field isothermal remanent magnetization (BIRM) using DC fields of -0.1 T (BIRM_{0.1}) and -0.3 T (BIRM_{0.3}). The BIRM and SIRM were used to obtain the S-ratios (BIRM_{0.1}/SIRM = S_{0.1}) and (BIRM.

$S_{0.3}/\text{SIRM} = S_{0.3}$) and hard isothermal remanent magnetization (HIRM). $\text{HIRM}_{0.1}$ is defined as $(\text{SIRM} + \text{BIRM}_{0.1}) / 2$, while $\text{HIRM}_{0.3}$ is defined as $(\text{SIRM} + \text{BIRM}_{0.3}) / 2$.

The magnetic parameters k , k_{ARM} and SIRM are all dependent on the concentration of magnetic material. Since k values for ferrimagnetic minerals (magnetite and maghemite) are 3 or 4 orders of magnitude greater than those of common antiferromagnetic minerals (hematite and goethite), k is usually dominated by the ferrimagnetic grains, and gives information on the concentration of this group of minerals. When the concentration of ferrimagnetic minerals is very low, k reflects variations in the concentration of paramagnetic (e.g. clay minerals, ferromagnesian silicate minerals) and diamagnetic (e.g. biogenic carbonate, silica) components. Like k , k_{ARM} and SIRM are also dominated by the concentration of ferrimagnetic grains in the sample. However, unlike k , which increases slightly with increasing grain-size (Dunlop, 1986; Maher, 1988), k_{ARM} and SIRM increase with decreasing grain-size (Maher, 1988). Because of this behavior, ratios of these parameters are grain-size dependent. The k_{ARM} ratios, k_{ARM}/k and $\text{SIRM}/k_{\text{ARM}}$, vary with the dominant ferrimagnetic grain-size of the magnetic minerals in the assemblage. k_{ARM}/k decreases when grain-size increases from approximately 1 to 20 μm (King et al., 1982), while $\text{SIRM}/k_{\text{ARM}}$ increases when grain-size increases from approximately 0.1 to 10 μm . For grain-sizes greater than approximately 10 μm this parameter decreases with increasing grain-size (Maher, 1988; Bloemendal et al., 1993). SIRM/k also decreases with increasing grain-size (Thompson, 1986).

The $S_{0.3}$ parameter can be used as an indicator of the proportion of antiferromagnetic (e.g. hematite) to ferrimagnetic (e.g. magnetite), but is only truly discriminatory when the proportion of antiferromagnetic material is greater than about 80% of the magnetic assemblage (Bloemendal et al., 1992, 1993). $\text{HIRM}_{0.3}$ can be used to estimate the concentration of hematite. The $S_{0.1}$ parameter is also sensitive to the

proportion of antiferromagnetic to ferrimagnetic minerals in the assemblage, but it exhibits a strong secondary response to ferrimagnetic grain-size (Robinson, 1986).

3.2.2 Hysteresis Parameters

Hysteresis parameters were determined on a Princeton Measurements Corporation Alternating Gradient Force Magnetometer (μ MAG) using ≈ 10 mg of sediment rolled in plastic wrap and coated in Vaseline to prevent dehydration. Values of saturation magnetization (M_S), saturation remanence (M_{RS}) and coercive force (H_C) were determined from hysteresis loops. Values of coercivity of remanence (H_{CR}) and an additional measure of M_{RS} were determined from backfield experiments. The hysteresis parameters; H_C , H_{CR} and the ratio M_{RS}/M_S are a function of magnetite grain-size and domain state (see Dunlop, 1986). Both H_C and M_{RS}/M_S decrease slowly with increasing grain-size above approximately $10 \mu\text{m}$. H_{CR} has a weaker size dependence than H_C (Dunlop, 1986); thus trends in the ratio H_{CR}/H_C over a broad size range reflect mainly variations in H_C . M_{RS}/M_S is considered to be the most sensitive to grain-size because of its large variation over the (0.025 - $230 \mu\text{m}$) size range (Dunlop, 1986). H_{CR}/H_C increases with increasing magnetite grain-size is biased toward larger grain-sizes due to the weak size dependence of H_C for large pseudo-single domain (PSD) to multidomain (MD) grains (Hartstra, 1982; Dunlop, 1986).

3.2.3 Low Temperature Remanence

Low-temperature measurements were made on a Quantum Design Magnetic Properties Measurement System (MPMS) using ≈ 500 mg samples of dried sediment packed in a gel cap and placed in a drinking straw. The samples were cooled to 10 K, given an isothermal remanent magnetization (IRM) using a 500 mT field and then allowed

to warm to 160 K as the remanence was periodically monitored. Upon warming through 110-120 K, magnetite undergoes a crystallographic phase transition from monoclinic to cubic spinel known as the Verwey transition (T_V) (Verwey, 1939). This transition is diagnostic of magnetite, and is accompanied by an abrupt change in coercivity, remanence intensity, and susceptibility. Single crystal studies show that T_V is a maximum (118 K) for pure stoichiometric magnetite, and can drop below 100 K with small amounts of impurities (Özdemir et al., 1993). The amplitude of the remanence reduction associated with T_V is a function of grain-size, and the largest reduction is associated with large MD magnetite. Significant remanence reduction below T_V can be related to superparamagnetism as grains in this size range ($< \approx 0.03 \mu\text{m}$) reach their unblocking temperature.

3.3 CORE CHARACTERISTICS

In core P-094, Hillaire-Marcel et al. (1994a) identified peaks in coarse fraction ($>125 \mu\text{m}$) (Fig. 3.2) and correlated these to the Younger Dryas (H0) and North Atlantic Heinrich layers H1-H6 (Bond et al., 1992a; 1993). Peaks in coarse fraction correspond to high detrital carbonate (DC) layers or low detrital carbonate (LDC) layers as determined from the bulk carbonate content (Fig. 3.2). The high resolution magnetic properties clearly delineate these rapidly deposited detrital layers (Fig. 3.3), allowing identification of at least seven DC and six LDC layers deposited during the last glacial interval. Several LDC layers not previously recognized on the basis of coarse fraction or carbonate content (at 10 cm sampling intervals) are clearly visible in the magnetic record (Figs 3.2 and 3.3). The 13 DC and LDC layers identified by the magnetic parameters are considered to represent the minimum number of rapidly deposited detrital layers contained within the last glacial sediment. The general association of light $\delta^{18}\text{O}$ events, interpreted as meltwater dilution, with these layers (Hillaire-Marcel, et al., 1994a,b) and (Hillaire-Marcel, C. unpublished

data), suggests significantly greater Laurentide ice sheet variability than can be accounted for by the present Heinrich event stratigraphy.

The sediment from glacial and deglacial intervals, in P-094, commonly contains sand with occasional gravel and is composed of gray to dark gray hemipelagic mud. The DC layers are interspersed grayish brown (2.5Y 5/1) sandy and silty muds commonly containing gravel that are generally deposited over sharp sedimentary contacts. LDC layers also show sharp sedimentary contacts, but no color change (Fig. 3.2). Distinct from other DC and LDC layers, LDC5/6 is composed of two turbidite layers (LDC5 and LDC 6), which show graded bedding from bottom units of foraminifera rich sand deposited above clear erosional surfaces. This sedimentary structure is not observed in any other DC or LDC layer from P-094 or P-013. Unlike these DC layers in P-094, Heinrich layers further east in the North Atlantic (e.g. core SU-9008, Grousset et al., 1993) are often characterized by lower than background bulk carbonate content. Though, the IRD within the Heinrich layers is much richer in carbonate content than the IRD of the background sediment (Bond et al., 1992a ; Grousset et al., 1993).

3.4 MAGNETIC CHARACTERISTICS OF DC AND LDC LAYERS

3.4.1 Bulk Magnetic Parameters

All DC and LDC layers are characterized by low values of SIRM and k_{ARM} (Fig. 3.3). Relatively high values for k are observed from most DC and LDC layers, with k values for DC0 and DC1 lower or just slightly above background values. High negative values of $S_{0.3}$ (<-0.9) and the low values of $HIRM_{0.3}$ indicate that magnetic properties in this core are dominated by a low coercivity mineral(s) (e.g., magnetite) (Fig. 3.4). However several intervals of a slightly higher coercivity are observed. Slightly less negative $S_{0.3}$ values are found for LDC1-3 during the last glacial maximum and for LDC4

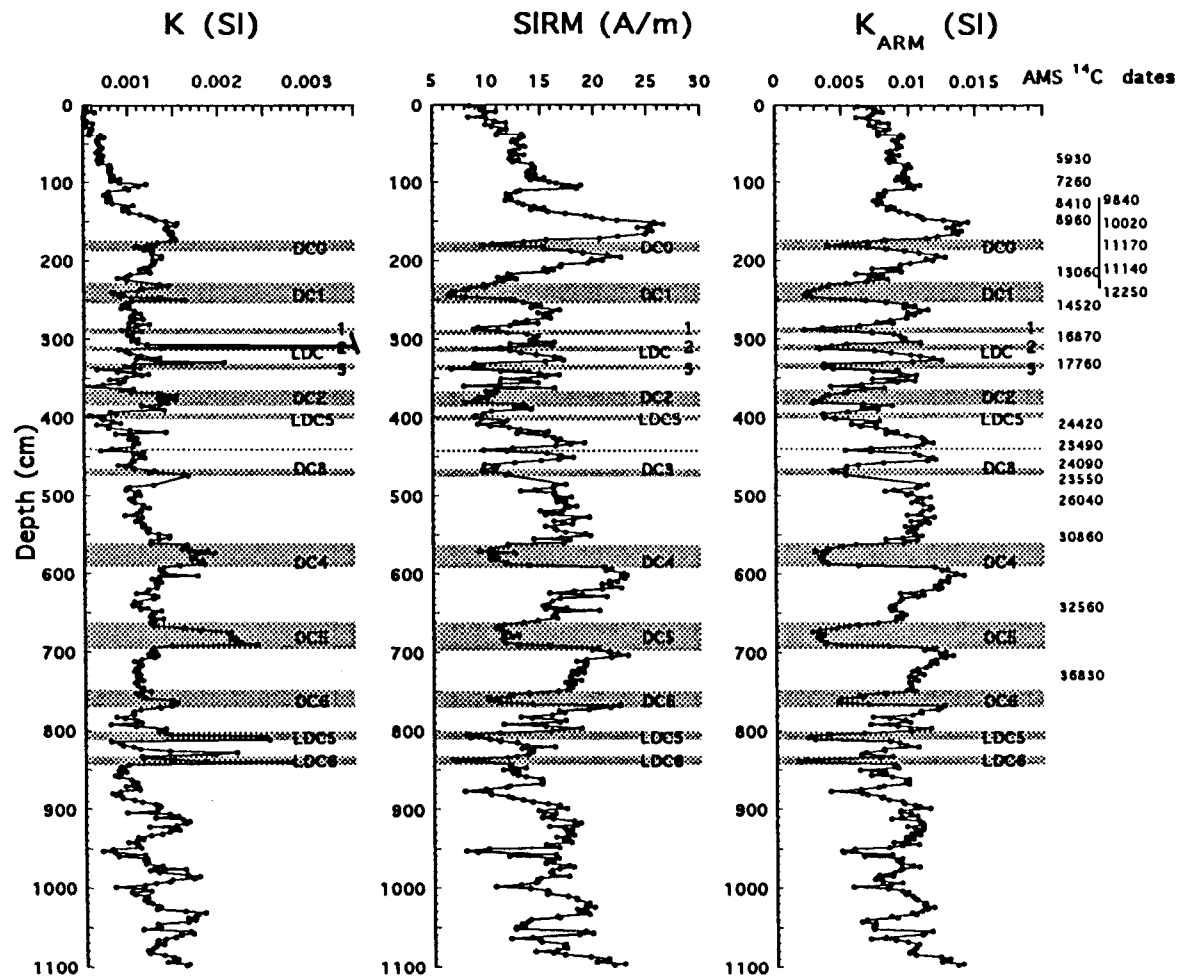


Figure 3.3 Down core profile (P-094) of concentration dependent rock magnetic parameters k , k_{ARM} and SIRM. Shaded areas indicate intervals of visually identified lithologic change.

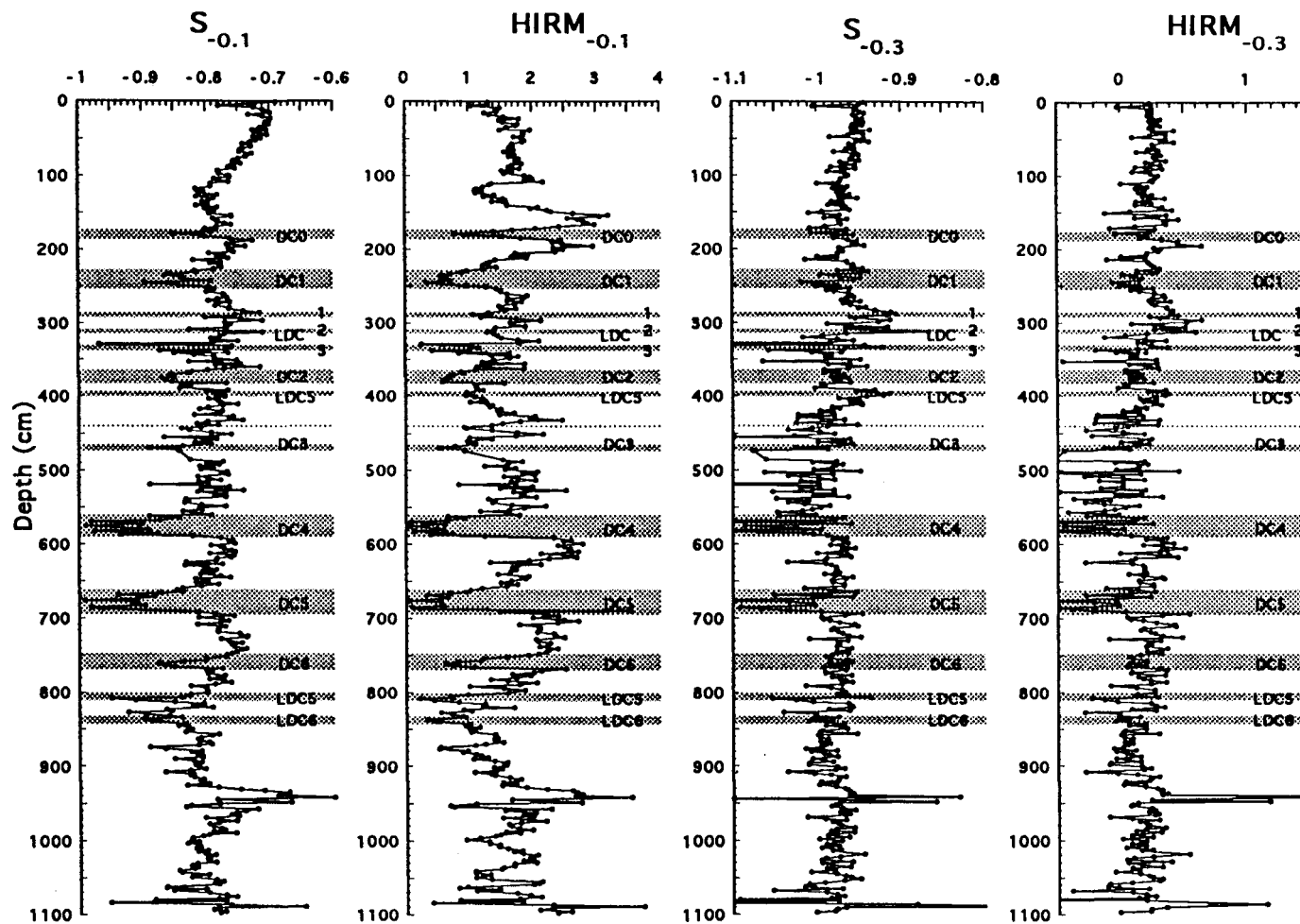


Figure 3.4. Down core profile (P-094) of coercivity dependent rock magnetic ratios S-0.1, S-0.3, and concentration high coercivity component parameters HIRM-0.1 and HIRM-0.3. Shaded areas indicate intervals of visually identified lithologic change.

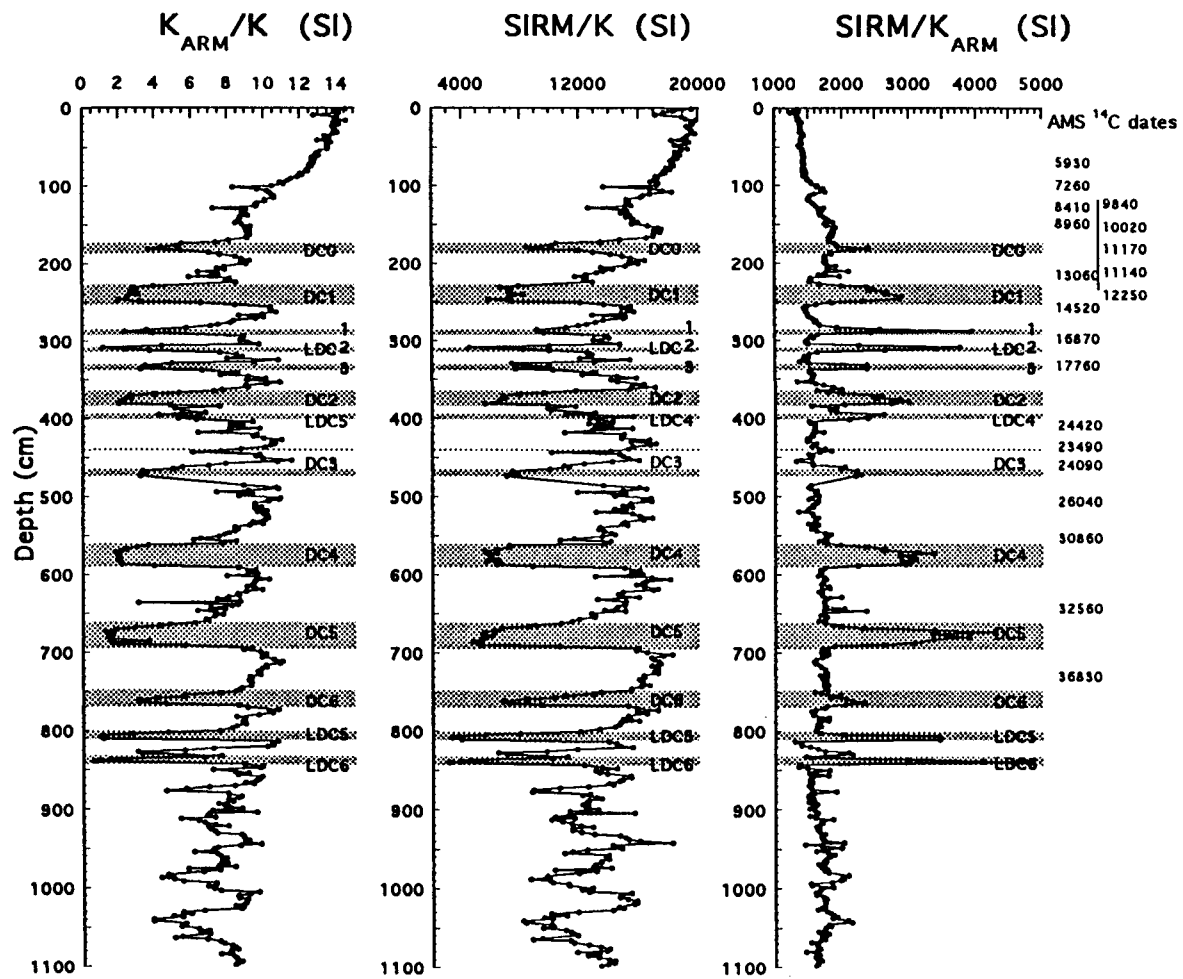


Figure 3.5. Down core profile (P-094) of magnetic grain-size sensitive ratios k_{ARM}/k , SIRM/ k and SIRM/ k_{ARM} . Shaded areas indicate intervals of visually identified lithologic change.

below DC2 (approximately 390-400 cm) (Fig. 3.4). Because of the dominant ferrimagnetic mineralogy and the very low k_f values indicating low superparamagnetic contribution, the ratios k_{ARM}/k , $SIRM/k$ and $SIRM/k_{ARM}$ are likely to be useful magnetite grain-size indicators (Fig. 3.5). According to all three parameters, the DC and LDC layers are intervals of larger magnetite grain-size. Therefore, most of the variation observed in the $S_{0.1}$ ratio can be related to a reduction in coercivity (due to increased magnetite grain-size) associated with the DC and LDC layers. The $HIRM_{0.1}$ pattern is very similar to that of $SIRM$ due to the generally low coercivity mineralogy of this core.

Dilution by detrital carbonate is one possible explanation for the low values of k_{ARM} and $SIRM$ during DC layers (Fig. 3.3), although it would not explain the generally high k values. One way to test the effect of carbonate on the magnetic parameters is to calculate them on a carbonate free basis. High resolution (1 cm sampling interval) carbonate data are available for a few selected intervals (including DC0, DC1, LDC1,2,3 and DC4) (150-350 cm and 520-620 respectively). Therefore, the effect of high carbonate content can be observed for these layers. For the intervening intervals the carbonate data were linearly interpolated to the same resolution as the magnetic data (Fig. 3.6). The concentration dependent parameters (k , $SIRM$, and k_{ARM}) were calculated on a carbonate-free basis (Fig. 3.7), according to the formula:

$$M_{CO_3} = M / (1 - (CO_3\% / 100))$$

where M is the magnetic parameter and M_{CO_3} is the magnetic parameter calculated on a carbonate-free basis. The lows associated with DC layers in the k_{ARM-CO_3} and $SIRM_{CO_3}$ records are smoothed (Fig. 3.7) compared to $SIRM$, and k_{ARM} (Fig. 3.3) but still exist, showing that carbonate dilution is not the main cause of decreased magnetite concentration. The two peak k pattern associated with DC1 (Fig. 3.7) is still present for k_{CO_3} (Fig. 3.7), indicating that this variation is also not a function of carbonate content. Therefore, the

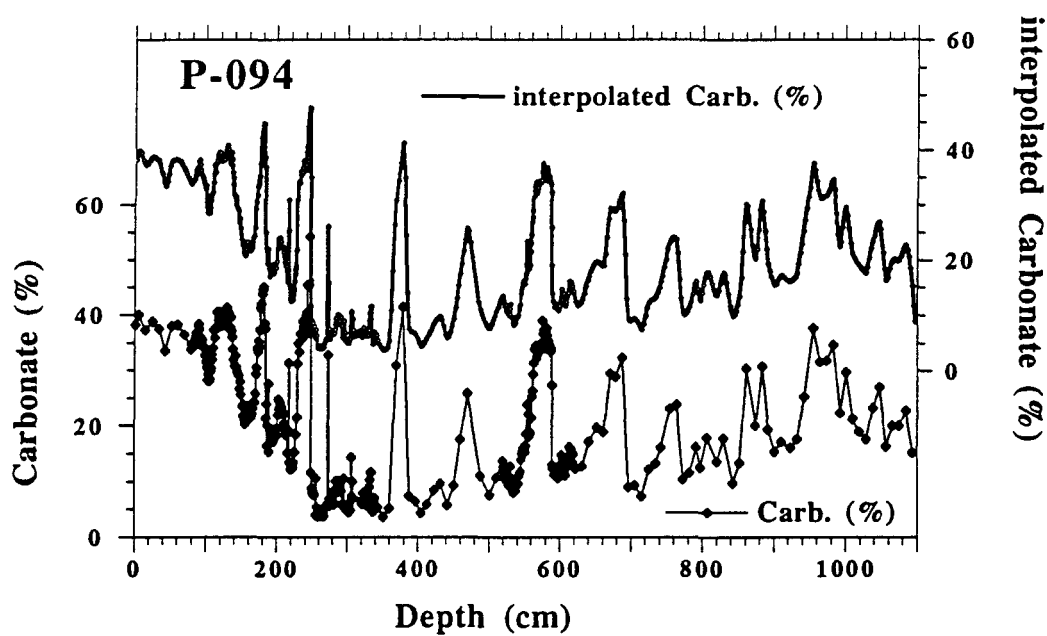


Figure 3.6. Down core profile (P-094) of carbonate (%) data (Hillaire-Marcel et al. 1994a,b) compared with linear interpolation used to calculated carbonate(%) data at the same resolution as the magnetic data.

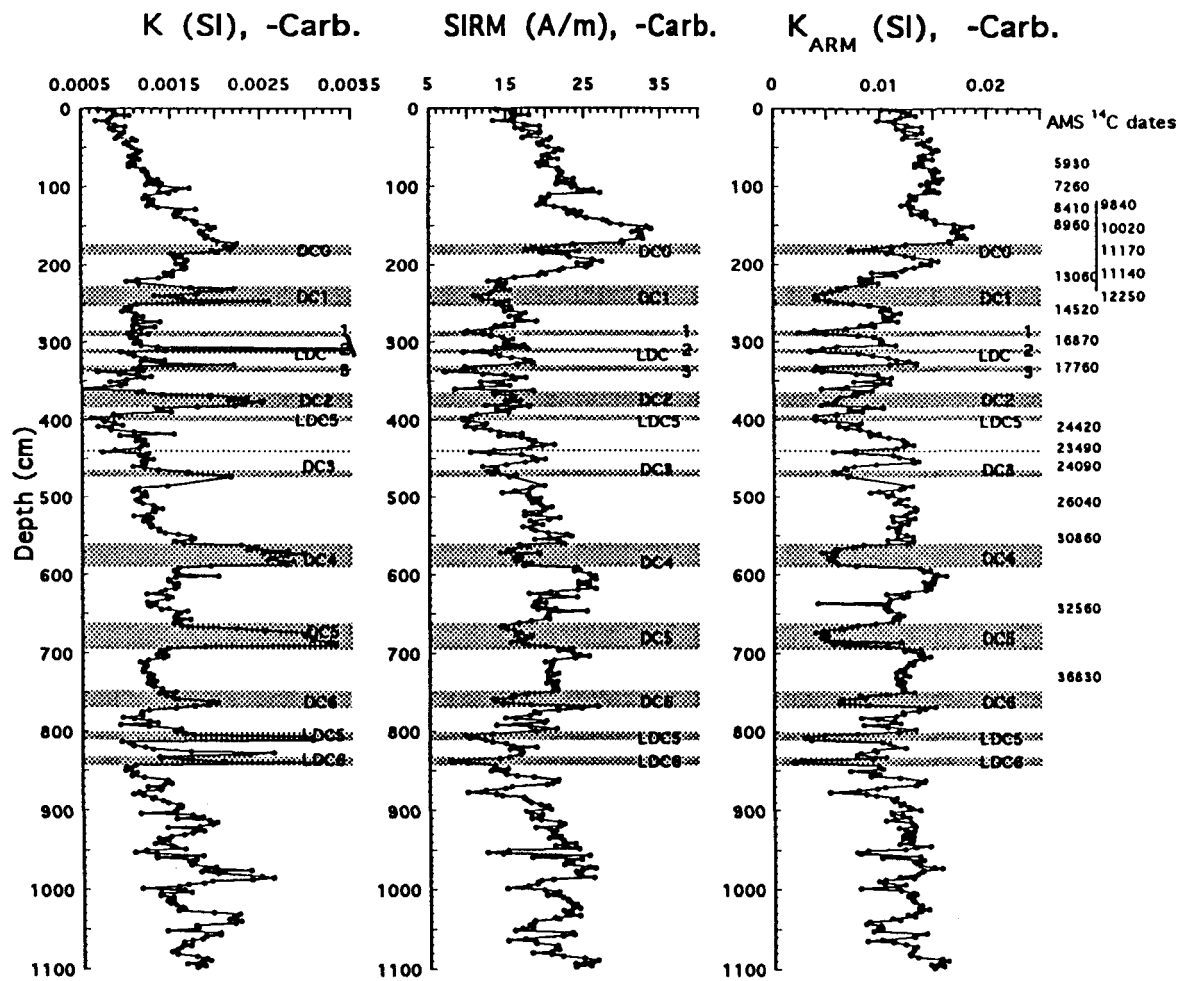


Figure 3.7 Down core profile (P-094) of concentration dependent rock magnetic parameters k , k_{ARM} and SIRM plotted on a carbonate free basis. Shaded areas indicate intervals of visually identified lithologic change.

inverse relationship between k and k_{ARM} , SIRM is likely due to the increased magnetite grain-size some of which is MD magnetite too large to carry a stable remanence. The MD magnetite component contributes to the high k values, but has little or no effect on SIRM and k_{ARM} .

3.4.2 Hysteresis Parameters

High field hysteresis parameters were measured on 316 samples from piston core P-094. All DC and LDC layers identified by rock magnetic parameters were sampled at high resolution (1 sample approximately every 2.5 cm) whereas the background sediment was sampled at intervals of approximately 5 to 7.5 cm. The hysteresis loops indicate a low coercivity magnetite mineralogy (Fig. 3.8). Samples from DC and LDC layers are characterized by extremely thin waisted loops with very small paramagnetic slopes (Fig. 3.8). Background sediment samples generally display a larger waisted loop indicative of the smaller average grain-size (Fig. 3.8). The high field slope correction for all samples was very small, suggesting a very minor paramagnetic contribution. All samples plot within the PSD to MD fields (Day et al., 1977), with ratios $M_{\text{rs}}/M_{\text{s}}$ ranging from 0.222 to 0.026 and $H_{\text{cr}}/H_{\text{c}}$ from 2.2 to 11.9 (Fig. 3.9). Parry (1980, 1982) showed that synthetic samples containing mixtures of PSD + MD or SD + MD magnetite, as well as samples containing discrete grain-sizes of magnetite or titanomagnetite, follow a power law relationship between $M_{\text{rs}}/M_{\text{s}}$ and $H_{\text{cr}}/H_{\text{c}}$.

$$M_{\text{rs}}/M_{\text{s}} = c (H_{\text{cr}}/H_{\text{c}})^m$$

For single sized magnetites, $m = -1.6$ (Parry, 1982) and if shape anisotropy is dominant, $c = 0.5$. For mixed-grain-size magnetite, both m and c are somewhat lower, while for single-sized titanomagnetite, both parameters have higher values than those for magnetite. Such a relationship is observed for the magnetic parameters in this core with an almost identical

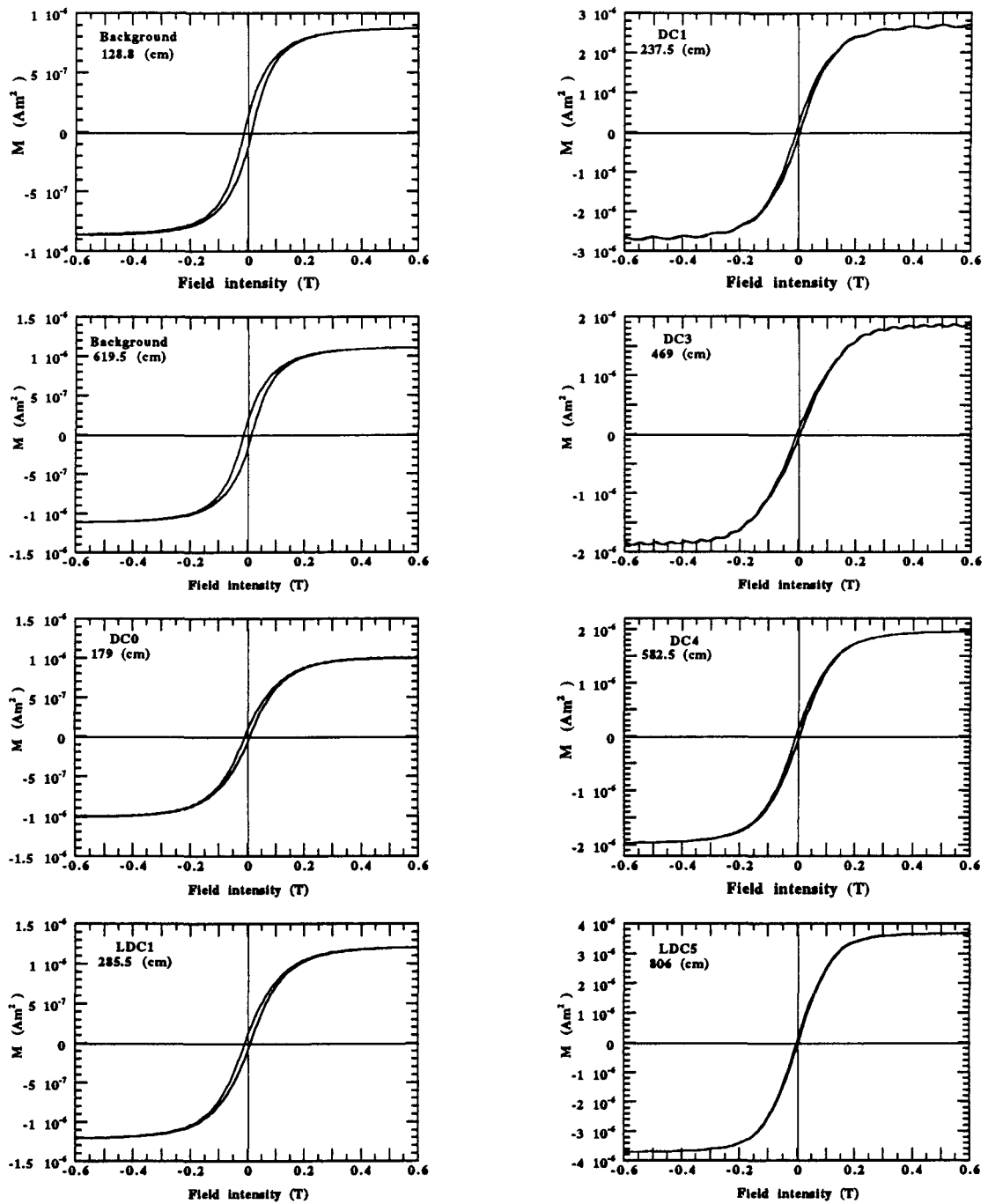


Figure 3.8. Hysteresis loops of selected samples from P-094.

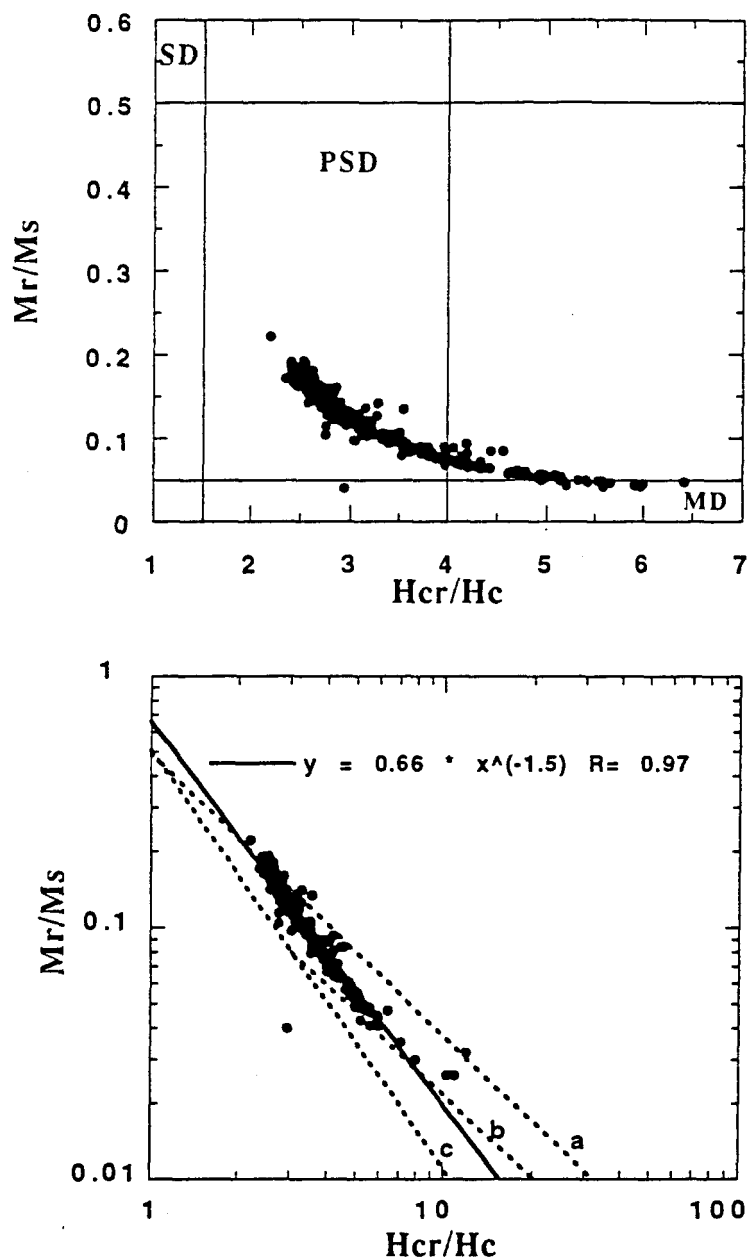


Figure 3.9. Top: Hysteresis parameters for all (316) samples from piston core P-094. M_{rs} , saturation remanence; M_s , saturation magnetization; H_{cr} , remanent coercivity; H_c , coercive force. a. Single domain (SD), pseudo-single domain (PSD), and multidomain (MD) fields after Day et al.(1977). Base: Logarithmic plot of hysteresis parameters with best fitting line plotted as solid line. The results of Parry (1980, 1982) for synthetic samples are shown for reference: broken line a, SD + MD mixtures; broken line b, PSD +MD mixtures; and broken line c, single size magnetite.

slope ($m = -1.5$) and a slightly higher intercept ($c = 0.66$). This suggests that the magnetic properties in this core are controlled by titanomagnetite of relatively constant grain-size (Fig. 3.9). A change in the slope observed from the samples with the highest H_{cr}/H_c and lowest M_{rs}/M_s values follows the trend suggested for a mixtures of PSD + MD grains (Parry, 1980; 1982). The power law relationship of the magnetic parameters in this core is consistent with magnetite grain-size mixing (Fig. 3.9).

The hysteresis parameters H_{cr} and H_c and the ratios M_{rs}/M_s and H_{cr}/H_c were plotted (Fig. 3.10). The DC and LDC layers are observed as intervals of increased magnetite grain-size, as indicated by H_c and both ratios. H_{cr}/H_c is a better marker for DC and LDC layers because it is more sensitive to variations in the large PSD to MD grain-size fraction and less sensitive than M_{rs}/M_s to the smaller grain-size fraction. Using a value of 4 in H_{cr}/H_c for the transition from PSD-MD grain-size (Day et al., 1977), all DC and LDC layers except DC0 and LDC4 are characterized by MD grains (Fig. 3.10). The empirical relationship between H_c and grain diameter for crushed grains ($H_c \propto d^{-0.5}$) (e.g. Day et al., 1977) implies that the mean magnetite grain diameter within DC and LDC layers is approximately 4 time larger ($\approx 10 \mu\text{m}$ vs. $2.5 \mu\text{m}$ for pure magnetite) than for sediment above and below. The grain-size estimates would be larger assuming an increased Ti content for the magnetite.

3.4.3 Low Temperature Remanence

Seventeen samples from P-094 were given an IRM in a field of 500 mT at 10 K then warmed to 160 K in approximately zero field and monitored at 5 K increments (Fig. 3.11). One sample from each DC and LDC event was measured. Three samples at 128.5 cm, 536.5 cm and 619.5 cm were measured to set background values. All samples display the Verwey transition with an abrupt drop in remanence for the DC and LDC sediment.

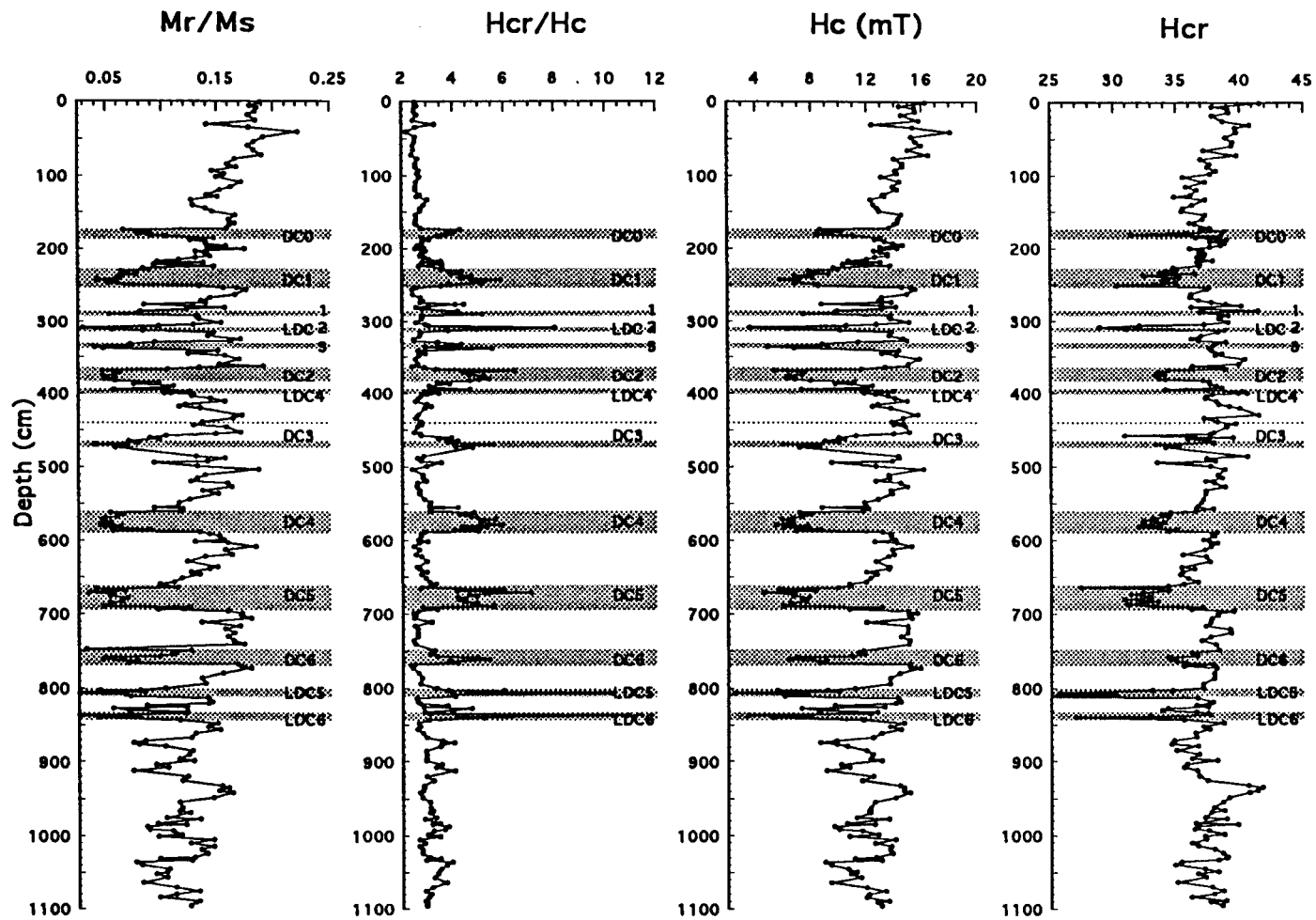


Figure 10. Down core profile (P-094) of hysteresis parameters M_{rs}/M_s , H_{rc}/H_c , H_{cr} and H_c . Shaded areas indicate intervals of visually identified lithologic change.

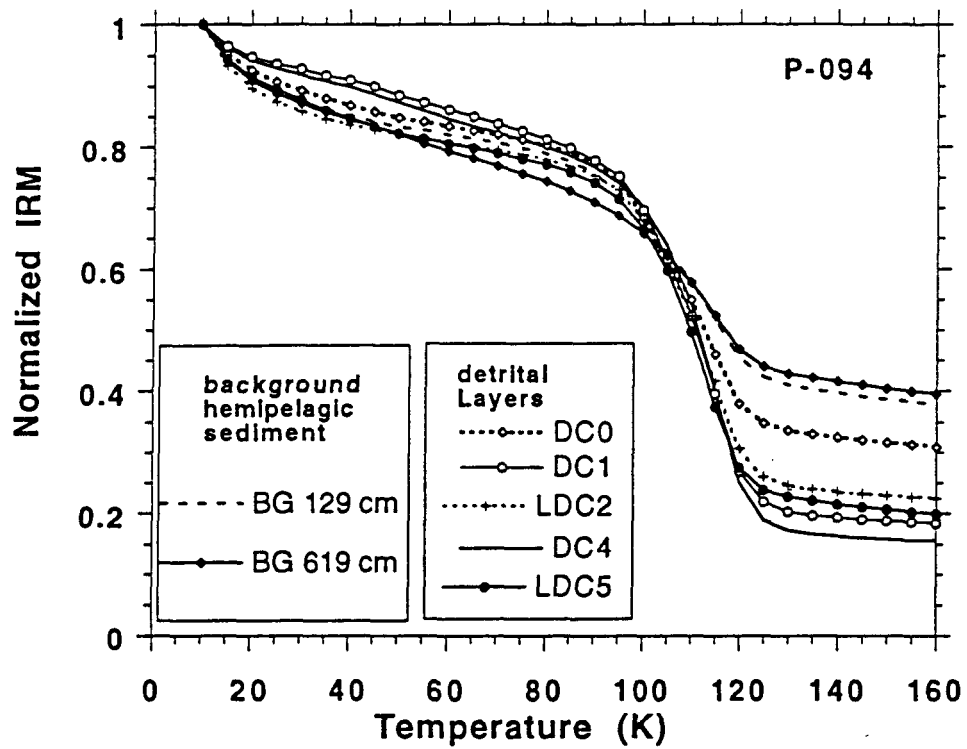


Figure 3.11 Normalized isothermal remanence curves of selected samples during warming from 10 K to 160 K. Isothermal remanence acquired in 500 mT field at 10 K.

The background sediment samples are characterized by a lower remanence decrease consistent with a reduced magnetite grain-size. DC0 has an intermediate remanence drop, consistent with a larger magnetite grain-size than the background sediment but smaller than the glacial DC and LDC layers (Fig. 3.11). A similar remanence drop was observed from a detrital carbonate bearing interval in stage 5 (DC7). No significant remanence drop was observed above or below T_v , suggesting little superparamagnetic contribution to the magnetic assemblage of this core

3.5 DEPOSITIONAL MECHANISM OF DC AND LDC LAYERS

Rock magnetic, hysteresis, and low temperature data indicate that the magnetic mineralogy of P-094 is dominantly magnetite with larger grain-size during DC and LDC layers. The large drop in remanence at the Verwey transition in all samples confirms that magnetite is the dominant magnetic mineral. Within individual DC and LDC layers, bulk rock magnetic ratios k_{ARM}/k and $SIRM/k$ and the hysteresis parameters H_{cr}/H_c , M_{rs}/M_s , and H_c are strongly correlated (Fig. 3.12). Magnetite grain-size is generally consistent between the DC and LDC layers (Fig. 3.13). Considering the difference in the size of the samples used (approx. 10 mg for hysteresis measurements and 12 g for bulk rock magnetic parameters), the strong correlation indicates that the increase in grain-size in DC and LDC layers is a property of the sediment matrix, rather than just an increased proportion of large MD magnetite due to increased IRD deposition.

A detailed comparison of magnetic properties, carbonate content and coarse fraction (% >125 μm) in the interval from 150 to 350 cm (Fig. 3.14) shows that coarse fraction in DC0 and DC1 is high at the base and top of the DC layer, but relatively low within the layer. The shaded areas in Figure 3.14 represents the visually (lithologically) distinct intervals. The increase in magnetic grain-size during these layers closely

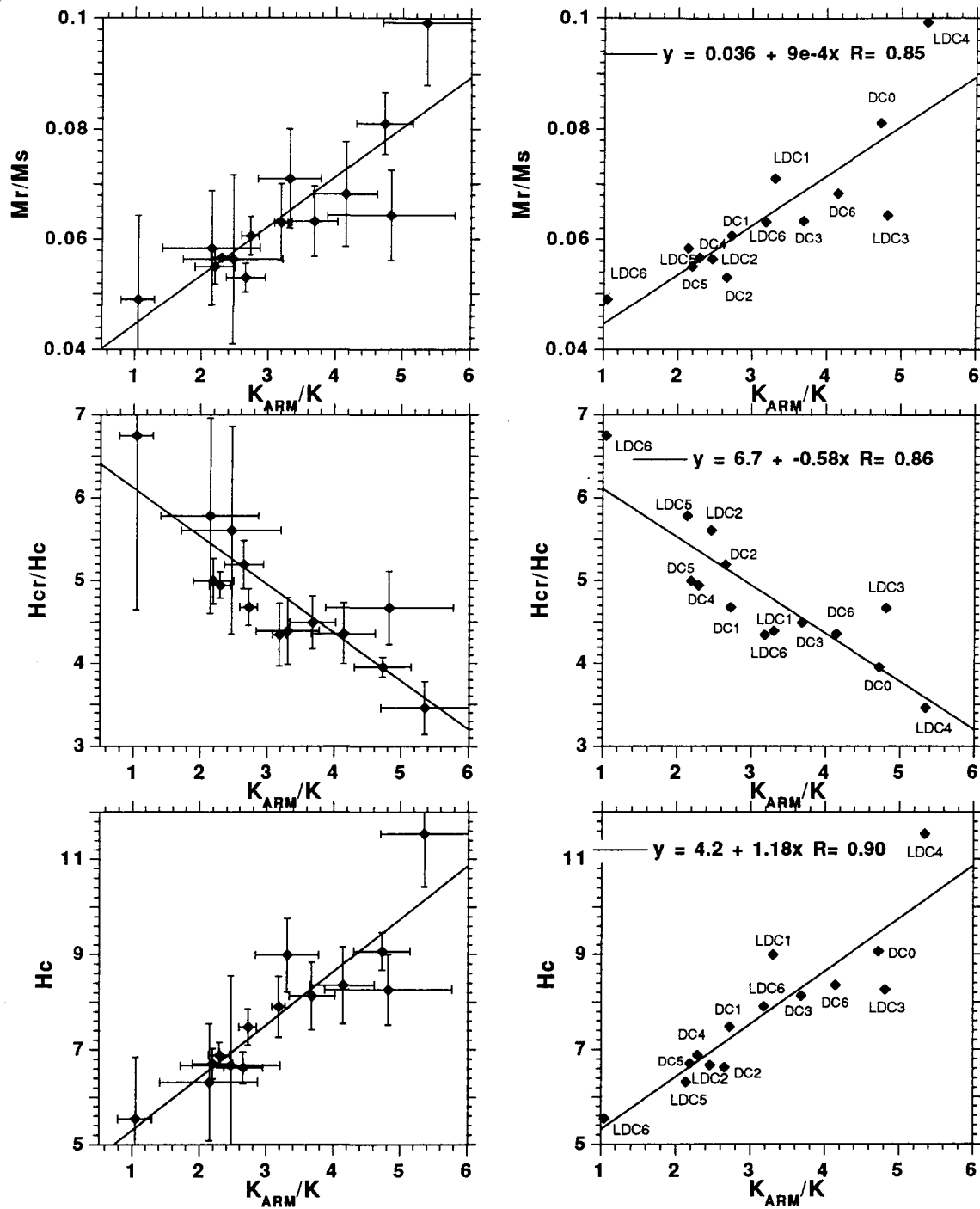


Figure 3.12. Bivalent plots of mean values of hysteresis parameters M_r/M_s , H_c , and H_{cr}/H_c plotted against mean values of rock magnetic parameter k_{ARM}/k for individual layers within P-094. Standard error of the mean for each layer shown on left, labels shown on right.

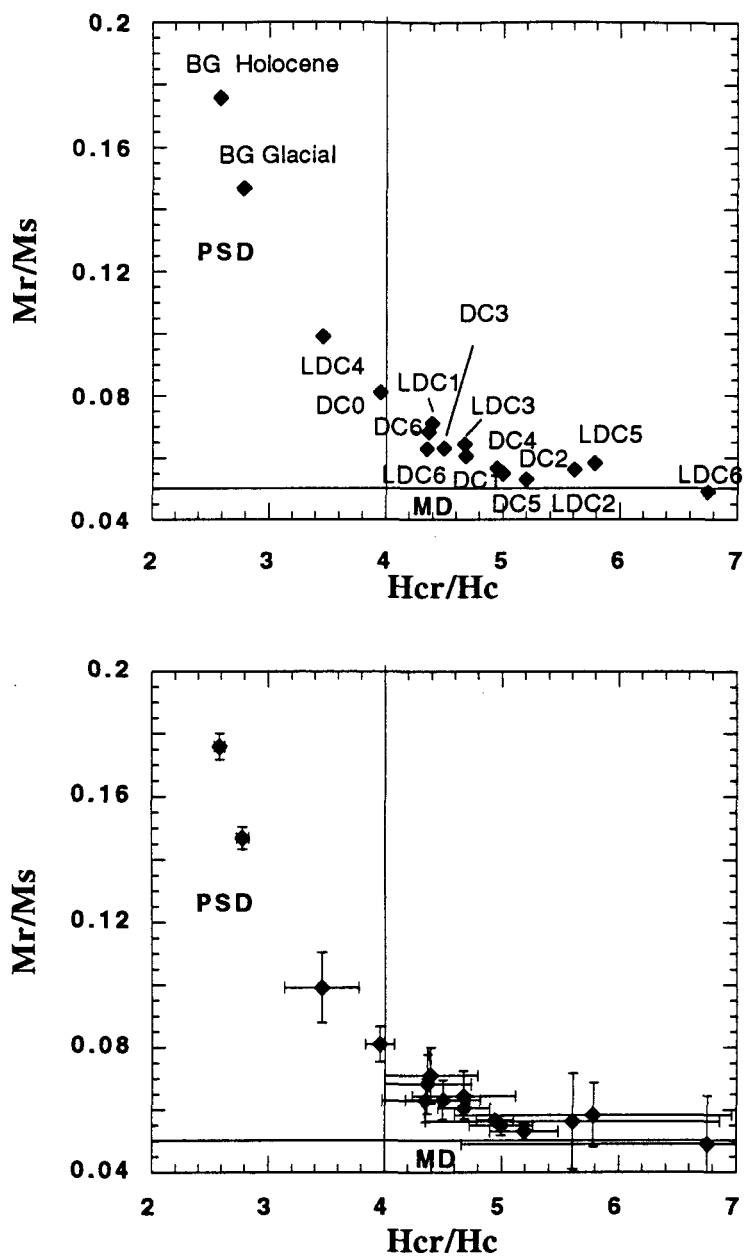


Figure 3.13. Hysteresis parameters of mean values from individual layers within P-094. Pseudo-single domain (PSD), and multidomain (MD) fields after Day et al.(1977). Top: Labels shown. Base: Standard error of the mean for each layer.

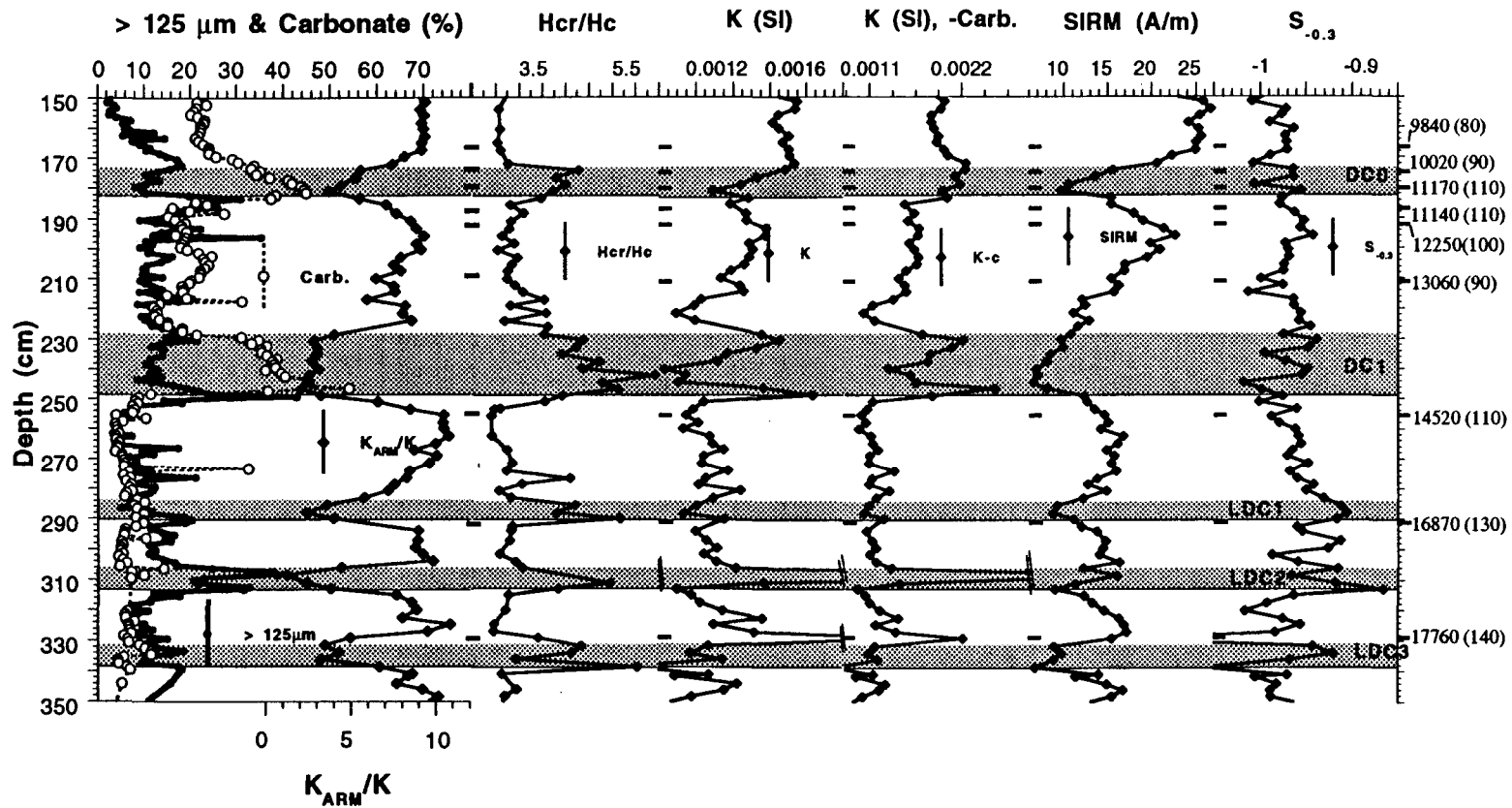


Figure 3.14. High resolution lithologic parameters coarse fraction ($>125 \mu\text{m}$) and carbonate (%) compared with magnetic parameters k_{ARM}/k , H_{cr}/H_c , k , $k\text{-CO}_3$, SIRM and $S_{0.3}$ for the interval from 150-350 cm from piston core P-094. Shaded areas indicate intervals of visually identified lithologic change; solid horizontal line indicates sharp sedimentary contact; black bars indicate AMS ^{14}C dated intervals, with dates to the right (Hillaire-Marcel et al. 1994a,b)

corresponds to the increased input of fine grained detrital carbonate and the visual record of sediment change. The peak in magnetite grain-size and carbonate occurs during a relative low in IRD compared to background deglacial values. The peaks in IRD, as identified from the coarse fraction (% >125 μm), begin below the basal and end above the upper contacts as visually identified (Fig. 3.14). k appears to mimic the coarse fraction (% >125 μm).

Hillaire-Marcel et al. (1994a) noted the decoupling between coarse fraction deposition and carbonate accumulation for DC0 and DC1. They proposed two depositional mechanisms for the DC layers, carbonate deposition related to density currents, and coarse sand deposition related to both gravity flow and ice rafting. The correspondence of increased grain-size of well sorted magnetite with the increase in fine grained detrital carbonate content but not with coarse fraction content precludes ice rafting as the primary depositional mechanism for these layers. However, since very similar magnetic properties are also observed in LDC layers, the increased magnetite grain-size is most likely not tied to the carbonate, but to the depositional mechanism.

In the northern Labrador Sea, similar DC layers are marked by high carbonate content, sharp or erosional basal contacts, relatively low susceptibility and coarse fraction (% >125 μm) (Andrews and Tedesco, 1992; Andrews et al., 1994a; Hillaire-Marcel et al., 1994a). In the eastern North Atlantic, correlative Heinrich layers are characterized by variable to low bulk carbonate, high coarse fraction and high susceptibility (Bond et al., 1992a,b; Grousset et al., 1993). This contrast between the magnetic properties of DC and LDC layers and Heinrich layers is consistent with IRD control of the k record, and increased magnetite grain-size in DC and LDC layers being due to settling of suspended sediment possibly produced by turbiditic flow down the nearby NAMOC.

In piston core P-013 on the Greenland rise (Fig. 1), layers correlating with DC1, DC2, DC4, DC5, DC6, and LDC5/6 are recognized from coarse fraction $\% > 125 \mu\text{m}$ (Hillaire-Marcel et al., 1994a). Three layers of high detrital carbonate are observed corresponding to DC2, DC4 and a layer within the initial part of substage 5e that contains no IRD. While high coarse fraction content ($\% > 125 \mu\text{m}$) is observed from many intervals within this record, increased magnetite grain-size is only observed from layers associated with high detrital carbonate (Fig. 3.15) or local Greenland deglaciation (Stoner et al., 1995). The lack of a large signal for many of these layers may be due to the location of P-013 largely, but not completely, outside the influence of the NAMOC (Fig. 1).

The DC and LDC layers may be denoting different sources for material entrained in NAMOC turbidites. High detrital carbonate has been shown to be associated with deposits from Hudson Strait (Josenhans et al. 1985, Chough et al., 1987; Andrews and Tedesco, 1992) and may indicate periods when the ice sheet in this region reached the outer shelf (Andrews et al., 1994b). We postulate that the ice surges which produced the IRD in P-094, P-013 and in correlative North Atlantic Heinrich layers also triggered turbiditic flows down the NAMOC. Estimates of the accumulation time for these layers using both excess ^{230}Th (Francois and Bacon 1994, Hillaire-Marcel et al., 1994b) and AMS ^{14}C dates (Bond et al., 1992a, 1993; Hillaire-Marcel et al, 1994a,b) range from approximately 500-1000 yrs. This time constant precludes these layers from being deposited from a single event. Therefore, it is suggested that these layers were deposited by a relatively uniform depositional process during a finite time interval. One possible scenario is that these layers were constructed from settling of suspended sediment produced by repetitive turbiditic flow down the nearby NAMOC possibly caused by seasonal variations during the lifetime of the ice surge. The concentration of IRD near the top and bottom of the DC layers (Fig. 3.14) may be explained either by rapid sedimentation of these layers within the time

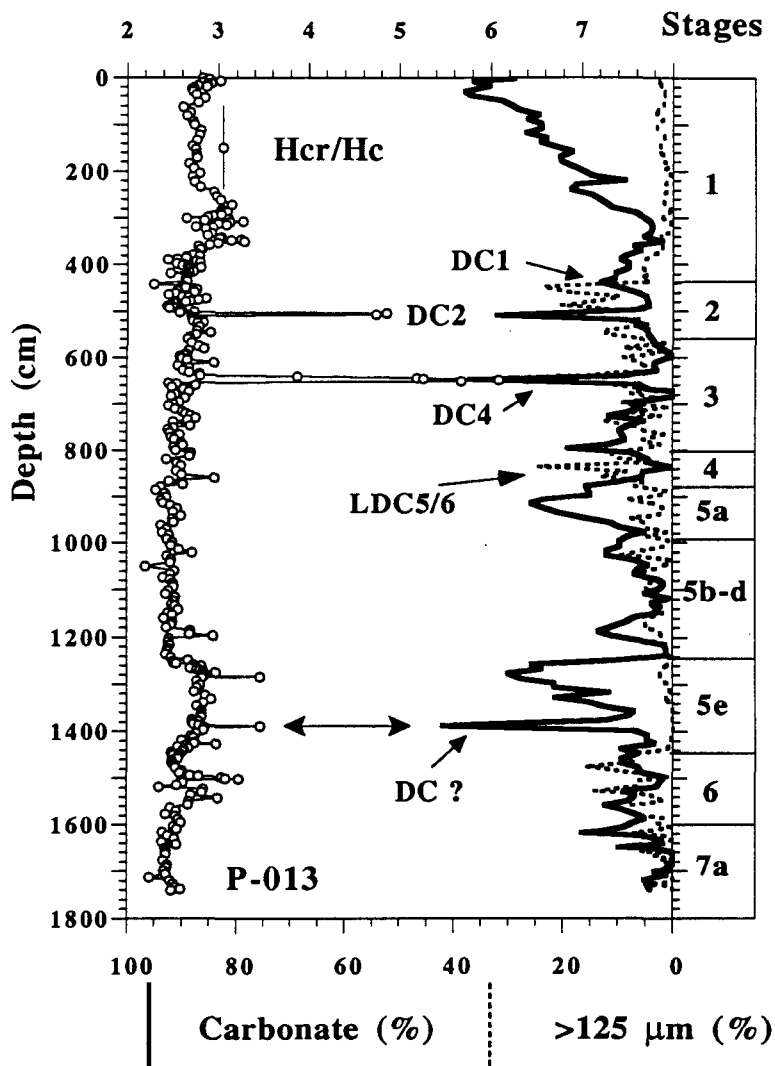


Figure 3.15. Down core plot from Greenland rise piston core P-013 of lithologic parameters coarse fraction >125 μm and carbonate (%) compared with hysteresis ratio H_{cr}/H_c . DC = detrital carbonate layers. LDC = possible low detrital carbonate layer.

interval of IRD deposition, and/or by two peaks in IRD flux predicted from the binge/purge model of Laurentide ice sheet variability (MacAyeal, 1993; Alley and MacAyeal, 1994).

3.6 CHRONOLOGY AND CORRELATION

The age control for P-094 is based on $\delta^{18}\text{O}$ measurements from planktonic foraminifera *N. pachyderma* (left-coiled) and 21 AMS ^{14}C dates from the upper 725 cm of the core (Hillaire-Marcel et al., 1994a,b) (Table 3.1). The oxygen isotope record and micropaleontological data indicate that the base of this core extends at least into isotopic substage 5a and likely 5b (Fig. 3.2) (Hillaire-Marcel et al., 1994a). All AMS ^{14}C dates are from a monospecific assemblage of *N. pachyderma* (left-coiled), corrected for 400 yr to account for the average difference between atmospheric and surface ocean ages (Stuiver et al. 1986). The high resolution AMS ^{14}C stratigraphy allows comparison and possible correlation of DC and LDC layers in P-094 with the DC layers observed in other Labrador Sea cores (e.g. Andrew et al., 1994b) and with North Atlantic Heinrich layers (Bond et al., 1992a, 1993) (Table 3.1).

Bond et al. (1992a, 1993) estimated ages from eastern North Atlantic cores of H1 (14.3 ka), H2 (21 ka), H3 (27 ka), H4 (35.5), H5 (50 ka) and H6 (66 ka), while Andrews et al. (1994b) dated DC0 at approximately 10.2 ka. The AMS ^{14}C stratigraphy for P-094 indicates that DC0, DC1, DC2 and DC5 fall within the age estimates for DC0 of Andrews et al. (1994b) and Heinrich layers H1, H2 and H4 of Bond et al. (1992a, 1993) respectively (Table 1). The age of 27 ka for Heinrich layer H3 (Bond et al., 1993), is suggested from the available AMS ^{14}C dates to be approximately 3 kyr older than DC3 and 4 kyr younger than DC4. A layer correlated with DC4 is observed from piston core P-013 off SW Greenland (Hillaire-Marcel et al., 1994a, Stoner et al., 1994) and constrained below at 31,310 (± 300) ^{14}C yr BP. From NW Atlantic core V23-16 (Fig. 1) a thick detrital

carbonate layer previously described as H3 is dated within at 31,230 (± 880) ^{14}C yr BP and constrained above at 28,240 (± 600) ^{14}C yr BP (Bond et al., 1992a). These dates associated with this layer in V23-16 are consistent with those associated with DC4 in P-094 and P-013 (Table 3.1), suggesting that these layers may be correlative and distinct from H3 in the North Atlantic. DC3 is not presently recognized from any other locality. In P-094, four AMS ^{14}C dates between 410 and 470 cm suggest a constant age for this sediment (Hillaire-Marcel et al., 1994a). The dates range from 23,490 (± 160) ^{14}C yr BP at 431 cm to 24,420 (± 230) ^{14}C yr BP at 413 cm. The lower two dates are within and just above the interval defined as DC3, the other two are above. There is no apparent age differential between the overlying sediment and DC3. DC3 is associated with light $\delta^{18}\text{O}$ values, suggesting that this layer reflects a variation of the Laurentide ice sheet. However, the relationship between DC3 and the overlying sediment is presently unclear.

AMS ^{14}C dates in P-094 and from the northern Labrador Sea (Andrews et al., 1994b) suggest that DC0 was deposited during the Younger Dryas. This layer has not been readily recognized in North Atlantic cores, though Bond et al. (1993) indicated higher detrital carbonate content within the Younger Dryas sediment at DSDP Site 609 and V23-81 (Table 3.1). In P-094, mean magnetite grain-size in DC0 is larger than in the background deglacial sediment, but not as large as observed in other DC and LDC layers (Figs. 3.12 and 3.13). While in the Northern Labrador Sea, DC0 has also been reported to be mineralogically distinct (high dolomite content) from the other DC layers (DC1, 2) (Andrews and Tedesco 1992). The correspondence of low K values with a relative low in coarse fraction (Fig. 3.14) suggests a reduced influx of (highly magnetic) IRD compared to other DC layers, possibly explaining the lack of a clear signal for this layer within the North Atlantic.

Three low detrital carbonate layers LDC1-3 occur just after the last glacial maximum (Figs 2,3 and 4). Two AMS ^{14}C dates, 16,870 (± 130) ^{14}C yr BP between LDC1 and 2, and 17,760 (± 140) ^{14}C yr BP between LDC 2 and 3, constrain the age of these layers (Table 3.1). These dates are consistent with the timing of light $\delta^{18}\text{O}$ events measured from piston cores taken from Davis Strait and the northern Labrador Sea cores (Hillaire-Marcel and de Vernal, 1989; Andrews et al., 1994a). A similar light $\delta^{18}\text{O}$ event corresponds to LDC2 in P-094 (Hillaire-Marcel et al., 1994a,b). Therefore, LDC 1-3 may also be associated with Laurentide ice sheet variability. The lack of detrital carbonate and the higher magnetic coercivity of the LDC layers suggests that these layers may not have been derived from ice surging down Hudson Strait. The lack of DC layer corresponding to the light $\delta^{18}\text{O}$ event from the northern Labrador Sea cores of Andrews et al. (1994a) also supports this suggestion. The higher coercivity of these intervals suggests that the iron formations of the Labrador Trough (part of the Circum-Ungava Geosyncline, New Quebec orogen) could provide a possible source for this detritus (Josenhans et al., 1986; Laymon, 1992). A rapidly deposited detrital layer attributed to Greenland ice sheet instability was observed in P-013 just after 16,990 (± 110) ^{14}C yr BP (Stoner et al., 1995). The correlation of these events within the Labrador Sea after the last glacial maximum may indicate a regionally significant ice sheet adjustment. To the best of our knowledge no similar lithologic layer has been observed from the North Atlantic during this interval. However, the timing of these layers are chronologically consistent with a warm-cold sea surface temperature oscillation observed from DSDP site 609 (Bond et al., 1993). This may link these events to the termination of a less pronounced version of the so called Bond cycles associated with North Atlantic Heinrich layers.

DC6 and LDC5/6 are beyond the range of AMS ^{14}C dating and therefore ages must be estimated from sedimentation rates and $\delta^{18}\text{O}$ stratigraphy. We assume a correlation of

DC6 to Heinrich layer H5 and LDC 5/6 to H6 (Hillaire-Marcel et al., 1994a). The $\delta^{18}\text{O}$ stratigraphy indicates that LDC5/6 in both P-094 and P-013 was deposited during isotopic stage 4, consistent with the estimates for H6 in the eastern North Atlantic (Bond et al., 1992a, 1993). In P-094, however, LDC5/6 is composed of two turbidite layers (LDC5 and LDC 6) which are associated with light $\delta^{18}\text{O}$ values (Hillaire-Marcel et al., 1994a). Similar light $\delta^{18}\text{O}$ values are observed in P-013 though the turbidite structure is not. The light $\delta^{18}\text{O}$ values suggest that these layers are related to ice sheet activity, while the lack of detrital carbonate in P-094 and P-013 suggest a source other than Hudson Strait. However, at present, the relationship (if any) between LDC5/6 and H6 is unclear until a more detailed correlation method becomes available.

3.7 CONCLUSIONS

1. The magnetic mineralogy of Labrador Sea piston core P-094 is dominated by magnetite.
2. Seven detrital carbonate (DC) layers and six low detrital carbonate (LDC) layers can be observed by larger than background magnetite grain-size during the last glacial cycle.
3. Some but not all DC and LDC layers can be correlated to previously recognized North Atlantic Heinrich layers.
4. The increase in magnetite grain-size within DC and LDC layers is believed to reflect an overall magnetite grain-size rather than an increased proportion of very large grained magnetite. For DC layers, the increase in magnetite grain-size appears to be coupled to carbonate and independent of the coarse fraction content (IRD proxy).
5. Very similar magnetic properties are seen in DC and LDC layers indicating that the magnetic properties (particularly those sensitive to grain-size) are not tied to the source

but related to depositional mechanism. We consider that the DC and LDC layers within this core were deposited from suspension generated by NAMOC overflows during periods of ice sheet surging to the shelf-slope break.

6. The susceptibility (k) appears to be controlled by highly magnetic IRD from the Canadian shield. As IRD deposition is the primary depositional mechanism associated with Heinrich layers within the North Atlantic, high k values are generally associated with these layers.

7. DC0, deposited during the Younger Dryas, has a smaller mean magnetite grain-size than for other DC and LDC layers. This event is associated with a relatively low IRD, which may account for its slightly smaller mean magnetite grain-size and for the fact that this event is not widely recognized in the North Atlantic.

REFERENCES

- Alley, R. B., and MacAyeal, D. R. 1994. Ice-rafted debris associated with binge/purge oscillations of the Laurentide Ice sheet, **9**: 505-511.
- Andrews, J. T., and Tedesco, K. 1992. Detrital carbonate-rich sediments, northwest Labrador Sea: implications for ice-sheet dynamics and iceberg rafting Heinrich events in the North Atlantic. *Geology*, **20**: 1087-1090.
- Andrews, J. T., Tedesco, K., and Jennings, A. E. 1993. Heinrich events: Chronology and processes, East-central Laurentide Ice Sheet and NW Labrador Sea. *In Ice in the Climate System, Nato ASI Series. I*, **12**:167-186.
- Andrews, J. T., Erlenkeuser, H., Tedesco, K., Aksu, A. E., and Jull, A. J. T. 1994a. Late Quaternary (stage 2 and 3) meltwater and Heinrich events, Northwest Labrador Sea. *Quaternary Research*, **41**: 26-34
- Andrews, J. T., Tedesco, K., Briggs, W. M., and Evans, L. M. 1994b. Sediments, sedimentation rates, and environments, SE Baffin Shelf and NW Labrador Sea 8 to 26 Ka. *Canadian Journal of Earth Sciences*, **31**: 90-103.
- Bloemendal, J. 1983. Paleoenvironmental implications of the magnetic characteristics of sediments from DSDP Site 514, Southeast Argentine Basin, Initial Reports of the Deep Sea Drilling Project, **71**: 1097-1108.
- Bloemendal J., and deMenocal, P. B. 1989. Evidence for a change in the periodicity of tropical climate cycles at 2.4 Myr from whole-core magnetic susceptibility measurements. *Nature*, **342**: 897-900.
- Bloemendal, J., Lamb, B., and King, J. W. 1988. Paleoenvironmental implications of rock-magnetic properties of Late Quaternary sediment cores from the eastern equatorial Atlantic. *Paleoceanography*, **3**: 61-87.
- Bloemendal J., King, J. W., Hall, F. R., and Doh, S.J. 1992. Rock magnetism of Late Neogene and Pleistocene deep-sea sediments: relationship to sediment source, diagenetic processes, and sediment lithology. *Journal of Geophysical Research*, **97**: 4361-4375.
- Bloemendal, J., King, J. W., Hunt, A. deMenocal, P. B., and Hayahida, A. 1993. Origin of the sedimentary magnetic record at ocean drilling program sites on the Owen Ridge, Western Arabian Sea. *Journal of Geophysical Research*, **98**: 4199-4219.
- Bond, G., Heinrich, H., Broecker, W., Labeyrie, L., McManus, J., Andrews, J., Huon, s., Jantsschik, R., Clasen, S., Simet, C., Tedesco, K., Kias, M., Bonani, G., and Ivy, S. 1992a. Evidence for massive discharges of icebergs into the North Atlantic ocean during the last glacial period. *Nature*, **360**: 245-249
- Bond, G., Broecker, W., Lotti, R., and McManus, J., 1992b. Abrupt color changes in isotope stage 5 in North Atlantic deep sea cores: implications for rapid change of

- climate-driven events. In. Start of a Glacial, G. J. Kukla and E. Went eds: NATO ASI Series. Vol 13 Springer-Verlag Berlin Heidelberg. 185-205
- Bond, G., Broecker, W., Johnsen, S., McManus, J., Laberyie, L., Jouzel, J., and Bonani, G. 1993. Correlations between climate records from North Atlantic sediments and Greenland ice. *Nature*, **365**: 143-147.
- Broecker, W.S., Bond, G., McManus, J., Klas, M., and Clarke, E. 1992. Origin of the Northern Atlantic's Heinrich events. *Climate Dynamics*, **6**: 265-273.
- Chough, S. K., Hesse, R., and Müller, J. 1987. The Northwest Atlantic Mid-Ocean Channel of the Labrador Sea. IV. Petrography and provenance of the sediments. *Canadian Journal of Earth Sciences*, **24**: 731-740.
- Day, R., Fuller, M., and Schmidt, V. A. 1977, Hysteresis properties of titanomagnetites: grain-size and compositional dependence. *Physics of the Earth and Planetary Interiors*, **13**: 260-267.
- Doh, S. J., King, J. W., and Leinen, M. 1988. A rock-magnetic study of Giant Piston Core LL44-GPC from the Central North Pacific and its paleoceanographic significance. *Paleoceanography*, **3**: 89-111.
- Dunlop, D. J., 1986. Hysteresis properties of magnetite and their dependence of particle size: A test of pseudo-single domain remanence models. *Journal of Geophysical Research*, **91**: 9569-9584.
- Francois, R. and Bacon, M. P., 1994. Heinrich events in the North Atlantic: radiochemical evidence. *Deep Sea Research*, **41**: 315-334.
- Grousset, F., Labeyrie, L., Sinko, A., Cremer, M. Bond, G., Duprat, J. Cortijo, E. and Huon, S. 1993. Patterns of ice-rafted detritus in the glacial North Atlantic (40-55°N). *Paleoceanography*, **8**: 175-192.
- Hartstra, R. L., 1982. A comparative study of the ARM and I_{SF} of some natural magnetites of MD and PSD grain size. *Geophysical Journal of the Royal Astronomical Society*, **71**: 497-518.
- Heinrich, H. 1988. Origin and consequences of cyclic ice rafting in the northeast Atlantic Ocean during the past 130 000 years. *Quaternary Research*, **29**: 143-152
- Hesse, R., Chough, S. K., and Rakofsky, A. 1987. The Northwest Atlantic Mid-Ocean Channel of the Labrador Sea. V. Sedimentology of a giant deep-sea channel. *Canadian Journal of Earth Sciences*, **24**: 1595-1624
- Hillaire-Marcel, C., and de Vernal, A. 1989. Isotopic and palynological records of the Late Pleistocene in Eastern Canada and adjacent ocean basins. *Géographie Physique et Quaternaire*, **43**: 263-290.

- Hillaire-Marcel, C., de Vernal, A., Bilodeau, G. and Wu, G. 1994a. Istone stratigraphy, sedimentation rates, deep circulation and carbonate events in the Labrador Sea during the last ~ 200 ka. *Canadian Journal of Earth Sciences*, **31**: 63-89.
- Hillaire-Marcel, C., Stoner, J. S., Vallières, S., Assameur, D. and Channell, J. E. T. 1994b. High resolution studies of "Heinrich" and detrital carbonate Layers in the the deep Labrador Sea: age, duration, frequency and depositional mechanisms. *Transactions. American Geophysical Union*, **75** (44): 186.
- Josenhans, H. W., Zevenhuizen, J. and Klassen, R. A. 1985. The quaternary geology of the Labrador Shelf. *Canadian Journal of Earth Sciences*, **23**: 1190-1213.
- Keigwin, L. D., and Lehman, S. J. 1994. Deep circulation change linked to HEINRICH event 1 and Younger Dryas in a middepth North Atlantic core. *Paleoceanography*, **9**: 185-194.
- Kent, D. V. 1982. Apparent correlation of paleomagnetic intensity and climatic records in deep-sea sediments. *Nature*, **299**: 538-539
- King, J. W., Banerjee, S. K., Marvin, J. and Ozdemir, O., 1982. A comparison of different magnetic methods for determining the relative grain size of magnetite in natural materials: some results from lake sediments. *Earth and Planetary Science Letters*, **59**: 404-419.
- Laymon, C. A. 1992. Glacial geology of western Hudson Strait, Canada, with reference to Laurentide Ice Sheet dynamics. *Geological Society of America Bulletin*, **104**: 1169-1177.
- MacAyeal, D. R. 1993. Binge/purge oscillations of the Laurentide Ice Sheet as a cause of the North Atlantic's Heinrich events. *Paleoceanography*, **8**: 775-784.
- Maher, B. A., 1988. Magnetic properties of some synthetic sub-micron magnetites. *Geophysical Journal of the Royal Astronomical Society*, **94**: 83-96.
- Martinson, D. G., Pisias, N. G., Hays, J. D., Imbrie, J., Moore, T. C. Jr. and Shackleton, N. J. 1987. Age dating and the orbital theory of the Ice Ages: development of a high-resolution 0 to 300,000-year chronostratigraphy. *Quaternary Research*, **27**: 1-29.
- Mayewski et al., 1994. Changes in atmospheric circulation and ocean ice cover over the North Atlantic during the last 41,000 years. *Science*, **263**: 1747-1751.
- Özdemir, Ö., Dunlop, D. J., and Moskowitz, B. M., 1993. The effect of oxidation on the Verwey transition in magnetite. *Geophysical Research Letters*, **20**: 1671-1674.
- Parry, L. G. 1980. Shape-related factors in the magnetization of immobilized magnetite particles. *Physics of the Earth and Planetary Interiors*, **22**: 144-154.
- Parry, L. G. 1982. Magnetization of immobilized particles dispersions with two distinct particle sizes. *Physics of the Earth and Planetary Interiors*, **28**: 230-241.

- Robinson, S. G. 1986. The Late Pleistocene palaeoclimatic record of North Atlantic deep-sea sediments revealed by mineral-magnetic measurements. *Physics of the Earth Planetary Interiors*, **42**: 22-46.
- Robinson, S. G. 1990. Applications of whole-core magnetic susceptibility measurements of deep-sea sediments, *In* Duncan, R. A., Backman, J., Peterson, L. C. et al., *Proceedings of the Ocean Drilling Program, Scientific Results*, **115**: 737-771.
- Stuiver, M., Pearson, G. W., and Braziunas, T. 1986. Radiocarbon age calibration of marine samples back to 9000 cal yr Bp. *Radiocarbon*, **28**: 980-1021.
- Stoner, J. S., Channell, J. E. T., Hillaire-Marcel C. and Mareschal J.-C., 1994. High resolution rock magnetic study of a Late Pleistocene core from the Labrador Sea. *Canadian Journal Earth Sciences*, **31**: 104-114.
- Stoner, J. S., Channell, J. E. T., and Hillaire-Marcel C., 1995. Magnetic properties of deep sea sediment off SW Greenland: Major differences between the last two deglaciations. *Geology*, **23**: 241-244.
- Thompson, R., 1986. Modeling magnetization data using SIMPLEX. *Physics of the Earth and Planetary Interiors*, **42**: 113-127.
- Verwey, E. J. W. 1939. Electronic conduction of magnetite (Fe_3O_4) and its transition point at low temperatures. *Nature*, **144**: 327-328.

CHAPTER IV

**LATE PLEISTOCENE RELATIVE GEOMAGNETIC FIELD
PALEOINTENSITY FROM DEEP LABRADOR SEA SEDIMENTS:
REGIONAL AND GLOBAL CORRELATION**

4.1 INTRODUCTION

The principal method of marine correlation during the Brunhes Chron is the oxygen isotope record. As a first approximation benthic foraminiferal tests linearly respond to changes in the oceans oxygen isotopic composition, providing a history of continental ice volume (Piasas et al., 1984; Shackleton, 1987; Martinson et al. 1987). In many locations, due to harsh environmental conditions or poor carbonate preservation, complete benthic $\delta^{18}\text{O}$ records cannot be developed. In the North Atlantic's subarctic basins, benthic $\delta^{18}\text{O}$ records are generally unavailable due to low foraminiferal concentrations. Planktonic foraminiferal $\delta^{18}\text{O}$ records can be developed and used for stratigraphic correlation (Shackleton and Opdyke 1973; Kellogg et al., 1977; Hillaire-Marcel et al., 1994). However, these $\delta^{18}\text{O}$ records may show large departure from the global $\delta^{18}\text{O}$ signal due to local surface water changes in temperature, salinity, or meltwater dilution (Kennett and Shackleton 1975, Leventer et al., 1982; Fairbanks et al., 1992; Wu and Hillaire-Marcel, 1994a), perturbing the planktonic $\delta^{18}\text{O}$ signal and inhibiting correlation.

The development of accelerator mass spectrometry (AMS) ^{14}C dating has provided precise correlation and chronometric control for, at most, the last 50,000 yrs (Duplessy et al., 1986, Broecker et al., 1988a,b; Andrews and Tedesco 1992, Bond et al., 1992, 1993 Hillaire-Marcel et al., 1994; Keigwin et al., 1994; Wu and Hillaire-Marcel, 1994b). Recent studies of Late Pleistocene marine sediments of Mediterranean Sea, Indian and Pacific

Oceans (Kent and Opdyke, 1977; Tauxe and Wu, 1990; Meynadier et al., 1992; Tric et al., 1992; Valet and Meynadier, 1993; Schneider, 1994; Tauxe and Shackleton, 1994; Yamazaki and Ioka, 1994) suggest that these sediments have recorded relative changes in dipole geomagnetic field intensity, which could provide a method for high resolution global correlation.

This paper presents Late Pleistocene relative paleointensity records from three deep Labrador Sea cores. The planktonic oxygen isotope stratigraphy from *N. pachyderma* (left-coiled) was established for the 3 cores and detailed AMS ^{14}C stratigraphies were obtained for 2 of these cores. Unlike other marine paleointensity records, these are from high latitude locations strongly affected by ice sheet-ocean interactions and are therefore characterized by variable sedimentation rates and mechanisms (Hillaire-Marcel et al., 1994, Stoner et al., 1995). These records provide a test of the measurement quality which can be derived from such sediments and of the usefulness of paleointensity data as a means of stratigraphic correlation.

4.2 CORE DESCRIPTIONS

Core HU90-013-012 (P-012) (lat. $58^{\circ}55.35\text{N}$, long. $47^{\circ}07.01\text{W}$, depth 2830 m) (Fig. 4.1) was obtained on the Greenland Slope. The oxygen isotope record from this 1240 cm core suggests that it extends, at least, into isotopic stage 6 (Hillaire-Marcel et al. 1994a). This core is characterized by two distinct sedimentation patterns: extremely low sedimentation rates for the Holocene and last interglacial (isotopic substage 5e) with approximately 20 cm of sediment for each, high sedimentation rates (10 cm/kyr) during the last glacial period. The low sediment accumulation during the interglacials is caused by winnowing and erosion due to a strong Western Boundary Undercurrent (WBUC) at this

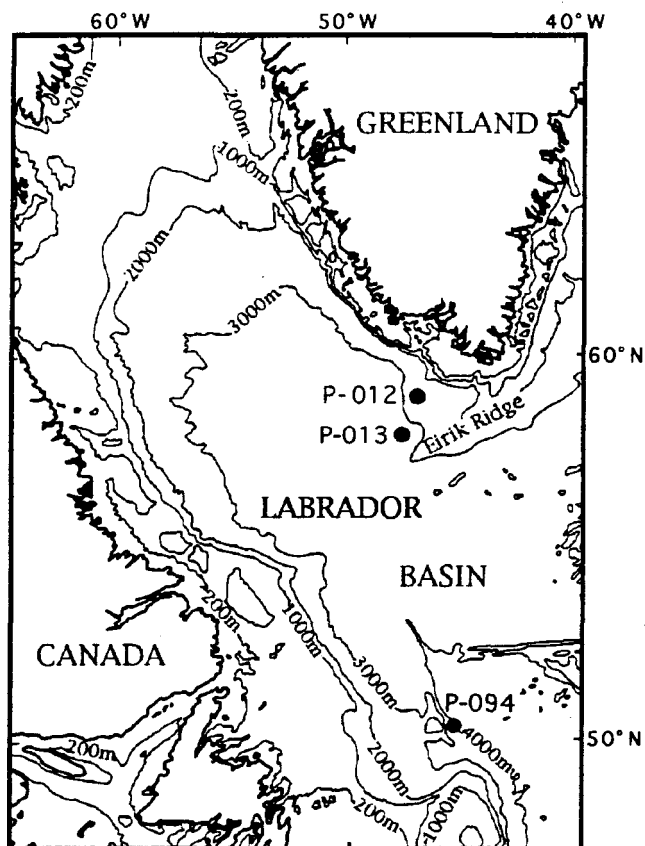


Figure 4.1. Map of the Labrador Sea showing the location of core sites used in this study. P-012 = piston core HU90-013-012; P-013 = piston core HU90-013-013; P-094 = piston core HU91-045-094.

site location. The high sedimentation rates during isotopic stages 2-5d and 6 indicate a weakened WBUC (Hillaire-Marcel et al., 1994).

The 1740 cm long piston core HU90-013-013P (P-013) (lat. 58°12.59N, long. 48°22.40W, depth 3380 m) (Fig. 4.1) was taken from the Greenland Rise, approximately 160 km away and 500 m deeper than P-012. The oxygen isotope record indicates that the base of this core corresponds to an interstadial period of isotopic stage 6 or late stage 7 (Hillaire-Marcel, 1994a,b). 21 AMS ^{14}C dates, also from *N. pachyderma* (left-coiled), show that sedimentation rates in P-013 are >30 cm/kyr in the Holocene and approach 100 cm/kyr during deglaciation. During glacial intervals sedimentation rates (~10 cm/kyr) are similar to, but slightly less than those inferred for P-012 on the Greenland Slope.

A third core HU91-045-094P (P-094) (lat. 50°12.26N, long. 45°41.14W, water depth 3448 m) (Fig. 4.1) was collected from a small deep channel SE of Orphan's Knoll on the Labrador rise (Hillaire-Marcel et al., 1994). The oxygen isotope record suggests that this 1098 cm long piston core extends into stage 5. The chronometry of this core is further constrained by 21 AMS ^{14}C dates. Sedimentation in P-094 is characterized by many rapidly deposited detrital carbonate (DC) (at least 8) and low detrital carbonate (LDC) (at least 5) layers (Hillaire-Marcel et al., 1994; Stoner et al., in press), some are correlated with North Atlantic Heinrich layers Heinrich, 1988; Andrews and Tedesco, 1992; Broecker et al., 1992 Bond et al., 1992). These layers are unsuitable for relative paleointensity determinations; because of abrupt changes in magnetite grain-size, concentration and accumulation rate, approximately one order of magnitude higher (Hillaire-Marcel et al., 1994; Francis and Bacon, 1994). However, the intervening hemipelagic sediment may preserve a reliable paleointensity record.

4.3 ROCK MAGNETIC PROPERTIES

Split core sections were sampled with 7 cc plastic cubes back-to-back down the central axis of each core. The cubic samples were used for rock magnetic measurements and were later subsampled for hysteresis, and low temperature remanence measurements. The rock magnetic measurements were made in the magnetically-shielded laboratory at the University of Florida, while the hysteresis, and low temperature remanence measurements were made at the Institute for Rock Magnetism at the University of Minnesota.

4.3.1 Mineralogy

Sedimentary relative paleointensity records must satisfy several criteria to be considered reliable (King et al., 1983; Tauxe, 1993). The magnetic remanence should be carried by magnetite of preferably pseudo-single domain (PSD) grain-size and should not vary in concentration by more than one order of magnitude. Saturation experiments ($S_{0.3}$, IRM acquisition) show that ferrimagnetic minerals dominate the magnetic assemblage of all three cores (Fig. 4.2 & 4.3). The shape of hysteresis loops (P-013 and P-094) are also characteristic of a magnetite mineralogy. Using the $S_{0.3}$ ratio, Stoner et al. (1994) recognized an interval of higher coercivity between 500 and 600 cm in P-013. During this interval the remanent coercivity (H_{cr}) increases abruptly from background values of 38 mT to approximately 60 mT. The higher coercivity could reflect a change in redox conditions where this interval did not pass through the zone of Fe reduction and was preserved as a relict oxidized zone. Because saturation is below 0.3 T (Fig. 4.2 & 4.3), the higher coercivity was suggested to be due to the presence of fine grained magnetite not preserved in the rest of the core. Low temperature remanence experiments show that the Verwey transition is suppressed in the high coercivity interval (Fig. 4.4a). Suppressed Verwey transition and increased coercivity have been associated with partially oxidized magnetites

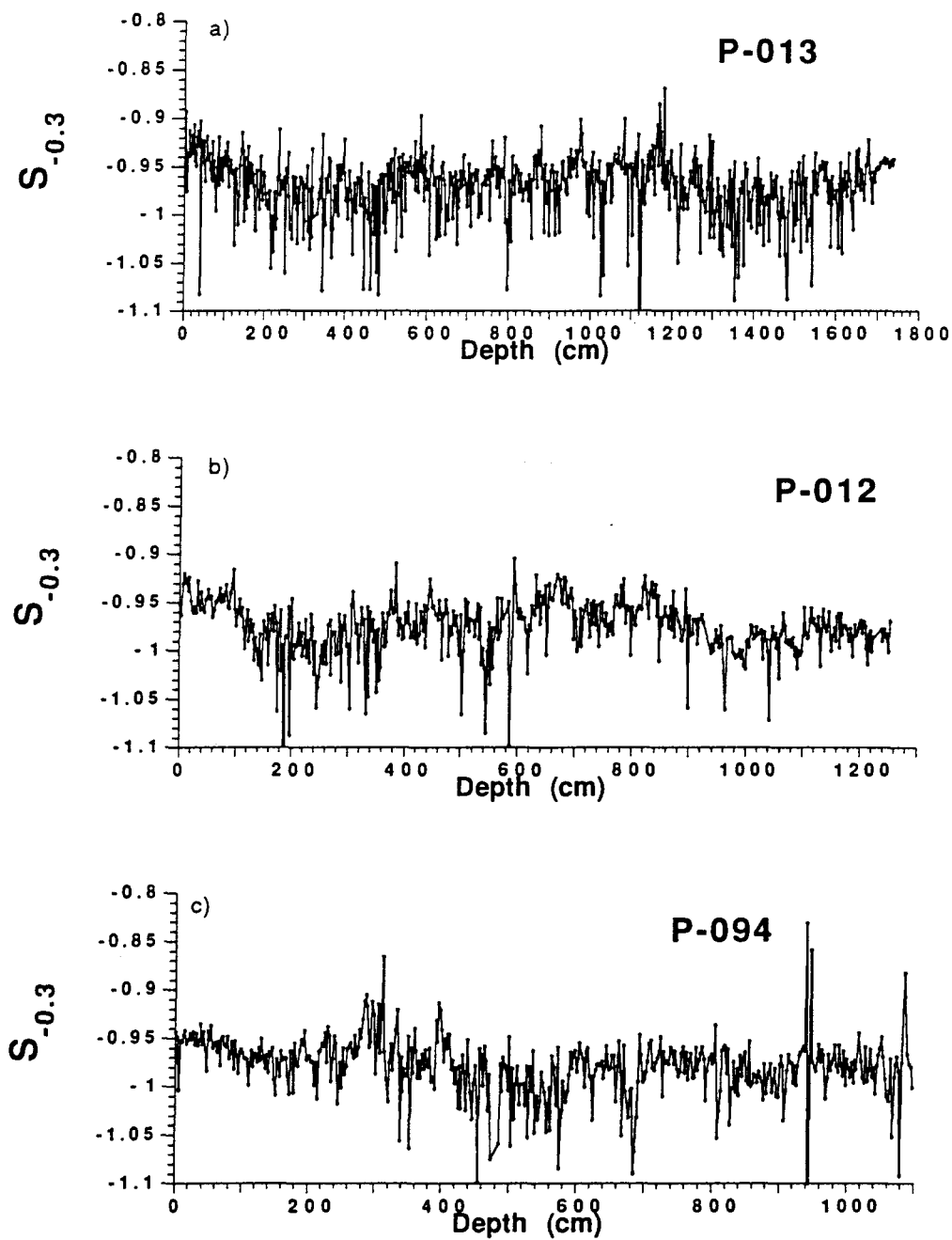


Figure 4.2. The $S_{-0.3}$ ratio versus depth for Labrador Sea piston cores . a.) P-013. b.) P-012. c.) P-094.

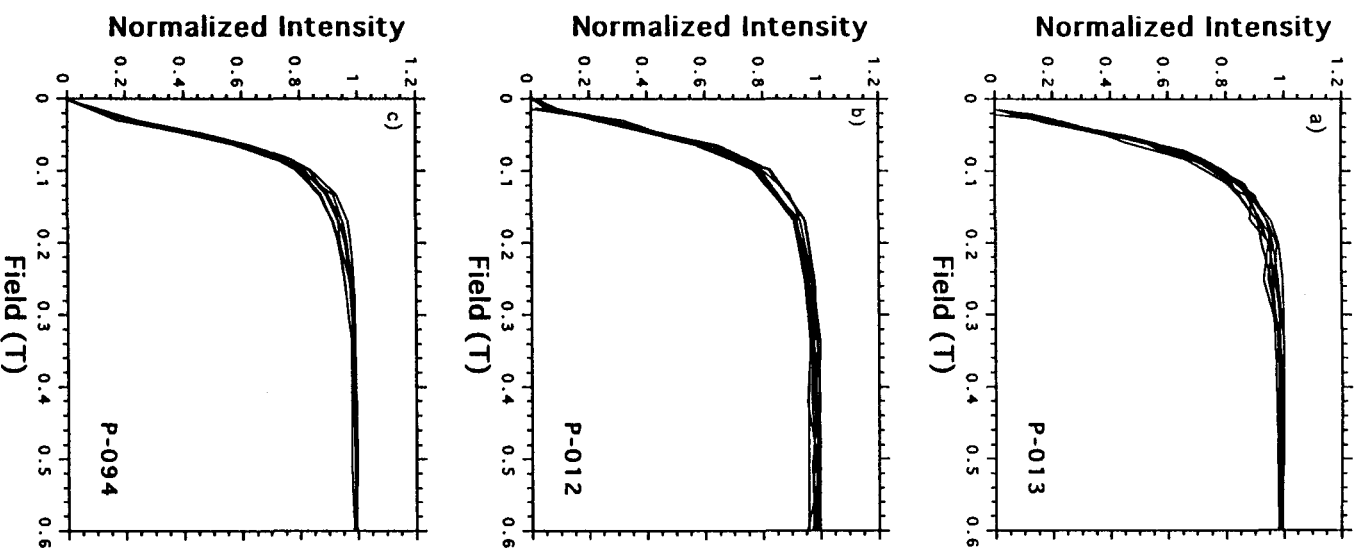


Figure 4.3. IRM acquisition curves of selected samples for Labrador Sea piston cores. a.) P-013. b.) P-012. c.) P-094

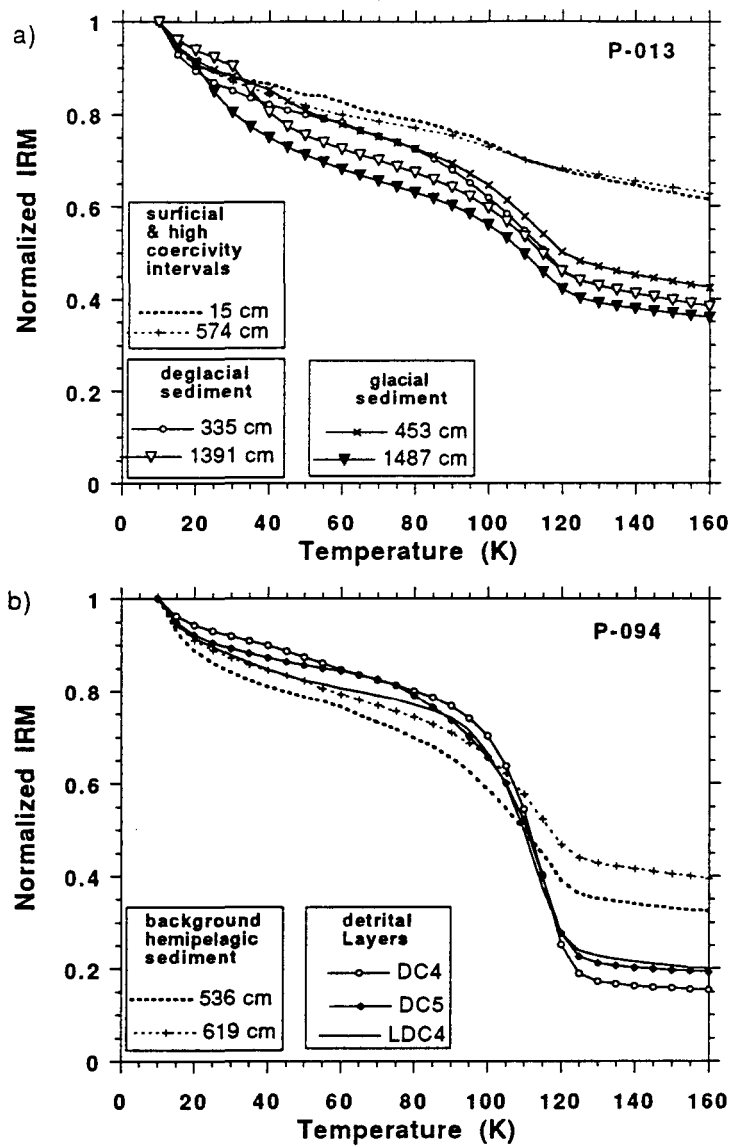


Figure 4.4. Normalized isothermal remanence curves for selected samples during warming from 10 K to 160 K. IRM acquired in 500 mT field at 10 K. a.) P-013. b.) P-094.

(Özdemir et al. 1993). A similar high coercivity interval in P-012 occurs from 70 to 120 cm. Isotopic stratigraphy reveals that these intervals are not coeval, further supporting a post-depositional cause for these intervals.

The dominance of low coercivity ferrimagnetic minerals does not preclude the presence of sulfide as a magnetic contributor. However, no low temperature pyrrhotite transition (Dekkers et al., 1989) was observed (Fig. 4.4). Therefore, based on saturation, hysteresis and low temperature experiments, magnetite is believed to be the dominant magnetic mineral in all three cores.

4.3.2 Concentration

Measurements of k , SIRM and k_{ARM} , show that the concentration of magnetic material varies downcore in P-012 and P-013 by less than a factor of 3 for all but a few samples (Fig. 4.5a, b). P-094 shows variations in magnetite concentration around one order of magnitude (Fig. 4.5c). If sediments associated with DC and LDC layers are discarded, the concentration especially for glacial age sediments varies by less than a factor of 2. Therefore, these cores pass the uniformity of concentration criteria (King et al., 1983; Tauxe, 1993).

4.3.3 Grain-size

Two methods were used for the determination of magnetite grain-size. For all three cores k_{ARM} vs. k plots (Fig. 4.6) were used as a test for consistency of magnetite grain-size, where changes in slope indicate changing grain-size (King et al., 1982, 1983). For P-013 and P-094, hysteresis ratios are also used to determine grain-size and domain state of magnetic particles (Fig. 4.7) (Day et al., 1977).

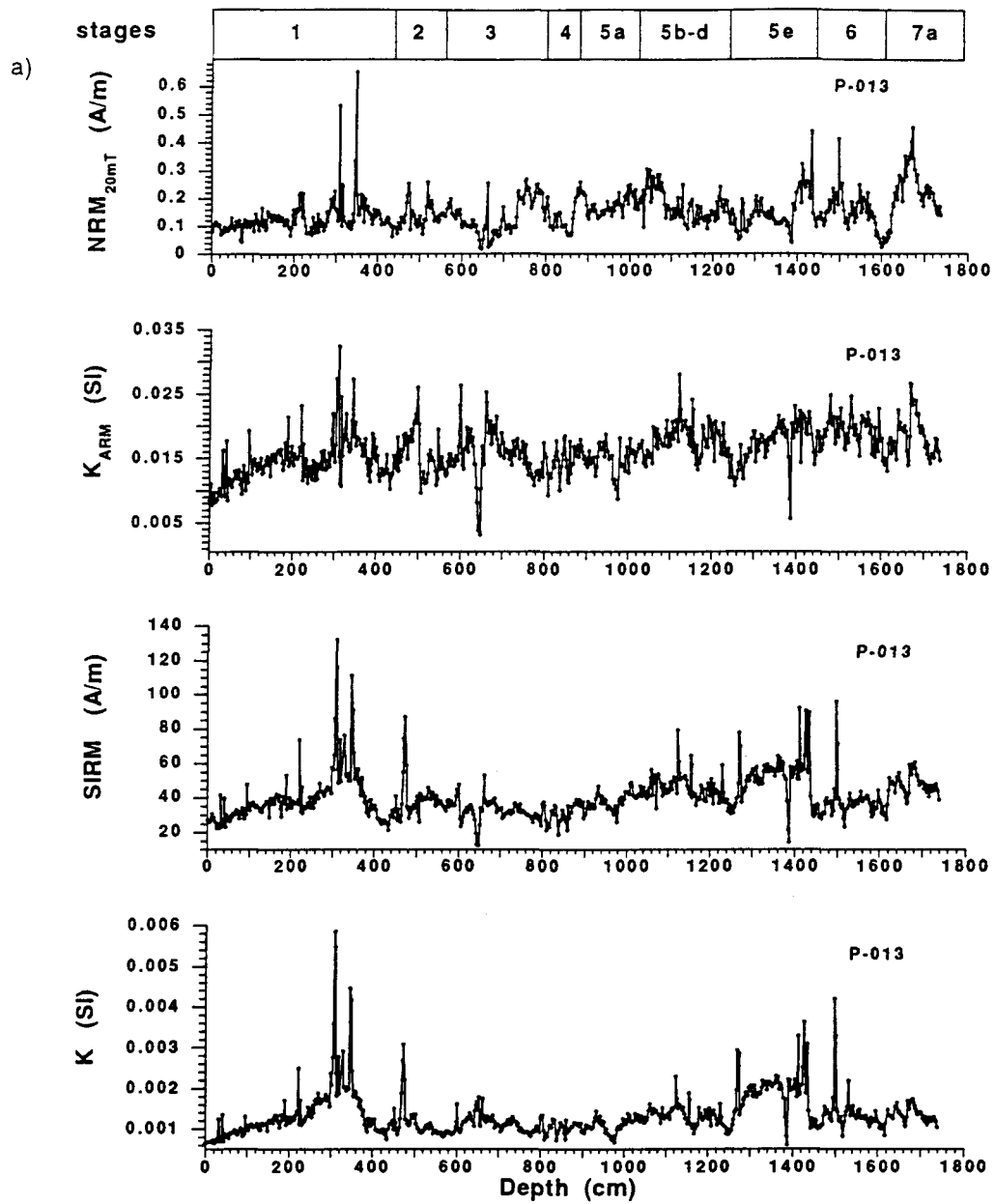


Figure 4.5. Down core profiles of concentration dependent rock magnetic parameters NRM_{20mT}, k , k_{ARM} and SIRM. a.) P-013.

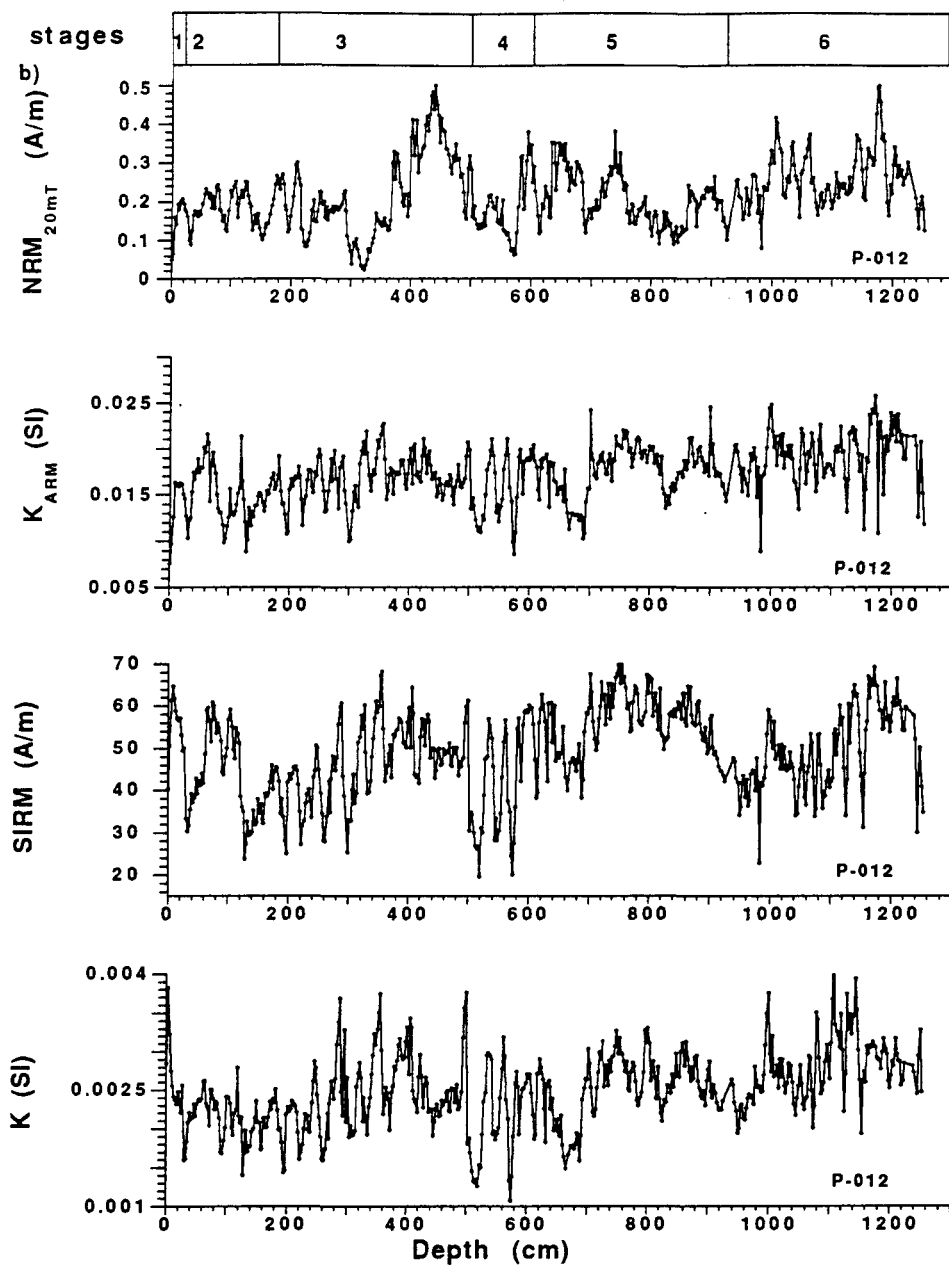


Figure 4.5. Down core profiles of concentration dependent rock magnetic parameters NRM_{20mT}, k , k_{ARM} and SIRM. b.) P-012.

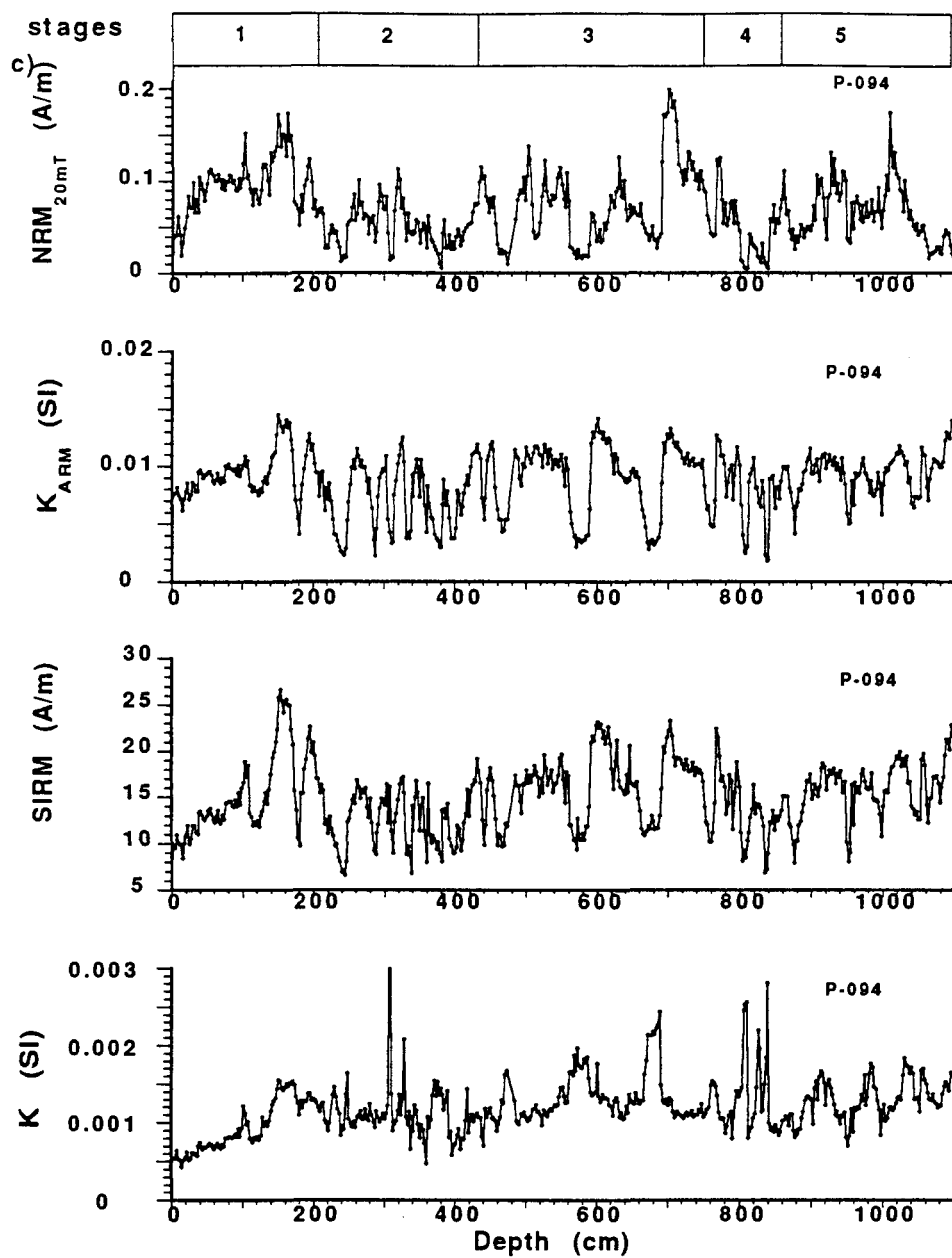


Figure 4.5. Down core profiles of concentration dependent rock magnetic parameters NRM_{20mT} , k , k_{ARM} and SIRM. c.) P-094.

An increase in magnetite grain-size was associated with the isotopic stage 6/5 and 2/1 glacial-interglacial transitions in P-013 (Stoner et al. 1994, 1995). The increase in magnetite grain-size and much higher sedimentation rates suggests that Holocene and last interglacial sediment may not be suitable for reliable paleointensity determinations and are removed from the record. Low interglacial sedimentation rates in P-012 suggest that only a small section of this core is unsuitable for paleointensity determinations. Similarly numerous detrital layers (DC and LDC) in P-094, characterized by large magnetite grain-size and rapid sedimentation, cannot be used for paleointensity determinations. Therefore, these layers were removed and the record was closed around them. The frequency of these events is significantly higher in the upper 500 cm than in the lower 600 cm of P-094. Therefore, a more complete paleointensity record may be derived from the lower section of this core. Several DC and LDC layers are also found within P-012 and P-013. The layers are significantly thinner in these two cores. However, when these layers correspond to changes in magnetite grain-size they are also extracted from the record.

Figure 4.6 shows the k_{ARM} vs. k plots both before and after extraction of sediment considered to unsuitable for paleointensity determinations. Sediment was determined to be unsuitable based sedimentological analysis, magnetite grain-size and sedimentation rate variations. Before extraction several distinct trends associated with different grain-size populations can be observed. After, the general linearity of the data indicates a consistency of grain-size for all cores. Figure 4.7 shows the hysteresis data both before and after extraction. For both P-013 and P-094, after extraction, all samples are constrained within a relatively narrow size range that falls within the PSD field (Day et al. 1977). However, for P-013, two distinct populations are noted. The group of data to the upper right is from the higher coercivity interval (≈ 500 to 600 cm). For P-012 the k_{ARM} vs. k plot indicates coarser magnetite than in the other cores (Fig. 4.6). Comparison between rock magnetic

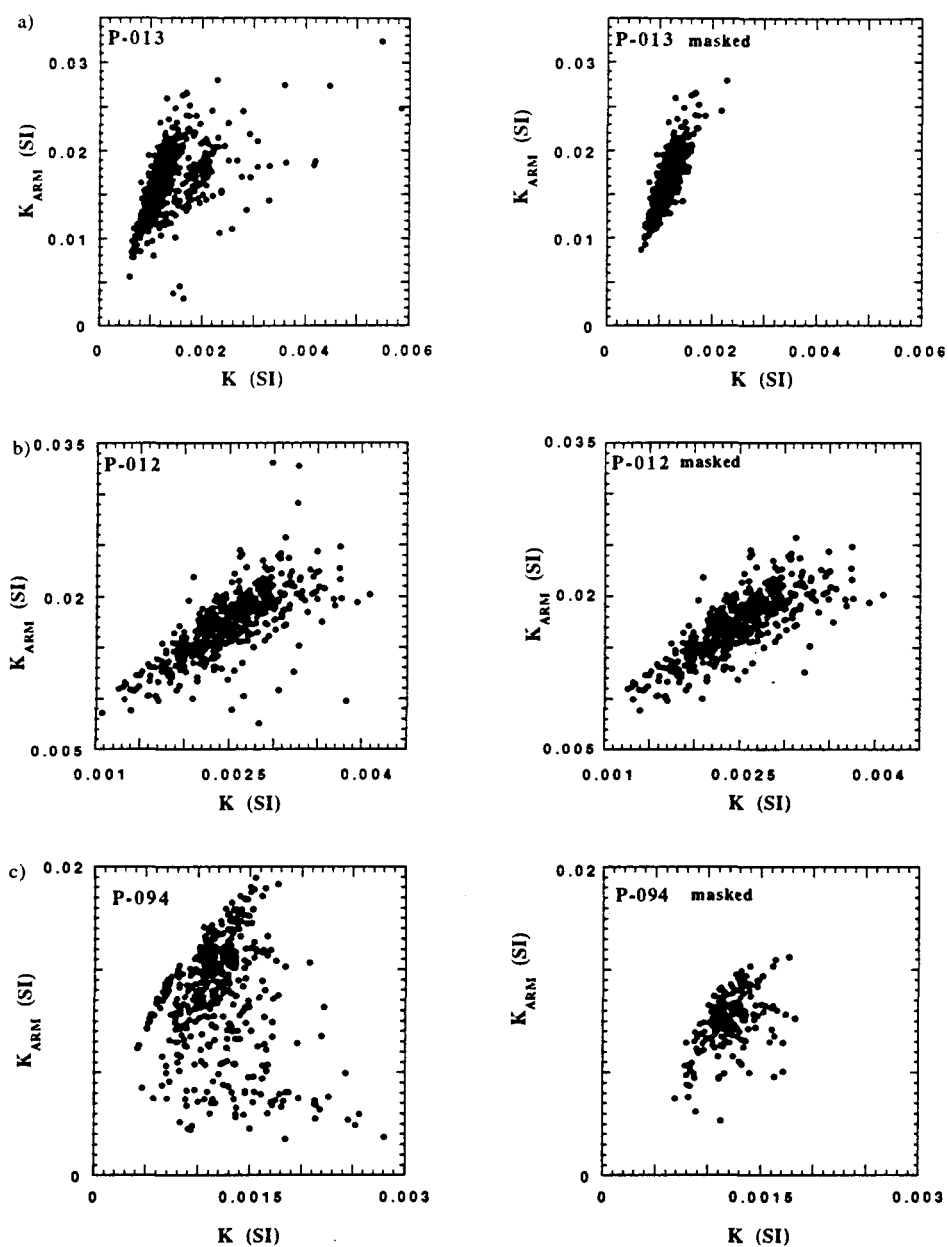


Figure 4.6. Bivariate plot of k_{ARM} versus k (King et al., 1992), both before (left) and after (right) removal of intervals associated with rapid deposition. a.) P-013. b.) P-012. c.) P-094.

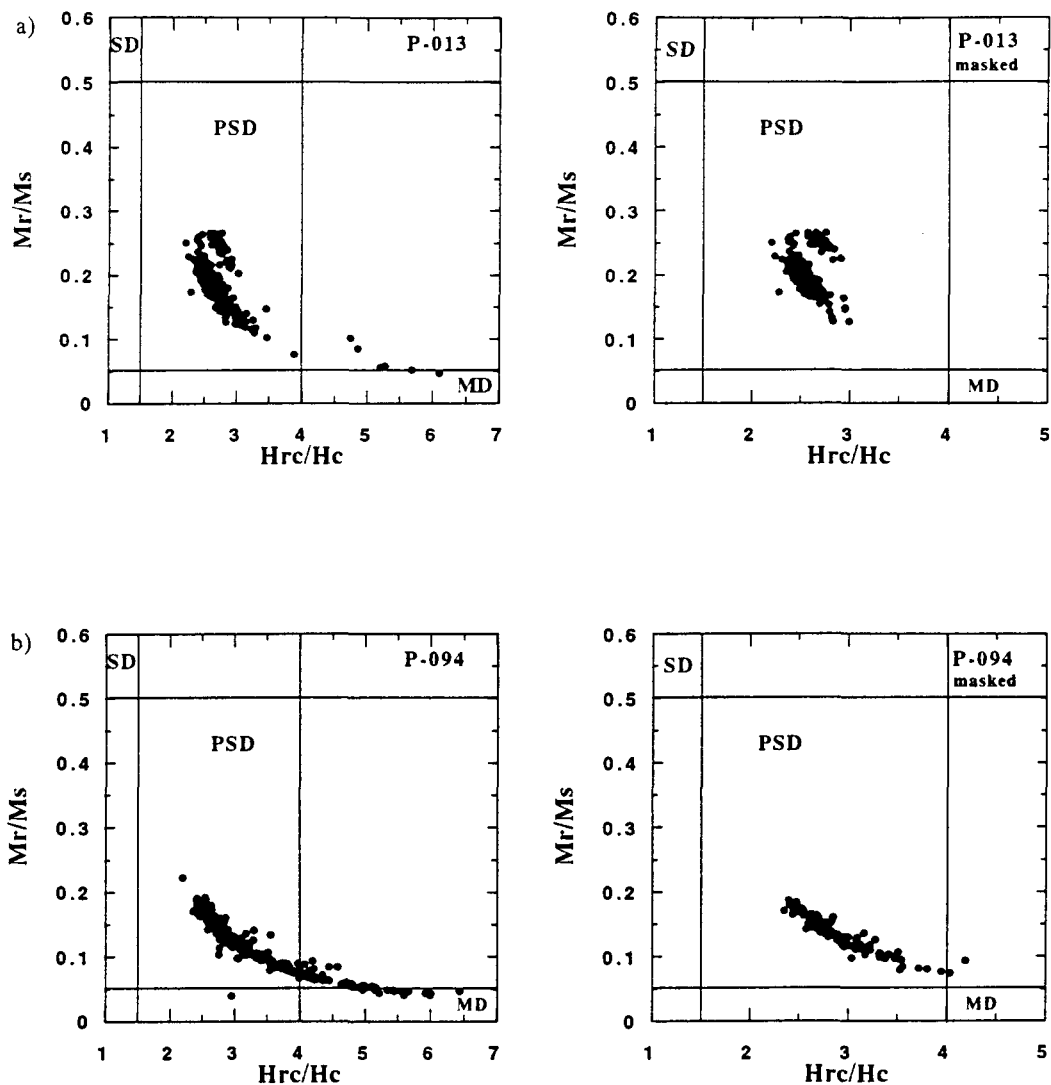


Figure 4.7. Hysteresis parameters both before (left) and after (right) removal of intervals associated with rapid deposition. a.) P-013. b.) P-094. M_{rS} , saturation remanence; M_s , saturation magnetization; H_{cr} , remanent coercivity; H_c , coercive force. Single domain (SD), pseudo-single domain (PSD), and multidomain (MD) fields after Day et al.(1977).

and hysteresis data in the other cores suggests the PSD magnetite is also dominant in P-012.

4.4 NATURAL REMANENT MAGNETIZATION

Stepwise alternating field (AF) demagnetization of the natural remanent magnetization (NRM) was carried out on selected pilot samples at 50 cm spacing in cores P-013, P-012 and P-094. The orthogonal projections of the demagnetization data (Fig. 4.8) indicate a clear linear trend toward the origin after removal of a soft secondary component by peak fields of 10-20 mT. Samples were not fully demagnetized at peak AF fields of 99 mT, although less than 10% of the NRM remained after demagnetization. Median destructive fields values generally ranged between 30 and 40 mT, with values close to 50 mT for high coercivity intervals of P-012 and P-013. On the basis of the orthogonal plots, all samples were treated with a blanket demagnetization at peak AF fields of 20 mT. At this demagnetization level, the secondary overprint was successfully removed from all pilot samples.

4.5 NORMALIZED REMANENCE

As NRM intensity is a function of magnetic concentration as well as magnetic field strength, the NRM record must be normalized in order to obtain a paleointensity record. The normalizer should activate the portion of the magnetic assemblage which carries the NRM, canceling out changes due to concentration and grain-size. Three normalizing parameters were used in this study: k_{ARM} , k , SIRM. For each core, the three normalized records are highly correlated (linear correlation coefficients, $r > 0.9$) (Fig. 4.9). Because normalized remanence is not correlated to the normalizing parameters (Fig. 4.10), normalized remanence variations are not caused by lithology.

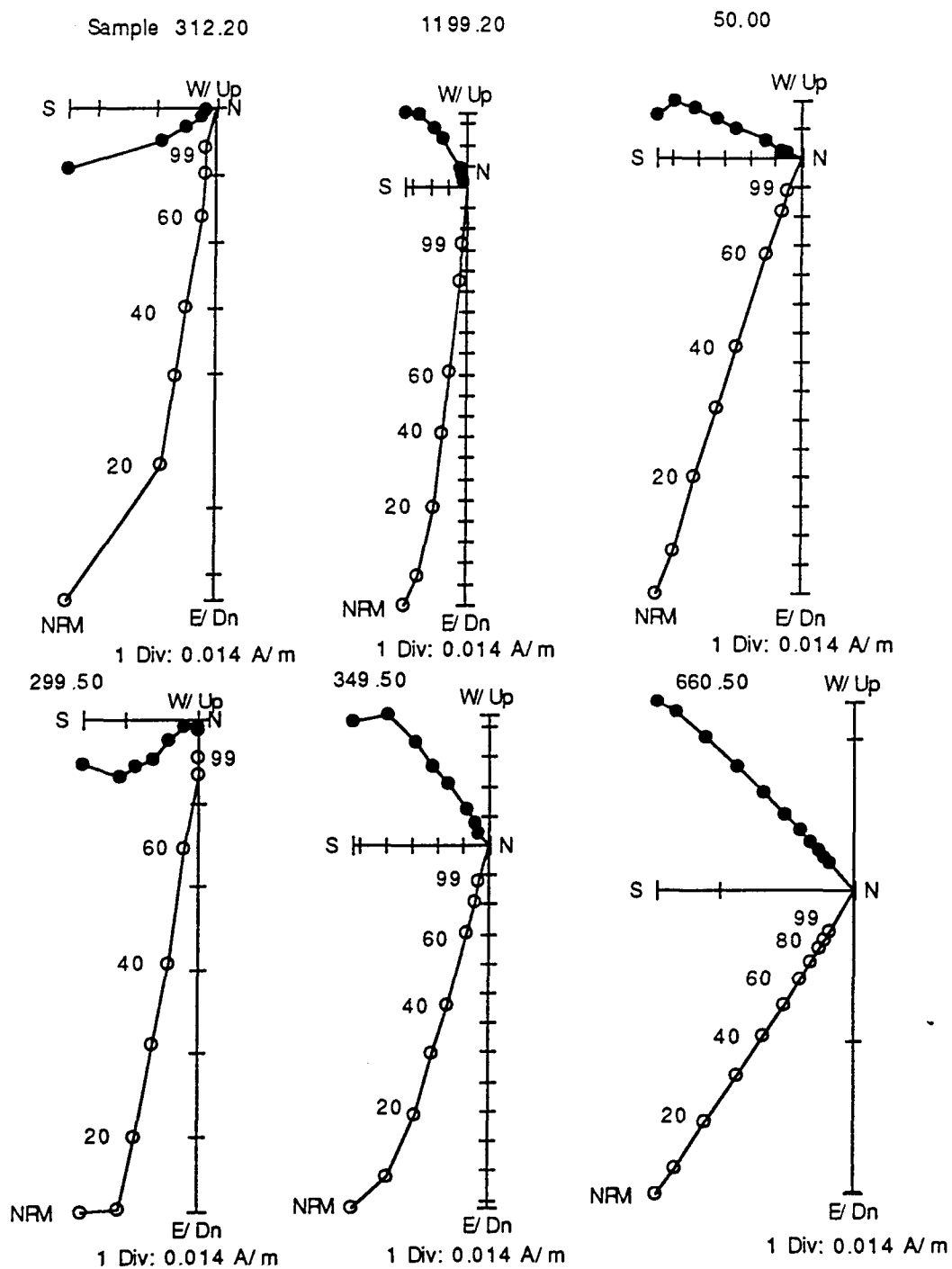


Figure 4.8. Orthogonal vector projections of alternating field demagnetization for samples from piston cores P-012. The declinations have not been corrected for core orientation. The solid (open) symbols represent the projection of the magnetic vector onto the horizontal (vertical) plane.

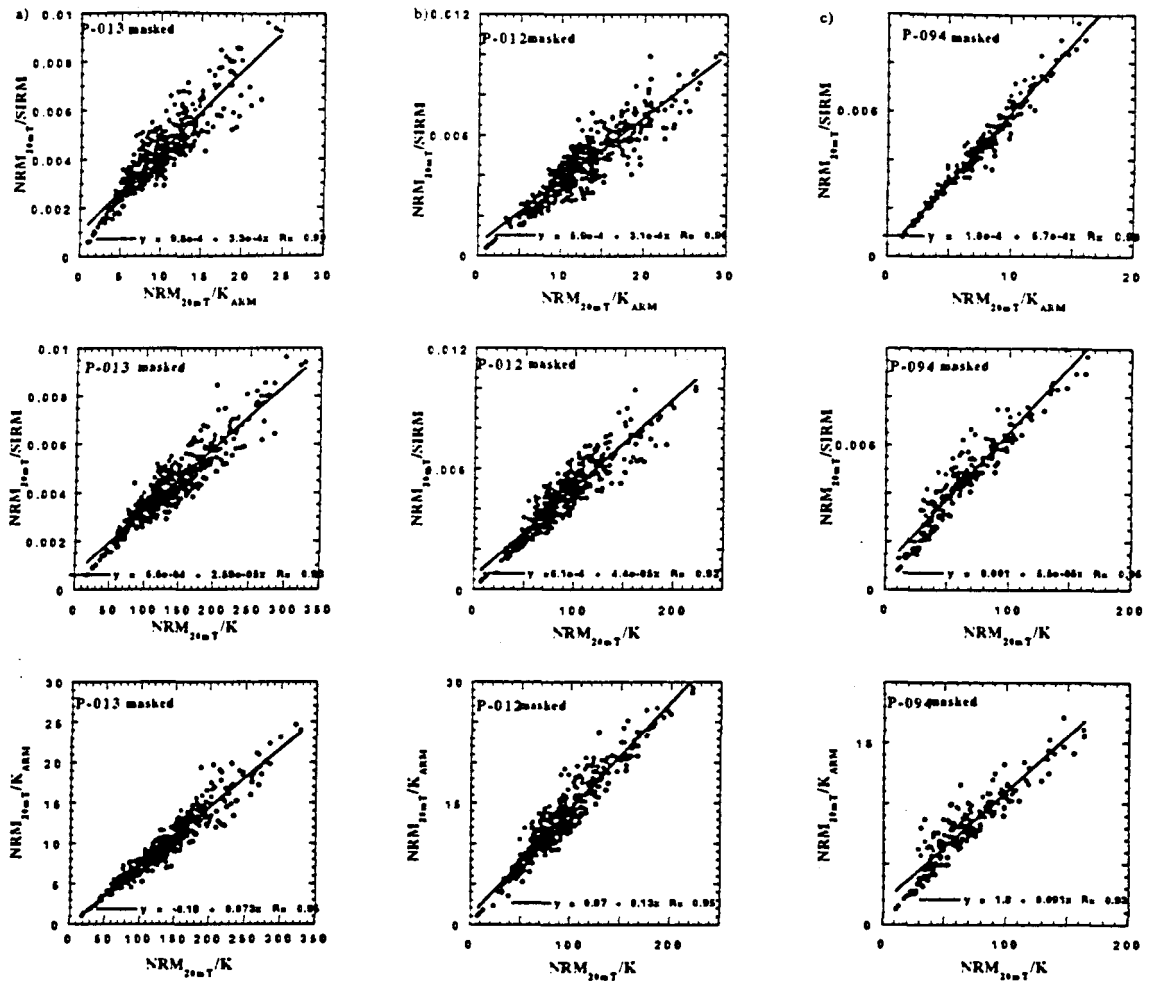


Figure 4.9. Comparisons of normalized remanence, using different normalizing parameters (k , SIRM, k_{ARM}) after removal of intervals associated with rapid deposition. a.) P-013. b.) P-012. c.) P-094

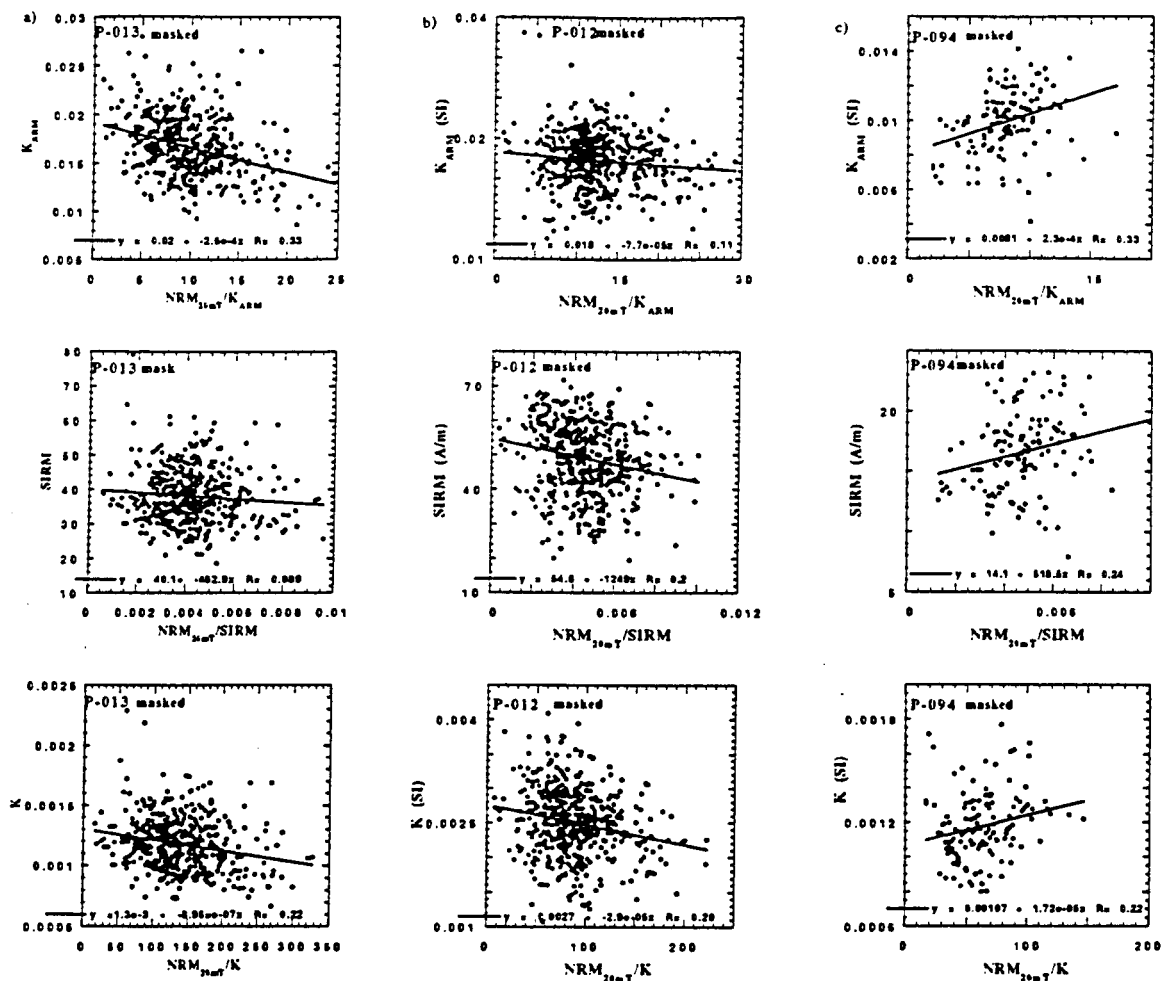


Figure 4.10. Normalized remanence versus the normalizing parameter (k , SIRM, k_{ARM}) after removal of intervals associated with rapid deposition. a.) P-013. b.) P-012. c.) P-094.

Figure 4.11, 4.12 and 4.13, show the normalized remanence plotted vs. depth for P-013, P-012 and P-094, respectively. Large variations in the normalized remanence are observed in all three cores. The detrital carbonate (DC) and (LDC) layers documented by Hillaire-Marcel et al. (1994) are not utilized in the paleointensity record but provide independent stratigraphic markers for core correlation. The consistent position of the DC and LDC layers on the normalized remanence records between cores indicates that normalized remanence records are reproducible within the Labrador Sea. Therefore, it is assumed that the normalized remanence in all three cores reflects the intensity of the Earth's magnetic field at the time of bioturbation in the upper ≈ 10 cm of the sediment column (Wu and Hillaire-Marcel 1994).

4.6 RELATIVE PALEOINTENSITY RECORD

Figure 4.14 shows the relative paleointensity records from P-012, P-013 and P-094 plotted on a common arbitrary depth scale. The correlation of these cores was based on the relative position of detrital layers (DC1, 2, 4, 5, 6 & 7 and LDC4, 5) in each core. No other tie points were used in this correlation. Intervals between DC and LDC layers were expanded or compressed by linear interpolation using the Analyseries software (Paillard and Labeyrie, 1993). Good correlation ($r = 0.66/k_{ARM}$, $0.709/SIRM$) is observed between P-013 and P-012. The correlation of the record from P-094 is not as strong at $r = 0.508$ (k_{ARM}), 0.631 (SIRM) for P-013; and 0.606 (k_{ARM}), 0.608 (SIRM) for P-012. Small offsets of paleointensity features are to be expected considering the large variability of sedimentation rates within and between these cores (Hillaire-Marcel et al., 1994) and the few tie points used (Fig. 4.14). The real strength of this correlation is that these tie points (DC and LDC layers) are completely independent of the paleointensity records. Improved correlations of paleointensity records for all cores are achieved when using SIRM as a

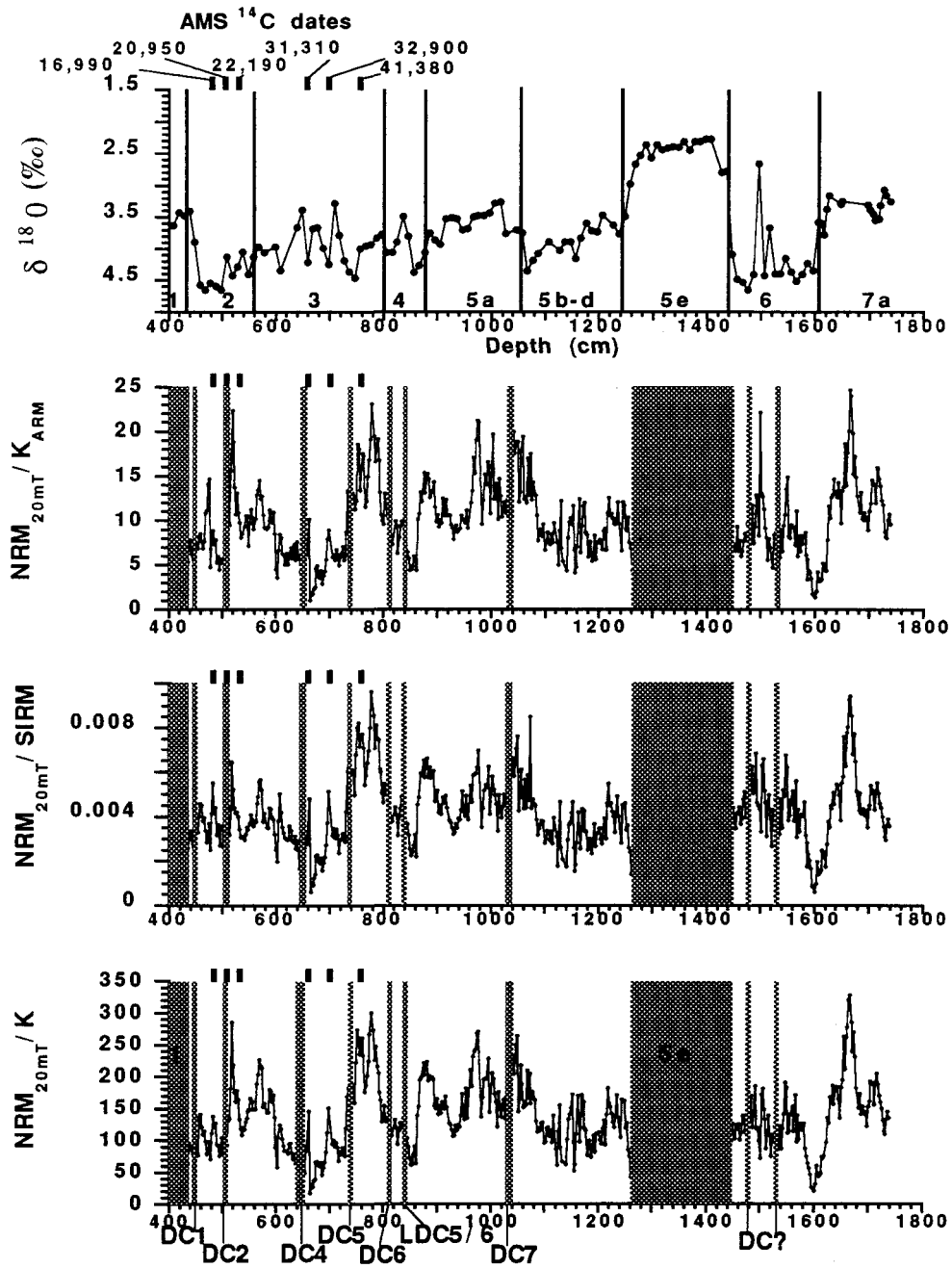


Figure 4.11. From the 400 to 1800 cm interval of P-013, the normalized remanence ($\text{NRM}_{20\text{mT}} / (\text{SIRM}, k_{\text{ARM}}$ and k) compared with the planktonic $\delta^{18}\text{O}$ (‰) and AMS ^{14}C stratigraphy derived from *Neogloboquadrina pachyderma* (L) versus depth (cm) (Hillaire-Marcel et al., 1994). Shaded areas indicate intervals of rapid sedimentation and lithologic events. DC= detrital carbonate event and LDC=low detrital carbonate event as defined by Stoner et al., (submitted).

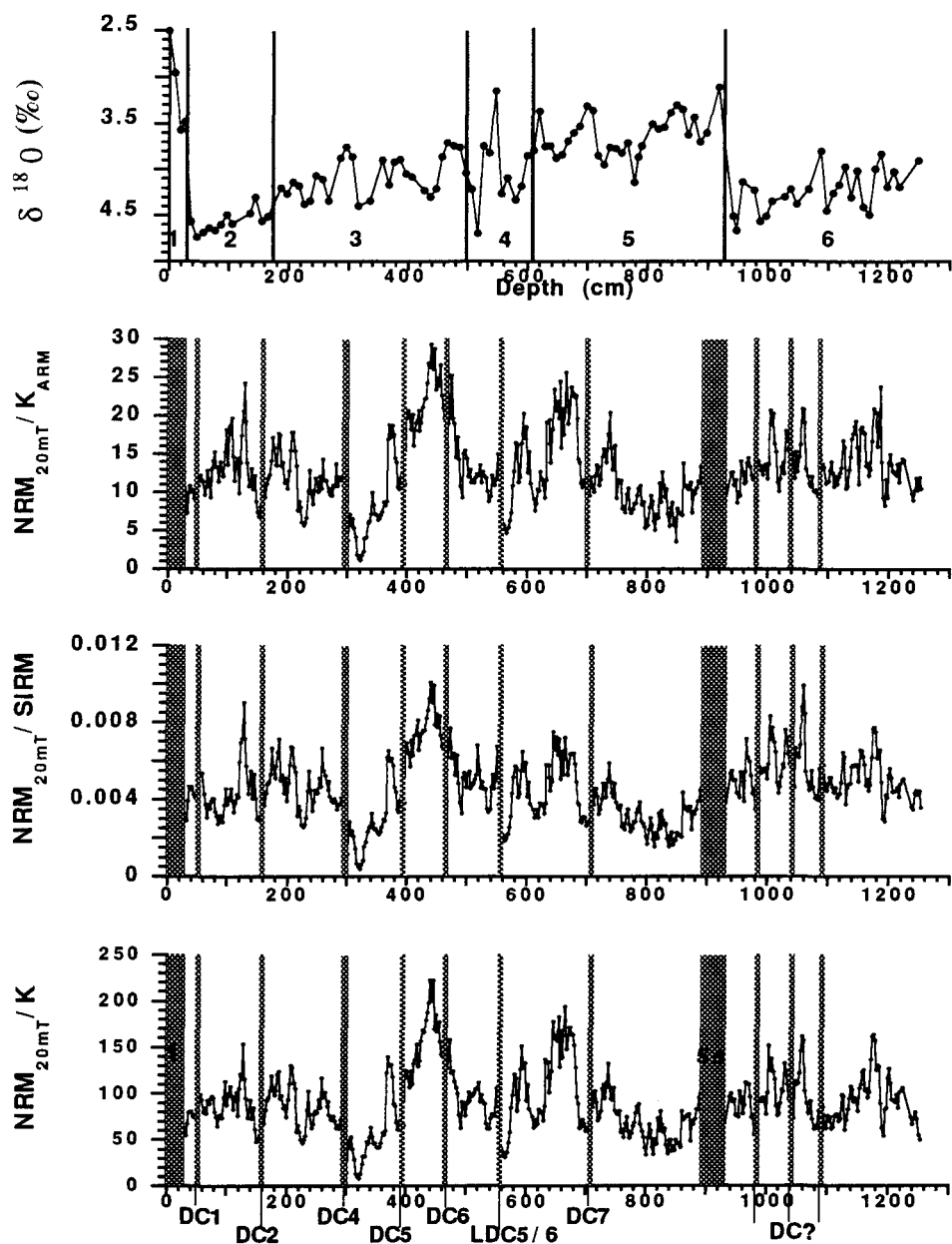


Figure 4.12. From piston core P-012, the normalized remanence ($NRM_{20mT}/(SIRM, k_{ARM}$ and k) compared with the planktonic $\delta^{18}O$ (‰) stratigraphy derived from *Neogloboquadrina pachyderma* (L) versus depth (cm) (Hillaire-Marcel et al., 1994). Shaded areas indicate intervals associated with lithologic events. DC= detrital carbonate event and LDC =low detrital carbonate event as defined by Stoner et al., (submitted).

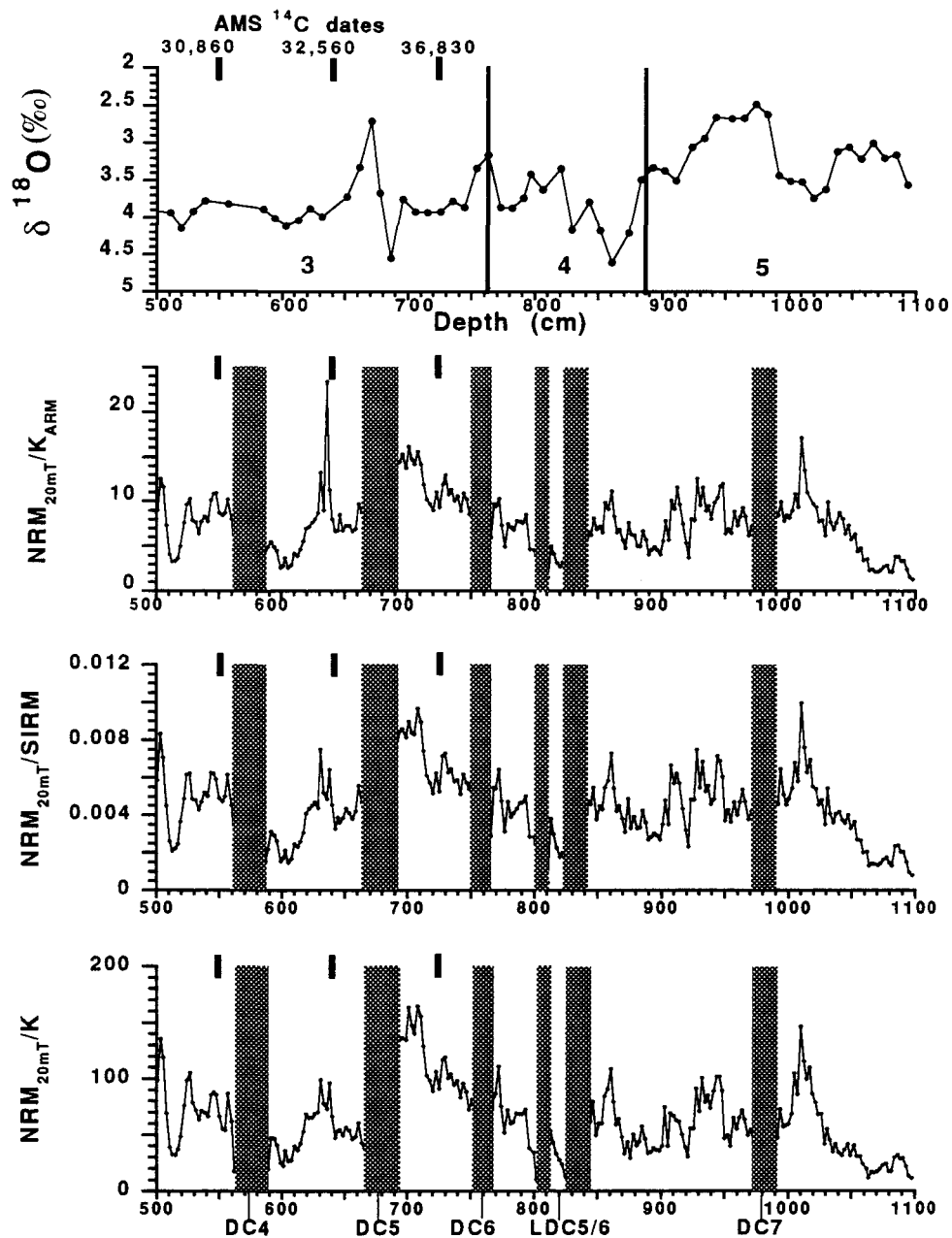


Figure 4.13. From the 500 to 1100 cm interval of piston core P-094, the normalized remanence ($\text{NRM}_{20\text{mT}}/(\text{SIRM}, k_{\text{ARM}}$ and k) compared with the planktonic $\delta^{18}\text{O}$ (‰) and AMS ^{14}C stratigraphy derived from *Neogloboquadrina pachyderma* (L) versus depth (cm) (Hillaire-Marcel et al., 1994). Shaded areas indicate intervals associated with lithologic events. DC= detrital carbonate event and LDC =low detrital carbonate event as defined by Stoner et al., (submitted).

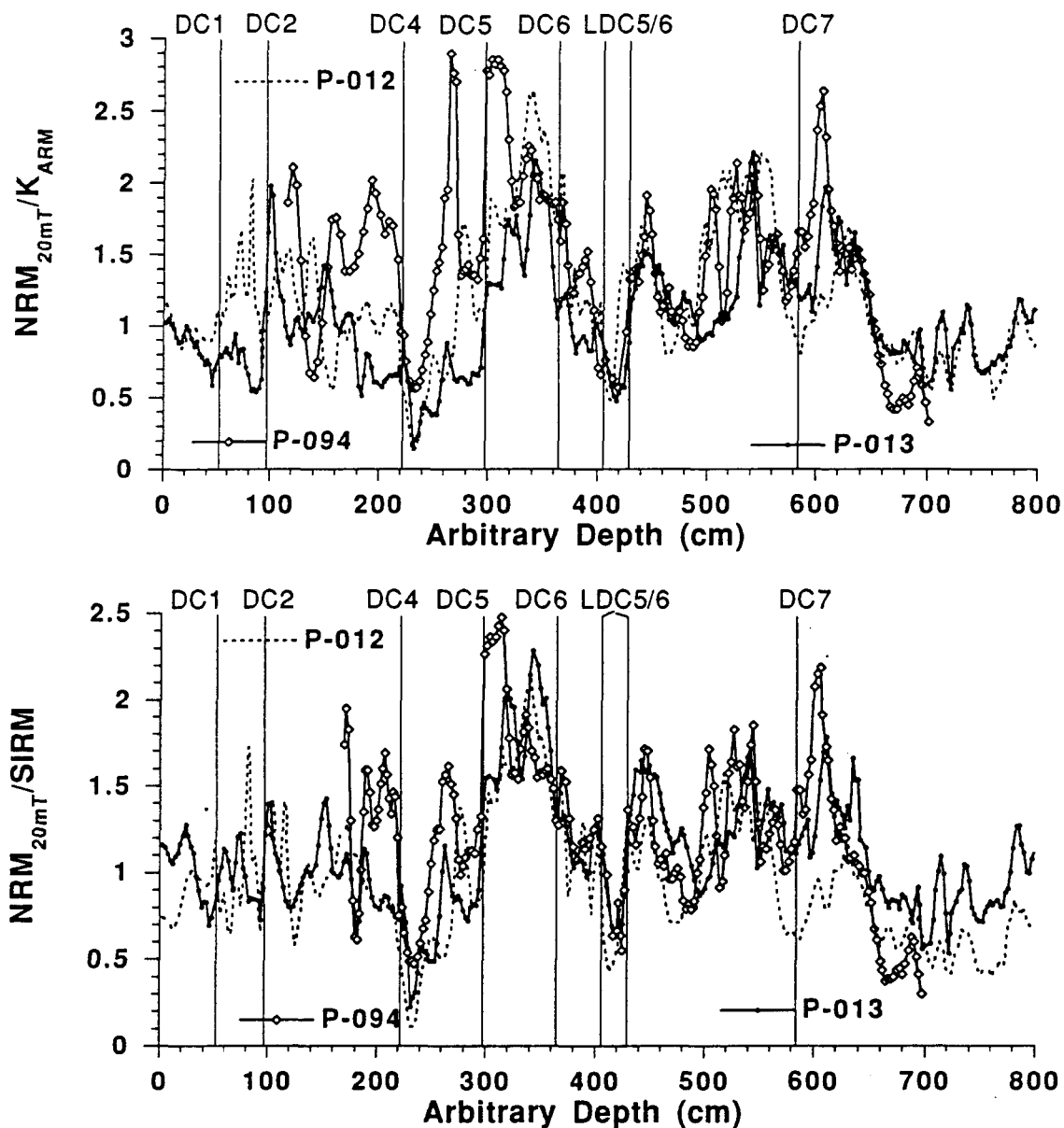


Figure 4.14. Normalized remanence plotted versus common arbitrary depth scale. Correlation of records using tie points (vertical lines) from detrital layers (DC1,2, 4,5,6,7 and LDC 5/6) as defined by Hillaire-Marcel et al. (1994) and Stoner et al. (submitted). a.) NRM_{20mT}/K_{ARM} versus arbitrary depth for P-013, P-012, and P-094. b.) $NRM_{20mT}/SIRM$ versus arbitrary depth for P-013, P-012, and P-094.

normalizer (Fig. 4.14). SIRM is, therefore, the preferred normalizer for these records. When these records are tuned by matching peaks and troughs, a higher level of correlation can be achieved (P-012 to P-013 $r = 0.77/k_{\text{ARM}}$, $0.803/\text{SIRM}$; P-094 to P-013 $r = 0.609/k_{\text{ARM}}$, $0.71/\text{SIRM}$; P-094 to P-012; $0.658/k_{\text{ARM}}$, $0.708/\text{SIRM}$) (Fig. 4.15). This suggests that the paleointensity record provides a climatically independent method of core correlation for the Labrador Sea.

4.7 CHRONOLOGY

To consider the paleointensity records versus age, a Labrador Sea chronometry is used based on AMS ^{14}C dates from P-013 and P-094, and planktonic $\delta^{18}\text{O}$ stratigraphy from P-013, P-012 and P-094 (Wu and Hillaire-Marcel, 1994; Hillaire-Marcel et al., 1994) (Fig. 4.16) All AMS ^{14}C dates are from a monospecific assemblage of *N. pachyderma* (left-coiled), corrected for 400 yr to account for the average difference between atmospheric and surface ocean ages (Stuiver et al. 1986). Isotopic stage boundary ages (Martinson et al., 1987), interpreted from the carbonate and oxygen isotope records, provide chronological control below the level of AMS ^{14}C dates. In all high latitude North Atlantic cores, the oxygen isotope stratigraphy is difficult to interpret and may be a source of error in the age model. Because of ambiguities in isotopic records and rapidly changing sedimentation rates, age control is relatively poor below the level of AMS ^{14}C dates and indistinct between substages 5a and 5e. The chronology is, therefore, restricted to approximately the last 100 kyr with much higher resolution and confidence in the upper 40 kyr than in the lower 60 kyr of the record.

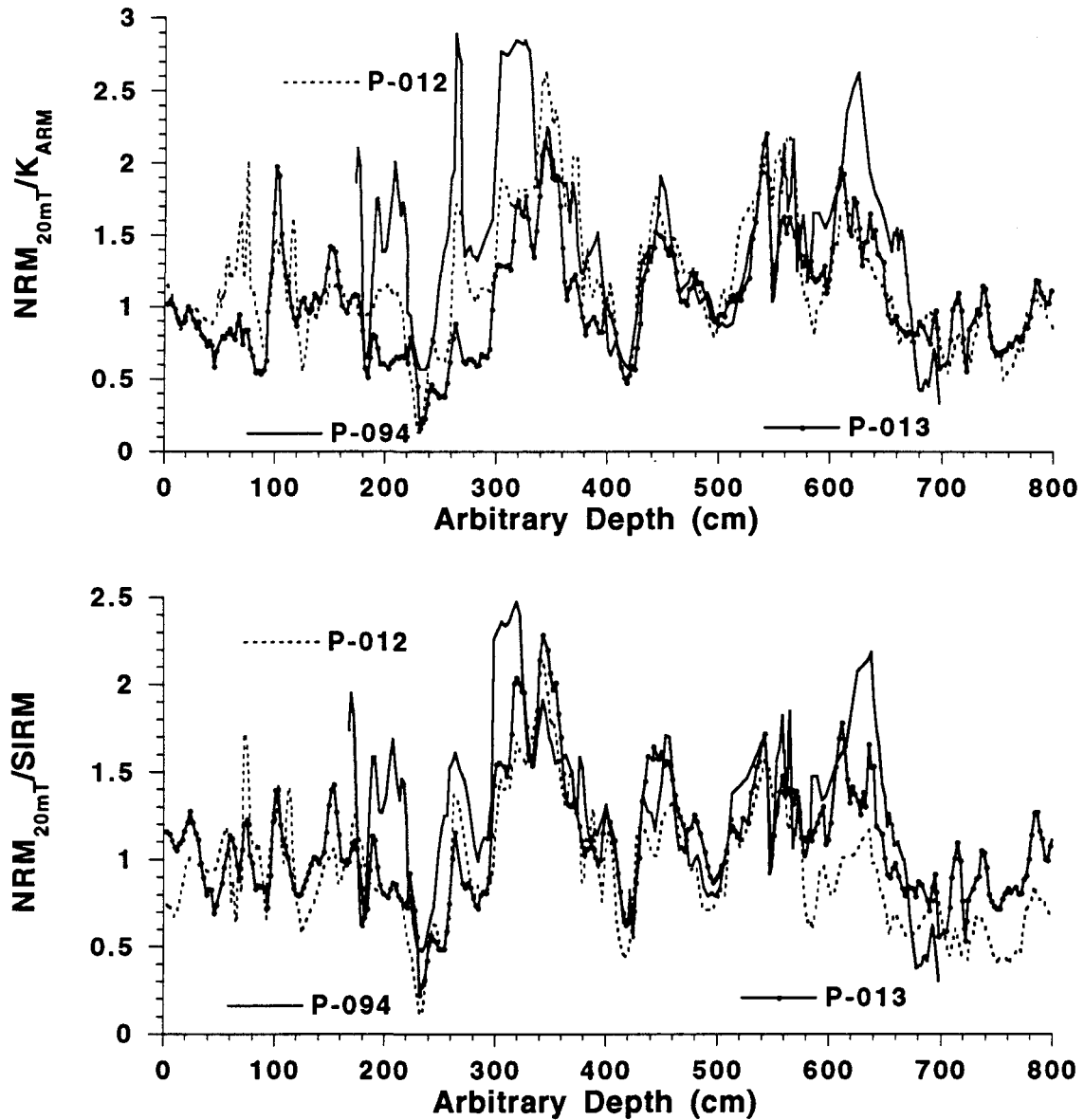


Figure 4.15. Normalized remanence plotted versus common arbitrary depth scale. Correlation of records based on tie points from detrital layers (DC1,2,4,5,6,7 and LDC 5/6) as defined by Hillaire-Marcel et al. (1994) and Stoner et al. (submitted) and visual peak matching. a.) NRM_{20mT}/k_{ARM} versus arbitrary depth for P-013, P-012, and P-094. b.) $NRM_{20mT}/SIRM$ versus arbitrary depth for P-013, P-012, and P-094.

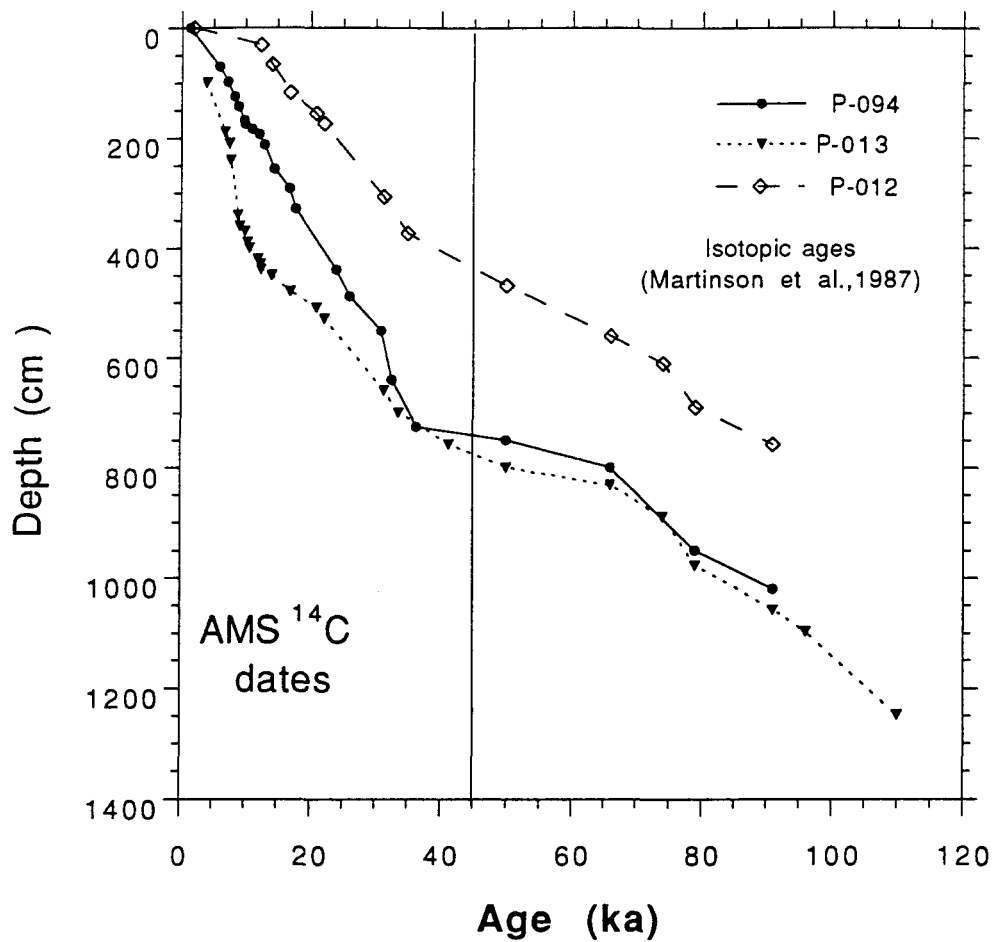


Figure 4.16. Age depth profile for P-013, P-012 and P-094.

4.7.1 Chronology of the Labrador Sea Paleointensity Records

A prominent feature in all three Labrador Sea records is a paleointensity low (Fig. 4.17) that occurs at approximately 660 cm in P-013 (Fig. 4.11), 310 cm in P-012 (Fig. 4.12), 600 cm in P-094 (Fig. 4.13) and 230 cm in the arbitrary depth scale of the stacked Labrador Sea records (Figs. 4.14 and 4.15). In P-013, the paleointensity low corresponds to a reservoir corrected AMS ^{14}C age of $31,310 (\pm 300)$ ^{14}C yr BP and is further constrained by 2 AMS ^{14}C dates 30 cm below of $33,520 (\pm 380)$ and $32,900 (\pm 340)$ ^{14}C yr BP (Fig. 4.11). In P-094 the paleointensity low lies between two AMS ^{14}C dates: $30,860 (\pm 280)$ ^{14}C yr BP above, and $32,560 (\pm 320)$ ^{14}C yr BP below (Fig. 4.13). The correlation of this paleointensity low between cores is facilitated by a lithologic event (DC4) (Hillaire-Marcel et al., 1994; Stoner et al., in press) which occurs directly above this interval in all records (Figs. 4.11, 4.12 and 4.13).

Above the $\approx 31,000$ ^{14}C yr BP paleointensity low, there is a relative high. Variations during this interval are more clearly defined in P-012 than in P-013. The high coercivity interval at 500 to 600 cm in P-013 may account for the lack of agreement between the two cores in this interval. The lower section of this feature appears to be preserved in the record from P-094.

Below the $\approx 31,000$ ^{14}C yr BP paleointensity low, a prominent high is observed in all three records (Figs 4.11, 4.12, and 4.13). Lithologic events DC5 and DC6 are observed on the ramps of this feature. DC5 is suggested to correlate with North Atlantic Heinrich layer H4 (Hillaire-Marcel et al., 1994; Stoner et al., in press). H4 has an AMS ^{14}C estimated age of 35.5 ka (Bond et al., 1993). This age is consistent with the AMS ^{14}C chronometry in P-013 and P-094 (Figs. 4.11 and 4.13) allowing an upper age limit to be placed on this paleointensity high.

Another prominent paleointensity low occurs within isotopic stage 4 (Figs. 4.11,

4.12, and 4.13). This paleointensity low occurs between two detrital layers (LDC5 and LDC6) in P-094. Only one lithologic layer (labeled LDC5) is clearly observed above the paleointensity low in P-012 and P-013. This event may correlate to Heinrich layer H6, defined in the North Atlantic (Heinrich, 1988; Bond et al., 1992).

Below the paleointensity low associated within stage 4 and LDC5/6 is another interval of higher paleointensity. This interval is characterized by three distinct highs in all cores. This intensity high occurs in stage 5a and appears to extend into 5b, although this part of the isotope record is ambiguous. A lithologic event associated with high detrital carbonate in P-094 and defined on the basis of high coarse fraction content in P-012 and P-013, is found between the bottom and middle peak in all records.

Features common to in the paleointensity records are more difficult to identify below isotopic stage 5. The records from both P-013 and P-012 indicate a broad "M" pattern in paleointensity through stage 6. A pronounced low, followed by a high below, is observed from the P-013 record at 1600 cm. This interval corresponds to the isotopic stage 6/7 transition (Hillaire-Marcel et al., 1994). Based on isotopic data, it is unclear whether P-012 extends into isotopic stage 7. The lack of a corresponding paleointensity feature suggests that P-012 terminates within stage 6.

4.8 GLOBAL CORRELATION

Figure 4.17 shows the stacked Labrador Sea (LS) paleointensity record from P-013 and P-012 compared with the stacked Mediterranean, Indian Ocean (MIO) paleointensity record (Meynadier et al., 1992). The stack of these records was derived from the arithmetic mean of the visually tuned correlation of the SIRM normalized records (Fig. 4.15b). The MIO stack was derived from 4 Mediterranean cores constructed to make a composite 8 to 80 ka record (Tric et al., 1992) and 3 Indian Ocean cores stacked for a 15 to 140 ka record

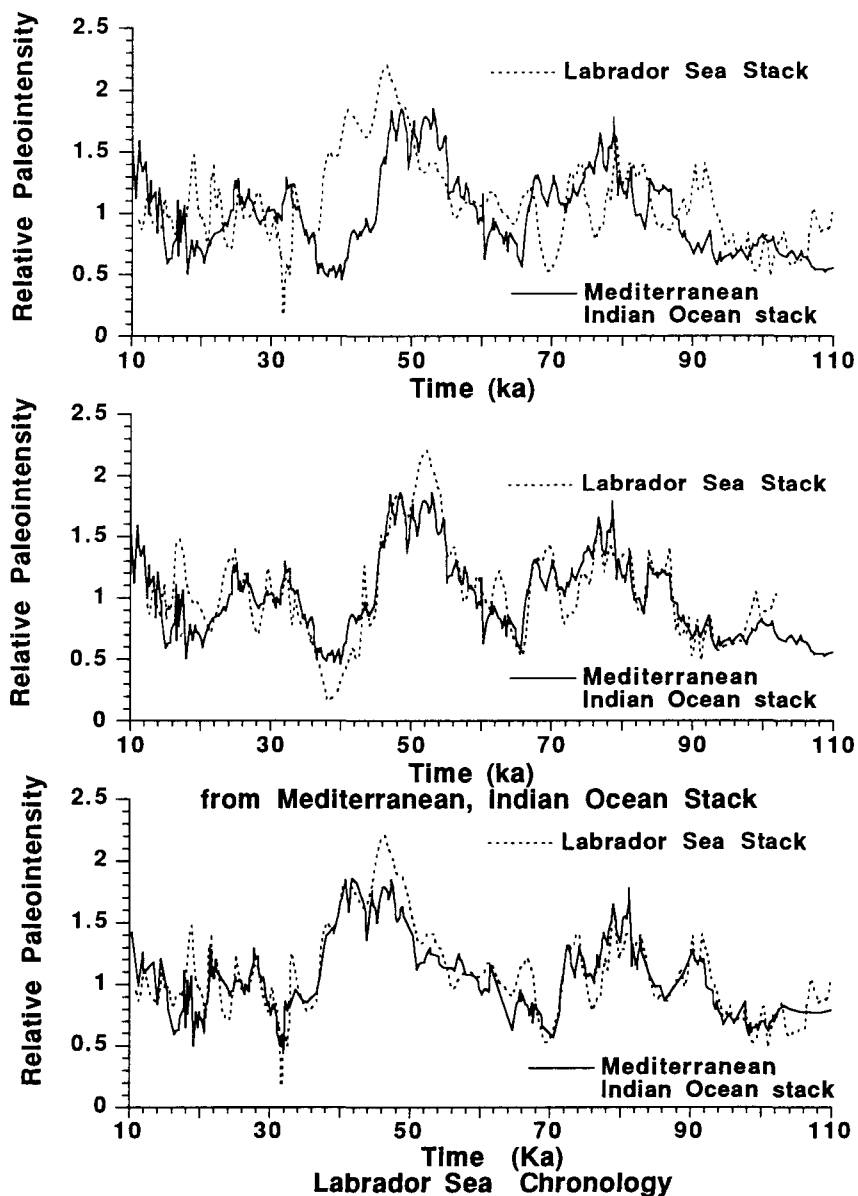


Figure 4.17. a.) The Labrador Sea relative paleointensity stack from P-013 and P-012 (dashed line) versus Labrador Sea age model derived from AMS ^{14}C dates, and isotopic stage determinations. Also plotted on the same scale, the Mediterranean, Indian Ocean paleointensity stack (solid line) (Meynadier et al., 1992; Tric et al., 1992) versus the bulk sediment $\delta^{18}\text{O}$ derived age model of Shackelton et al., (1993) (Indian Ocean) and $\delta^{18}\text{O}$, tephrochronology derived age model of Paterne et al., (1986) (Mediterranean). No correction was made for the difference between ^{14}C and calendar years. b.) Labrador Sea stack correlated to Mediterranean, Indian Ocean time scale. c.) Mediterranean, Indian Ocean paleointensity stack correlated to Labrador Sea time scale.

(Meynadier et al., 1992). In Figure 4.17a the LS stack and the MIO stack are placed on their respective time scales. Figure 4.17a illustrates that significant differences in chronology are present. However, when the LS and MIO stacks respective time scales are adjusted to achieve a maximum fit (LS; Figure 4.17b or MIO; Figure. 4.17c) the stacked records strongly correlate ($r = 0.87$).

The chronological disparities observed in the LS and MIO stacks are most probably due to the different methods used in the construction of the time-scales. The LS time-scale is strongly controlled by two cores with more than 20 AMS ^{14}C dates in each. This provides a high resolution absolute chronometry which can be cross-checked by the relative position of DC and LDC events for the upper 40,000 ^{14}C yr BP of these records. This chronometry is generally consistent with other North Atlantic AMS ^{14}C chronometries (Bond et al., 1992; 1993). However, in older parts of the LS time-scale, age interpretations based on planktonic foraminiferal determined isotopic stages may be distorted due to local environmental effects.

The MIO time-scale based on bulk sediment $\delta^{18}\text{O}$ analysis (Shackleton et al., 1993) for the Indian Ocean record and the planktonic $\delta^{18}\text{O}$ and tephrChronology for Mediterranean (Paterne et al., 1986, Tric et al., 1992) indicate consistently older ages within isotopic stage 3 (Fig. 4.17a). A similar offset was observed by Mazaud et al. (1994) when comparing ^{10}Be flux from the Antarctic Vostok ice core with a synthetic ^{10}Be profile based on geomagnetic intensity records of Meynadier, et al. (1992) and Tric et al. (1992). The lack of absolute age control (AMS ^{14}C dates) for the cores in which paleointensity was determined may be responsible for slight offsets in the chronological interpretations during the relatively indistinct isotope stage 3. For example, the prominent paleointensity low that occurs just below DC 4 in all Labrador Sea records (Figs 4.11, 4.12 and 4.13) and is AMS ^{14}C dated to approximately 31,000 ^{14}C yr BP in two cores is dated at 39 ka in the

Mediterranean (Tric et al., 1992) and at 37 ka in the Indian Ocean (Meynadier et al, 1992). Even after the proposed correction of AMS ^{14}C years into calendar years (Bard et al., 1990, Stuiver et al., 1991, Mazaud et al, 1991) the age of the paleointensity low in the LS record is considerably younger than in the MIO record. However the corrections of Bard et al. (1990) and Stuiver et al. (1991) are only applicable for the last 30 ka, while the results of Mazaud et al. (1991) are based on the Mediterranean paleointensity record (Tric et al, 1992) and may have to be adjusted. Therefore, a reevaluation of the age model may have to be undertaken.

Similarly, the age discrepancy between the older parts of the LS and MIO apparent paleointensity records (Fig. 4.17a) illustrates the difficulty of chronological interpretations from planktonic $\delta^{18}\text{O}$ records in high latitude areas, where continuous benthic records are unavailable. Once a strong chronology can be correlated to paleointensity variations, then the relative paleointensity record will become very useful as a high resolution correlation tool. From this initial study, the consistent correlation of lithologic events to paleointensity variations within the Labrador Sea implies that the paleointensity record has considerable potential as a correlation tool.

4.9 CONCLUSIONS

1. Normalized remanence from each of three deep Labrador Sea piston cores is highly correlated using three normalizing parameters (k_{ARM} , k , SIRM). Normalized remanence is not correlated to the normalizing parameters and is assumed to reflect the intensity of the Earth's magnetic field at the time of bioturbation in the upper ≈ 10 cm of the sediment column.

2. The correlation between the cores based on lithologic features beyond the limit of AMS ^{14}C chronometry, is supported by the consistency of paleointensity curves relative

to DC and LDC layers and the good correlation observed between all three cores.

3. The precise sequence of lithologic events to paleointensity variations within the Labrador Sea suggest that at least locally this record can be used for correlations. (Figs 4.14 and 4.15)

4. The similarity of large scale paleointensity features for P-012, P-013 and P-094 within the Labrador Sea, and for records from the Mediterranean and Indian Ocean suggests that the Labrador Sea sediments carry a record of geomagnetic dipole field intensity (Fig. 4.17). There are, however, major differences between the chronology of the Labrador Sea and that of the other records. In the Labrador Sea, correlation of detrital carbonate (DC) layers on either side of the paleointensity low indicates that the same event is observed in all three records. The AMS ^{14}C chronometry from P-094 and P-013 give very similar age estimates ($\approx 31,000$ ^{14}C yr BP) for the paleointensity low. The chronology of the records of Tric et al. (1993) and Meynadier et al. (1993), should be reexamined to determine whether or not the low at approximately 40 ka is distinct from that at 31 in the Labrador Sea. If global synchronicity could be established for paleointensity variations, then the relative paleointensity record would provide a high resolution global correlation tool.

REFERENCES

- Bard, E., Hamelin, B., Fairbanks, R. G., and Zindler, A., 1990. Calibration of the ^{14}C timescale over the past 30,000 years using mass spectrometric U-Th ages from the Barbados corals. *Nature*, **345**: 405-410.
- Bond, G., Heinrich, H., Broecker, W., Labeyrie, L., McManus, J., Andrews, J., Huon, S., Jantsschik, R., Clasen, S., Simet, C., Tedesco, K., Kias, M., Bonani, G., and Ivy, S. 1992. Evidence for massive discharges of icebergs into the North Atlantic ocean during the last glacial period. *Nature*, **360**: 245-249.
- Bond, G., Broecker, W., Johnsen, S., McManus, J., Labeyrie, L., Jouzel, J., and Bonani, G. 1993. Correlations between climate records from North Atlantic sediments and Greenland ice. *Nature*, **365**: 143-147.
- Broecker, W. S., Andree, M., Bonani, G., Wolfi, W., Klas, M., Mix, A. and Oeschger, H. 1988a. Comparison between radiocarbon ages obtained on coexisting planktonic foraminifera. *Paleoceanography*, **3**: 647-657.
- Broecker, W. S., Andree, M., Bonani, G., Wolfi, W., Oeschger, H, Klas, M., Mix, A. and Curry, W. 1988b. Preliminary estimates for the radiocarbon age of deep water in the glacial ocean. *Paleoceanography*, **3**: 659-669.
- Day, R., Fuller, M., and Schmidt, V. A. 1977, Hysteresis properties of titanomagnetites: grain-size and compositional dependence. *Physics of the Earth and Planetary Interiors*, **13**: 260-267.
- Dekkers, M. J., Mattéi, J-L, Fillion, G. and Rochette, P. 1989. Grain-size dependence of the magnetic behavior of pyrrhotite during its low-temperature transition at 34K. *Geophysical Research Letters*, **16**: 855-858.
- Duplessy, J-C, Arnold, M., Maurice, P, Bard, E., Duprat, J., and Moyes, J. 1986, Direct dating of the oxygen-isotope record of the last deglaciation by ^{14}C accelerator mass spectrometry: *Nature*, **320**: 350-352.
- Fairbanks, R.G., Charles, C. D., and Wright, J. D. 1991. Origin of the global meltwater pulses. *In Radiocarbon after Four Decades* R. E. Taylor et al. eds. pp 473-500 Springer-Verlag, Berlin.
- Francois, R. and Bacon, M. P., 1994. Heinrich events in the North Atlantic: radiochemical evidence. *Deep Sea Research*, **41**: 315-334.
- Heinrich, H. 1988. Origin and consequences of cyclic ice rafting in the northeast Atlantic Ocean during the past 130 000 years. *Quaternary Research*, **29**: 143-152
- Hillaire-Marcel, C., and de Vernal, A. 1989. Isotopic and palynological records of the Late Pleistocene in Eastern Canada and adjacent ocean basins. *Géographie Physique et Quaternaire*, **43**: 263-290.

- Hillaire-Marcel, C., de Vernal, A., Bilodeau, G. and Wu, G. 1994. Isotope stratigraphy, sedimentation rates, deep circulation and carbonate events in the Labrador Sea during the last ~ 200 ka. *Canadian Journal of Earth Sciences*, **31**: 63-89.
- Jones, G. A. and Keigwin, L.D, 1988. Evidence from the Fram Strait (78 N) for early deglaciation. *Nature*, **336**: 56-59.
- Keigwin, L. D., and Jones, G. A., 1994. Western North Atlantic evidence for millennial-scale changes in ocean circulation and climate. *Journal of Geophysical Research*, **99**: 12,397-12,410.
- Kellogg, T. B., Duplessy, J.-C., and Shackleton, N. J., 1978, Planktonic foraminiferal and oxygen isotopic stratigraphy and paleoclimatology of Norwegian Sea deep-sea cores. *Boreas*, **7**: 61-73.
- Kennett, J. P., and Shackleton, N. J., 1975. Laurentide ice sheet meltwater recorded in Gulf of Mexico deep-sea cores. *Science* **188**: 147-150.
- Kent, D. V., and Opdyke, N. 1977. Paleomagnetic field intensity and climatic records in deep-sea sediment core. *Nature*, **266**: 156-159.
- King, J. W., Banerjee, S. K., Marvin, J., and Ozdemir, O. 1982. A comparison of different magnetic methods for determining the relative grain size of magnetite in natural materials: some results from lake sediments. *Earth and Planetary Science Letters*, **59**: 404-419.
- King, J.W., Banerjee, S.K., and Marvin, J. 1983. A new rock magnetic approach to selecting sediments for geomagnetic intensity studies: application to paleointensity for the last 4000 years. *Journal of Geophysical Research*, **88**: 5911-5921.
- Leventer, A., Williams, D. F., and Kennet, J. P., 1982. Dynamics of the Laurentide ice sheet during the last deglaciation: evidence from the Gulf of Mexico. *Earth and Planetary Science letters*, **59**: 11-17
- Mangerud, J., and Gulliksen, S. 1975. Apparent radiocarbon ages of recent marine shells from Norway, Spitsbergen, and Arctic Canada. *Quaternary Research*, **5**: 263-273.
- Martinson, D. G., Pisias, N. G., Hays, J. D., Imbrie, J., Moore, T. C. Jr. and Shackleton, N. J. 1987. Age dating and the orbital theory of the Ice Ages: development of a high-resolution 0 to 300,000-year chronostratigraphy. *Quaternary Research*, **27**: 1-29.
- Mazaud, A., Laj, C., Bard, E., Arnold, M., and Tric, E., 1991. Geomagnetic field control of ¹⁴C production over the last 80 ky: implications for the radiocarbon time-scale. *Geophysical Research Letters*, **18**: 1885-1888.
- Mazaud, A., Laj, C., and Bender, M. 1994. A geomagnetic chronology for antarctic ice accumulation. *Geophysical Research Letters*, **21**: 337-340

- Meynadier, L., Valet, J.P., Weeks, R., Shackleton, N.J., and Hagee, V.L. 1992. Relative geomagnetic intensity of the field during the last 140 ka. *Earth and Planetary Science Letters*, **114**: 39-57.
- Özdemir, Ö., Dunlop, D. J., and Moskowitz, B. M., 1993. The effect of oxidation on the Verwey transition in magnetite. *Geophysical Research Letters*, **20**: 1671-1674.
- Paillard, D. and Labeyrie, L.D., 1993. A user friendly Macintosh software for rapid correlations of paleoclimatic signals and treatments. Centre des Faibles Radioactivités PNEDC/INSU Internal Report, Gif-sur-Yvette, France.
- Paterne, M., Guichard, F., Labeyrie, J., Gillot, P. Y. and Duplessy, J. C. 1986. Tyrrhenian sea tephrochronology of the oxygen isotope records for the past 60,000 years. *Marine Geology*, **72**: 259-285.
- Piasas, N. G., Martinson, D. G., Moore, T. C., Jr., Shackleton, N. J., Prell, W., Hays, J., and Boden, G. 1984. High resolution stratigraphic correlations of benthic oxygen isotopic records spanning the last 300,000 years. *Marine Geology*, **56**: 119-136.
- Schneider, D.A., 1994. An estimate of late Pleistocene geomagnetic intensity variation from Sulu Sea sediments. *Earth and Planetary Science Letters*, **120**: 301-310.
- Shackleton, N., 1987, Oxygen isotopes, ice volume and sea level: *Quaternary Science Reviews*, **6**: 183-190.
- Shackleton, N.J., and Opdyke, N.D. 1973. Oxygen Isotope and Paleomagnetic Stratigraphy of Equatorial Pacific Core V28- 238: Oxygen Isotope Temperatures and Ice Volumes on a 10^5 and 10^6 Year Scale. *Quaternary Research* **3**: 39-55.
- Shackleton, N. J., Hall M. A., Pate, D., Meynadier, L., and Valet, P. 1992. High-resolution stable isotope stratigraphy from bulk sediment. *Paleoceanography*, **8**: 141-148.
- Stoner, J. S., Channell, J. E. T., Hillaire-Marcel C. and Mareschal J.-C., 1994. High resolution rock magnetic study of a Late Pleistocene core from the Labrador Sea. *Canadian Journal Earth Sciences*, **31**: 104-114.
- Stoner, J. S., Channell, J. E. T., and Hillaire-Marcel C., 1995. Magnetic properties of deep sea sediment off SW Greenland: Major differences between the last two deglaciations. *Geology*, **23**: 241-244
- Stoner, J. S, Channell, J. E. T. and Hillaire-Marcel, C., (in press) The magnetic signature of rapidly deposited detrital layers from the deep Labrador Sea: relationship to North Atlantic Heinrich layers. *Paleoceanography*.
- Stuiver, M., Pearson, G. W., and Braziunas, T. 1986. Radiocarbon age calibration of marine samples back to 9000 cal yr Bp. *Radiocarbon*, **28**: 980-1021.

- Stuiver, M., Braziunas, T.F., Becker, B., and Kromer, B., 1991. Climatic, solar, oceanic, and geomagnetic influence on last-glacial and Holocene atmospheric $^{14}\text{C}/^{12}\text{C}$ change. *Quaternary Research*, **35**: 1-24.
- Tauxe, L. 1993. Sedimentary records of relative paleointensity of the geomagnetic field: theory and practice. *Reviews of Geophysics*, **31**: 319-354.
- Tauxe, L., and Wu, G. 1990. Normalized remanence in sediments from western equatorial Pacific: relative paleointensity of the geomagnetic field. *Journal of Geophysical Research*, **95**: 12337-12350.
- Tauxe, L., and Shackleton, N.J. 1994. Relative paleointensity records from the Ontong-Java plateau. *Geophysical Journal International* **117**: 769-782.
- Tric, E., Valet, J.P., Tucholka, P., Paterne, M., Labeyrie, L., Guichard, F., Tauxe, L., and Fontugne, M. 1992. Paleointensity of the geomagnetic field for the last 80,000 years. *Journal of Geophysical Research*, **97**: 9337-9351.
- Valet, J.-P., and Meynadier, L., 1993. Geomagnetic field intensity and reversals during the last four million years. *Nature*, **366**: 234-238.
- Wu, G. and Hillaire-Marcel, C. 1994a. Oxygen isotope compositions of sinistral *Neogloboquadrina pachyderma* tests in surface sediments: North Atlantic Ocean. *Geochimica et Cosmochimica Acta*, **58**: 1303-1312.
- Wu, G. and Hillaire-Marcel, C. 1994b. AMS radiocarbon stratigraphies in deep Labrador Sea Cores: paleoceanographic implications. *Canadian Journal of Earth Science*, **31**: 38-47.
- Yamazaki, T., and Ioka, N., 1994. Long-term secular variation of the geomagnetic field during the last 200 kyr recorded in sediment cores from the western equatorial Pacific. *Earth and Planetary Science Letters*, **128**: 527-544.

GENERAL CONCLUSIONS

Based on the study of the magnetic properties and paleointensity records from Late Quaternary Labrador Sea sediments, several general conclusions can be made. 1). The Labrador Sea provides an ideal location for using magnetic parameters for high resolution characterization and description of lithologic stratigraphy. The very high terrigenous content of these sediments, derived from old cratonic rocks of Greenland and Labrador, provide a source of dominantly pseudo-single domain magnetite at high concentrations. These sediments are characterized by more than one order of magnitude greater ferrimagnetic concentration than those observed from eastern North Atlantic sites (Bloemendal, et al., 1992). The generally oxic conditions of the sediment led to minimal diagenetic alteration of the magnetic minerals and, therefore, a high fidelity record of environmental change. However, relict oxic zones do occur and are clearly delineated by distinct magnetic properties. Due to the high magnetite concentration and sedimentation rates within the Labrador Sea, variation in the magnetic properties reflect changes in the sediment matrix and therefore, reflect fundamental changes in the environmental condition or depositional mechanisms. The magnetic properties are much less responsive to secondary depositional sources (i.e. IRD).

2). The interpretation and conclusions made in this study were possible because of the multidisciplinary nature of the study (see; Hillaire-Marcel, C. *Can. J. Earth Sci.*, 31(1), 1994; special issue, entitled "The Labrador Sea during the late Quaternary"). Lithologic, isotopic and geochemical studies have shown that short term variations in high resolution magnetic data reflect significant depositional changes, rather than noise in the magnetic signal. The covariance of the magnetic parameters with lithologic, isotopic, geochemical, micropaleontological changes implies very little noise in the magnetic signal. Features in the magnetic records occurring over a few centimeters, and corresponding to less than a few hundred years, appear to have paleoenvironmental significance.

3). Although the sedimentary record within the Labrador Sea is strongly influenced by climatic and ice sheet variability on both Milankovitch and sub-Milankovitch time scales, these sediments yield high fidelity records of geomagnetic field intensity. The paleointensity records from the Labrador Sea are well correlated between three well studied Labrador Sea cores (see; Hillaire-Marcel, C. *Can. J. Earth Sci.*, 31(1), 1994) indicating the utility of these records for regional correlation. The correlation to geomagnetic paleointensity records outside the NW Atlantic indicates that relative paleointensity measurements are recording dipole field intensity, with potential for global correlation. The potential advantages of the paleointensity record as a correlation tool over traditional methods (i.e. $\delta^{18}O$) include: (1) The geomagnetic paleointensity record is not limited to marine sediments and therefore may be applicable to other continuous depositional sequences such as lakes, loess deposits, and ice cores as reconstructed from ^{10}Be profiles (Mauzaud et al., 1994). (2) The geomagnetic paleointensity record is not directly related to environmental conditions, therefore, chronometric determinations may be greatly simplified. The quality of the record is, however, dependent on the environmental conditions. (3) Geomagnetic paleointensities, if due to the dipole field, are globally synchronous. (4) Significantly greater variability is

observed within paleointensity record than in the $\delta^{18}\text{O}$ record, suggesting that higher resolution correlations and chronometric determinations are possible. However, the global synchronicity of high frequency paleointensity variations, as suggested from this study, have yet to be established.

REFERENCES

- Bloemendal J., King, J. W., Hall, F. R., and Doh, S.J. 1992. Rock magnetism of Late Neogene and Pleistocene deep-sea sediments: relationship to sediment source, diagenetic processes, and sediment lithology. *Journal of Geophysical Research*, **97**: 4361-4375.
- Mazaud, A., Laj, C., and Bender, M. 1994. A geomagnetic chronology for antarctic ice accumulation. *Geophysical Research Letters*, **21**: 337-340
- Hillaire-Marcel, C. coordinator 1994. The Labrador Sea during the late Quaternary. *Canadian Journal of Earth Science*., **31(1)**, 158p.

APPENDICES

Table A.1 Generalized table of downcore magnetic parameters and their interpretations.

Parameters	Interpretation
Bulk Magnetic Parameters	
Generally measured on 7 cc orientated cubic samples.	
<p>Natural Remanent Magnetization (NRM) The fossil magnetization preserved within the sediment. NRM includes the declination, inclination, and intensity.</p>	Dependent on mineralogy, concentration, and grain-size of the magnetic material as well as mode of acquisition and intensity of the geomagnetic field.
<p>Volumetric Magnetic Susceptibility (k_v) A measure of the concentration of magnetizable material.</p>	<p>k_v is a first order measure of the amount of ferrimagnetic material (e.g., magnetite). However, k_v also responds to antiferromagnetic (e.g., hematite), paramagnetic (e.g., Fe, Mg silicates), superparamagnetic (SP) (e.g. magnetite < 0.03μm) and diamagnetic material (e.g. carbonate) which may complicate the interpretation.</p>
<p>Isothermal Remanent Magnetization (IRM) Magnetization acquired under the influence of DC magnetic field. Commonly expressed as a saturation IRM or SIRM when a field greater than 1T is used. An IRM may also be given as a backfield (BIRM) when magnetized in the opposite orientation.</p>	SIRM primarily responds the concentration of magnetic, principally ferrimagnetic material has a secondary response to changes in grains-size and mineralogy.
<p>Anhyseretic Remanent Magnetization (ARM) Magnetization acquired when a biasing field is imparted on a sample within a decreasing alternating field. Commonly expressed as an Anhyseretic susceptibility (k_{ARM}) when normalized by the biasing field used.</p>	<p>k_{ARM} is primarily a measure of the concentration of ferrimagnetic material, however it is also strongly grain-size dependent. k_{ARM} preferentially responds to smaller grain-sizes, and is therefore useful in the development of grain-size dependent ratios.</p>
<p>The "hard" IRM (HIRM) This is derived by imparting a back field of typically 0.1 or 0.3 T on a sample previously given an SIRM. BIRM which has a negative sine is used to derive the HIRM. $HIRM = (SIRM + BIRM)/2$.</p>	HIRM is a measure of the concentration of magnetic material with a higher coercivity than the backfield. This gives information on the concentration of the non-ferrimagnetic or very fine grained ferrimagnetic component depending on the backfield is chosen.

Table A.1 Generalized table of downcore magnetic parameters and their interpretations (continued).

Ratios

Ratios of different magnetic parameters are essentially concentration independent, therefore downcore variations in these ratios may be interpreted as variations in grain-size and/or mineralogy

<p>S-ratios</p> <p>These are derived by imparting a backfield of typically 0.1 or 0.3 T on a sample previously given an SIRM. The BIRM is then normalized by the SIRM value providing a measure of the proportion of higher coercivity material to total magnetic assemblage. $S = \text{BIRM/SIRM}$</p>	<p>The S-ratios can be used to estimate the magnetic mineralogy (i.e., magnetite or hematite) Downcore variations may be associated with changing mineralogy Values close to 1 indicate lower coercivity and a general ferrimagnetic mineralogy (i.e., magnetite), values closer to 0 indicate a higher coercivity possibly antiferromagnetic (i.e., hematite) mineralogy. S-ratio with a backfield of 0.1 T is very sensitive mineralogic and grain-size changes, but is not mineralogically discriminatory. While 0.3 T is discriminatory, it is not very sensitive.</p>
<p>k_{ARM}/k</p> <p>Indicates changes in magnetic grain-size, if the magnetic mineralogy is dominantly magnetite.</p>	<p>If the magnetic mineralogy is dominantly magnetite k_{ARM}/k varies inversely with magnetic grain-size from approximately 1-15μm. However, the interpretation of this ratio may be compromised by significant amounts of SP or paramagnetic material.</p>
<p>SIRM/k</p> <p>Indicates changes in magnetic grain-size, if the magnetic mineralogy is dominantly magnetite.</p>	<p>If the magnetic mineralogy is dominantly magnetite SIRM/k varies inversely with magnetic particle size. SIRM/k is more sensitive to changes in the large (>10μm) and small (< 1μm) and can, therefore, be difficult to interpret. SIRM/k may also be compromised by SP or paramagnetic material.</p>
<p>SIRM/k_{ARM}</p> <p>Indicates changes in magnetic grain-size, if the magnetic mineralogy is dominantly magnetite.</p>	<p>SIRM/k_{ARM} increases with increasing magnetic grain-size, but is less sensitive and can be more difficult to interpret than the other two. A major advantage of SIRM/k_{ARM} is that it only responds to remanence carrying magnetic material and is therefore not compromised by SP or paramagnetic material.</p>
<p>Frequency dependent magnetic Susceptibility (k_f)</p> <p>The ratio of low-frequency k (0.47kHz) to high frequency k (4.7 kHz)</p>	<p>k_f is used to indicate the presence of SP material. SP material in high concentrations can compromise the grain-size interpretation made using the k ratios</p>

Table A.1 Generalized table of downcore magnetic parameters and their interpretations (concluded).

Hysteresis Parameters

Hysteresis parameters provide an independent method to assess magnetic grain-size and mineralogic changes. Because these parameters are not influenced by paramagnetic material they may provide a more accurate estimate of grain-size changes. However, care must be taken with sediments that are not strongly homogenous because of the small sample size (approximately 0.01 g) typically used.

<p><u>Saturation Magnetization (M_s)</u> M_s is the magnetization within a saturating field.</p> <p><u>Saturation Remanence (M_{rs})</u> M_{rs} is the remanence remaining after removal of the saturating field</p>	<p>These parameters are typically used in the ratio M_{rs}/M_s which for magnetite decreases with increasing grain-size. This ratio is considered to be the most sensitive because it shows large variations over the (0.025 to 230 μm) size range.</p>
<p><u>Coercive force (H_c)</u> The field required to rotate saturation magnetization to zero within an applied field.</p> <p><u>Coercivity of Remanence (H_{cr})</u> The field required to rotate saturation magnetization to zero remanence</p>	<p>These parameters are typically used in the ratio H_{cr}/H_c which for magnetite increases with increasing grain-size. This ratio is biased toward larger grain-sizes due to the weak size dependence of H_c for larger grain-sizes.</p>

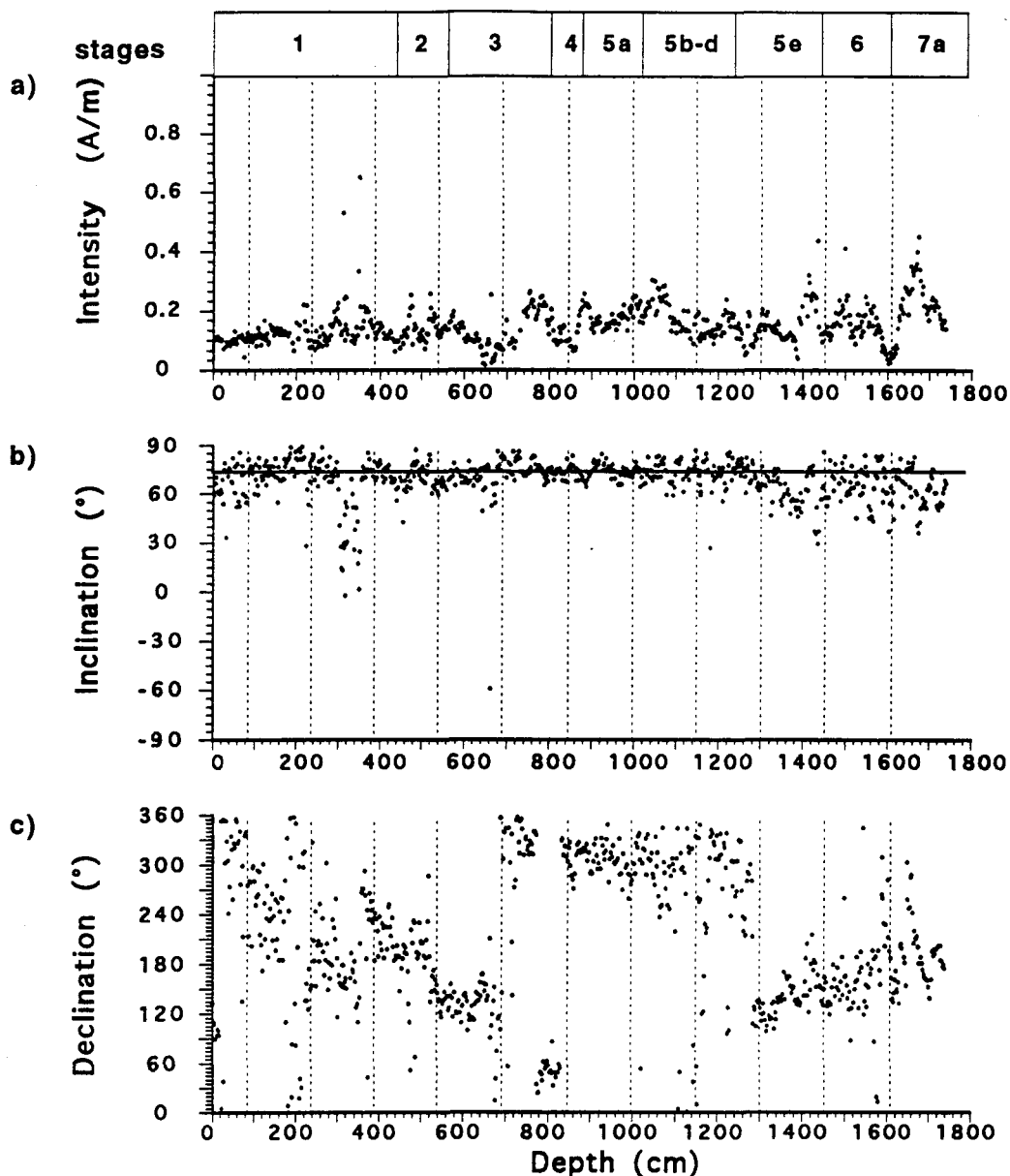


Figure A.1. Paleomagnetic remanence data after 20 mT AF demagnetization for core HU90-013-013 (P-013). a.) Magnetic intensity shown with isotopic stage determinations (Hillaire-Marcel et al., 1994). b.) Magnetic inclination with solid horizontal line indicating expected geocentric axial dipole inclination for this site. c.) Magnetic declination. Dashed vertical lines indicate piston core section breaks.

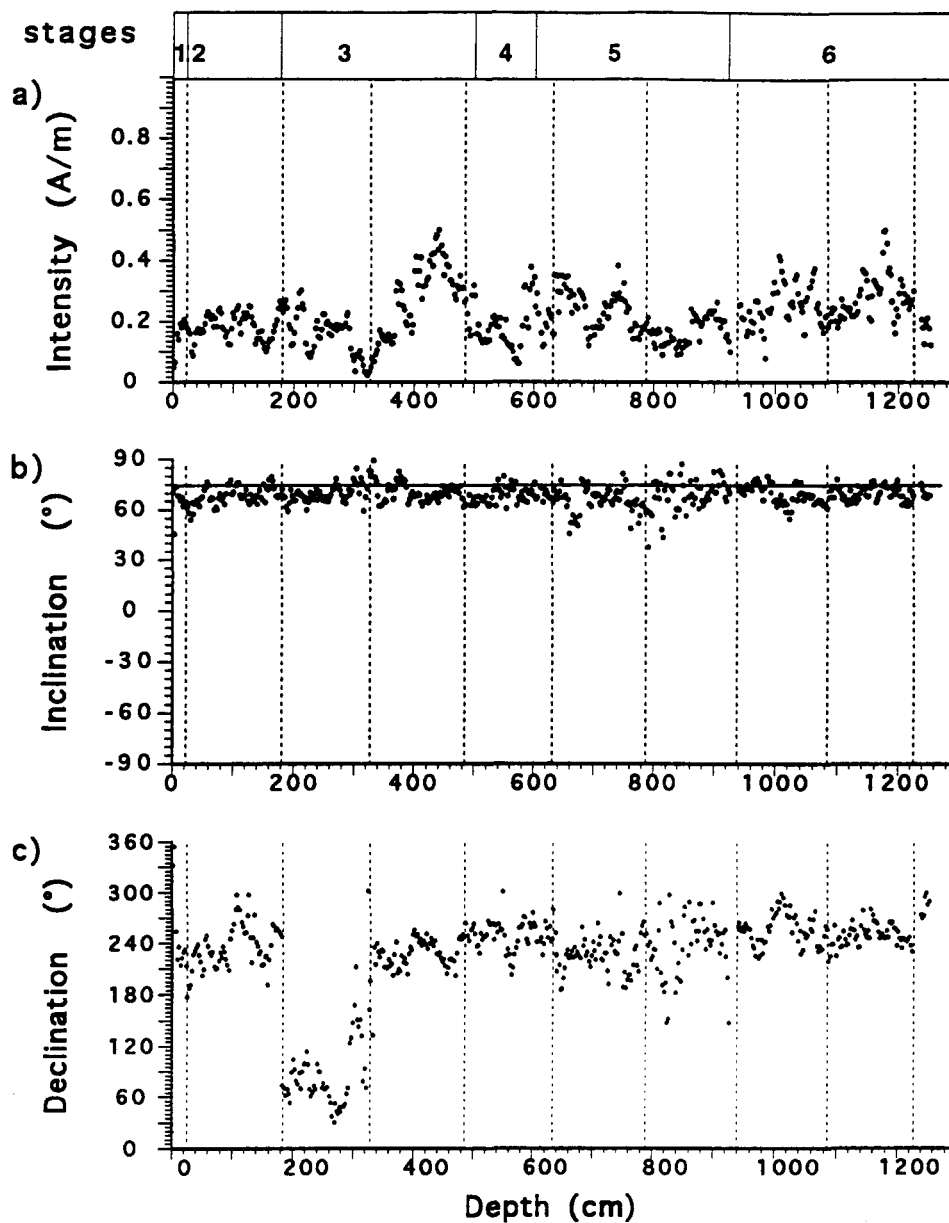


Figure A.2. Paleomagnetic remanence data after 20 mT AF demagnetization for core HU90-013-012 (P-012). a.) Magnetic intensity shown with isotopic stage determinations (Hillaire-Marcel et al., 1994). b.) Magnetic inclination with the solid horizontal line indicating expected geocentric axial dipole inclination for this site. c.) Magnetic declination. Dashed vertical lines indicate piston core section breaks.

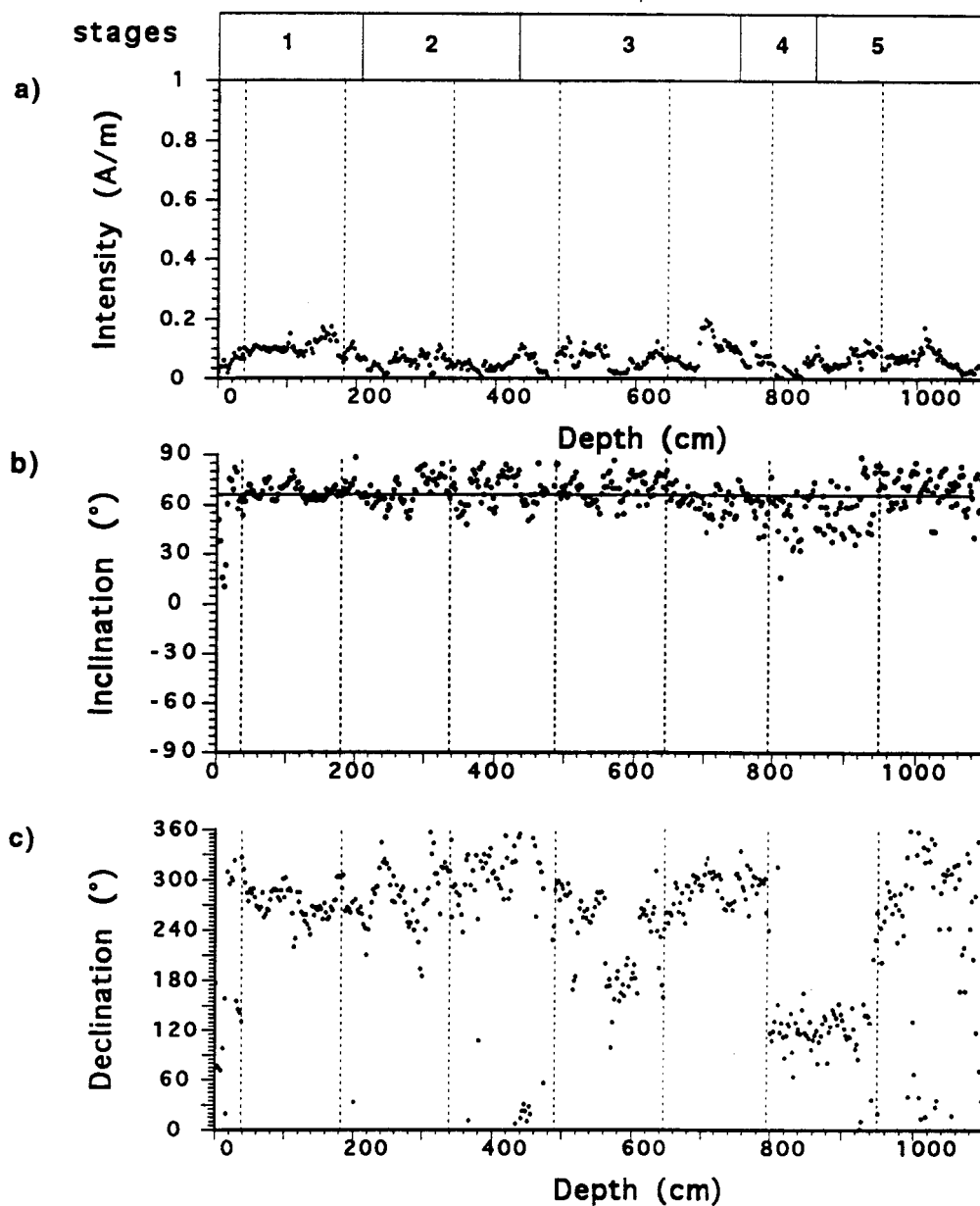


Figure A.3. Paleomagnetic remanence data after 20 mT AF demagnetization for core HU91-045-094 (P-094). a.) Magnetic intensity shown with isotopic stage determinations (Hillaire-Marcel et al., 1994). b.) Magnetic inclination with solid horizontal line indicating expected geocentric axial dipole inclination for this site. c.) Magnetic declination. Dashed vertical lines indicate piston core section breaks.